SEMI-ANNUAL STATUS REPORT

on

Research Grant NGR 06-002-088

"Electrochemical Studies in Aluminum Chloride Melts"

Grant Period: August 15, 1969 – August 14, 1971

Report Period: August 15, 1970 – February 14, 1971

Principal Investigator

R. A. Osteryoung

Associated Personnel

Dr. Larry Boxall (National Research Council
of Canada Fellow)
Dr. H. Lloyd Jones

Department of Chemistry

COLORADO STATE UNIVERSITY

Fort Collins, Colorado 80521

N71-19562   N71-19566

FACILITY FORM 602

(ACCESSION NUMBER)
128
(PAGES)
CR-117056
(NASA CR OR TMX OR AD NUMBER)

(THRU)
(J-3
(CODE)
06
(CATEGORY)

TABLE OF CONTENTS

LIST OF TABLES

SUMMARY

An extensive literature survey has been carried out on the use of $AlCl_3$ containing solvent systems as organic reaction media. They offer the advantages of short reaction times, ease of product recovery and saving on solvent costs. Numerous organic reactions are found to take place in these $AlCl_3$ solvent systems, the three largest catagories being condensation-addition, rearrangement-isomerization and dehydrogenation-addition reactions. Dehydration, exchange and reduction-chlorination reactions have also been found to occur. $AlCl_3$ solvent systems where one of the components is an organic compound, e.g., the $AlCl_3$-pyridine system, have been used as media for organic reactions. A limited number of mechanistic studies have been carried out. Only two reports have appeared on the electrochemical behavior of organic compounds in $AlCl_3$ solvent systems. One of these involved a preliminary study on the electro-oxidation of several polynuclear hydrocarbons while the other involved electro-initiated polymerization of aromatic hydrocarbons.

The present study has, thus far, been limited to the equimolar NaCl-$AlCl_3$ system. A simple versatile experimental cell for the $NaAlCl_4$ melts has been designed. The acid-base equilibria in these melts are reviewed to point out some serious discrepancies in the published data on the system. An unknown solid with an apparent equimolar NaCl-$AlCl_3$ composition has been found to form in the $NaAlCl_4$ melts at temperatures below $225°$ C. Carbon, platinum and tungsten electrodes have been used as indicator electrodes in the present study.

Hydrogen chloride gas was bubbled through the NaAlCl$_4$ melt and a reduction potential of 1.15 volts vs. aluminum for H$^+$ was observed. No reoxidation of the hydrogen was observed and the reduction potential of the H$^+$ is a direct function of the Cl$^-$ ion concentration in the melt in a similar fashion to that observed for the aluminum electrode.

Iron was added to the system by anodizing iron wire and by adding anhydrous ferric chloride. Cyclic voltammetry, pulse polarography, chronoamperommetry and chronopotentiometry were used to study this system. The Fe^{+3}/Fe^{+2} couple has a E$_{\frac{1}{2}}$ value of 1.53 volts and the reduction potential of Fe^{+2} to Fe is 0.64 volts vs aluminum. The Fe^{+3}/Fe^{+2} couple appears to be completely reversible and the diffusion coefficient for Fe^{+3} at 175° C. is 8.8 x 10^6 cm^2/sec. The results indicate the Fe^{+2} ion is moderately adsorbed at 0.64 volts and only weakly adsorbed at 1.53 volts.

The electro-oxidation of ferrocene in a NaAlCl$_4$ melt was investigated using several electrochemical techniques. It appears that ferrocene undergoes a reversible one-electron oxidation with possible product adsorption. However, we have found differences between several of the measured and calculated electrochemical parameters and it is obvious that further work must be done to verify the behavior of ferrocene.

The current state of the development of a system for the computerization of electrochemical measurements in fused salts is discussed. Several improvements have been made to existing programs and electronic interfacing. A chronoamperometric program which automatically compensates for background has been developed to measure electrode areas and for diffusion coefficients. The plans for a pulse polarography program utilizing a dropping mercury electrode is included in this report.

INTRODUCTION

The present work is a continuation of work reported previously, plus one significant change. We have embarked on investigating the behavior of organic species in the aluminum halide melts. The initial step was to carry out an intensive literature survey, and the results of that survey are included as Part I of this report.

One of the perplexing problems associated with studies of the aluminum halide melts by modern electrochemical techniques is a question of melt purity. Since both iron and hydrogen ion have been reported as melt impurities, the electrochemical behavior of these species seemed worth studying. The results on iron, while perhaps preliminary, appear valid and indicate that certain previous reports on melt impurities may not be correct. The results on hydrogen are preliminary, but appear to indicate that proton reacts electrochemically in the system. Finally, a preliminary study of ferrocene was carried out to aid in the establishment of a reference point which might be expected to be independent of the acidity of the melt.

The question of techniques which are readily applicable in fused salts has long been of interest. Our computerized system is being modified to permit better experimental control; the value of this system may be seen in the studies on the iron and ferrocene.

ALUMINUM CHLORIDE CONTAINING SOLVENT SYSTEMS

AS ORGANIC REACTIONS MEDIA — A LITERATURE SURVEY

Some reactions have been carried out in molten salts since organic
chemistry's beginning. A few of these are still found in the standard
synthetic repertory. Although new media [NH$_3$(ℓ), HF(ℓ), dipolar aprotic
solvents] have been introduced and extensively exploited, fused salt
reactions have apparently never been regarded as a class or subjected
to systematic investigation. When, in recent years, organic fused salt
reactions have been considered as such, a general distinction has proved
useful [1] between (1) homogeneous reaction and (2) high-temperature
processes in which an organic reactant gas phase is contacted with an
inorganic melt in which it is poorly soluble. Study of the latter,
which are often efficient replacements for heterogeneous catalysis by
solids, has been spurred by industrial interest, and this type of process
forms the principal subject matter of a review by Sundermeyer[2]. An
excellent review by Gordon[3] provides a collection of the necessary
practical information for planning fused salt experiments, together
with a summary of known organic fused salt reactions.

Three areas of organic chemical interest in molten salts are
taking form:

(1) Synthesis, where we can expect to see old reactions
     improved and altered, and new reactions discovered
     through the use of fused salt media. Modification
     of the reactivity of nucleophilic and electrophilic

reagents, and acids and bases; the appearance of new redox systems; and electrochemical and other modes of generation of reactive intermediates are among the foreseeable developments.

(2) Separation techniques in which one or more molten salt phases take part in chromatographic solvent-extraction, ion-exchange and electrophoretic procedures.

(3) Physical-organic investigations in which ionic liquids constitute new tools in kinetic and equilibrium problems employing electrochemical, spectroscopic, cryoscopic, and other type measurements.

Although the two reviews cited above mentioned the use of fused aluminum chloride and aluminum chloride containing melts, hereafter called $AlCl_3$ solvent systems, as organic reaction media, a comprehensive review was not presented. It is the purpose of this section of this report to present a thorough review of this area. At the same time, some other pertinent studies concerning the interaction of aluminum chloride with organic molecules will be discussed. While many different organic reactions have been carried out in $AlCl_3$ solvent systems, there are three reaction types which have been studied extensively. These are (1) condensation-addition reactions, (2) rearrangement-isomerization reactions and (3) dehydrogenation-addition reactions, the Scholl reaction. Each of these reaction types has been observed in other solvents in the presence of aluminum chloride and

other Lewis acid type catalyst. However, advantages such as short
reaction times, ease of product recovery, saving on solvent cost,
etc. make $AlCl_3$ solvent systems worthy of study. Other types of
reactions that will be discussed are exchanges, dehydrations, and
chlorination reductions.

A. Condensation-Addition Reactions.

Condensation-addition reactions are formally analogous to the well
known Friedel-Crafts reaction. There appears to be only one physio-
chemical study of Friedel-Crafts type reaction in $AlCl_3$ solvent sys-
tems. Komagorov, Baeva, and Koptyug[4] using infrared spectroscopy
studied the formation of acylium cations from aromatic carboxylic
acids and acid chlorides. In a 60:40 mole % $AlCl_3$:NaCl melt in the
temperature range 25-160°C the formation of the acylium ion, $ArCO^{\oplus}$,
where Ar = phenyl, o-chlorophenyl, p-chlorophenyl and o-methoxyphenyl
could be followed by its infrared absorption at $2240cm^{-1}$. Acylium ion
concentration was found to increase with temperature and disappear
reversibly on cooling, with appreciable concentrations of the ion oc-
curring only at temperatures greater than 130°C.

An example of the Friedel-Crafts hydrocarbon synthesis which was
carried out in an $AlCl_3$ solvent system is the reaction of benzene with
ethyl chloride or ethyl bromide at 150-170°C to yield ethylbenzene.
However, large amounts of tarry products are formed[5].

Many examples of condensation type reactions have been carried
out in $AlCl_3$ solvent systems. In general, one of the reactants
has either been carboxylic acids, dicarboxylic acids, acid anhydrides or

lactones, while the other has been aromatic or heterocyclic compounds

which were not severely deactivated. In the following discussion, we

will discuss the use of these various reactants. One of the simplest

cases is the reaction between phenol and benzoic acid in a 68:32 mole %

$AlCl_3$:NaCl melt to give o- and p-hydroxybenzophenone as illustrated:

OH CO_2H 68:32 Mole % $AlCl_3$:NaCl OH C=O + C=O OH
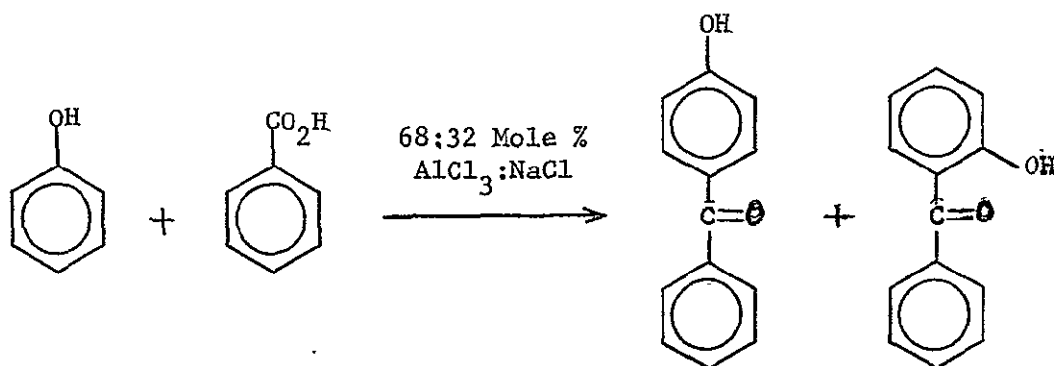
The earliest reports of condensation reactions in $AlCl_3$ solvent

systems invariably involved the use of acid anhydrides as one of the

reactants. As we will see, the products one obtains are dependent on

the reaction temperature. Keto-acids are obtained at lower temperature

while quinones are obtained at higher temperature, no doubt by conden-

sation of the keto-acid. We will first discuss the reaction where

phthalic anhydride and its derivatives are one of the reactants.

Waldmann and Sellner[6] reported that when phthalic anhydride

and pyrocatechol were heated at 110°C in an $AlCl_3$,NaCl melt the

product was the keto-acid and not hystazarin, the corresponding

anthraquinone:
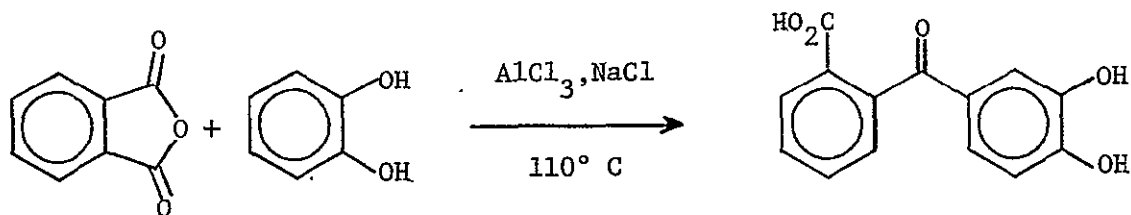
However, at temperatures of approximately 200°, quinones are secured. In this way, hydroquinone with phthalic anhydride yields quinizarin[7]:
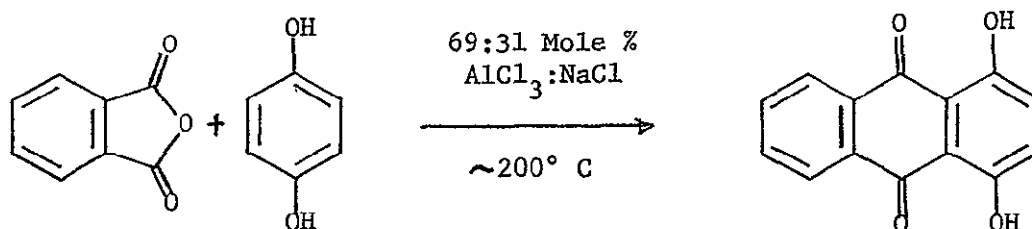
Another example of the effect of temperature on the product is the reaction between phthalic anhydride and o-cresol[6]. At 120-130°C in a 65:35 mole % $AlCl_3$:NaCl melt, a mixture of isomeric keto-acids is obtained. However, if the reaction mixture is heated at 165°C, the product is a mixture of the corresponding anthraquinones.

Aromatic amines also undergo condensation with phthalic anhydride. β-Naphthylamine adds normally to phthalic anhydride in an $AlCl_3$,NaCl melt at 110-115°C to yield aminonapthoylbenzoic acid[8]. Kranzlein[9] has also been successful in preparing keto-acids from a number of polynuclear amines and phthalic anhydride reactants with an $AlCl_3$, NaCl melt at temperatures of 110-120°C. Further heating at about 150°C results in ring closure. This is illustrated for 4-aminobiphenyl:
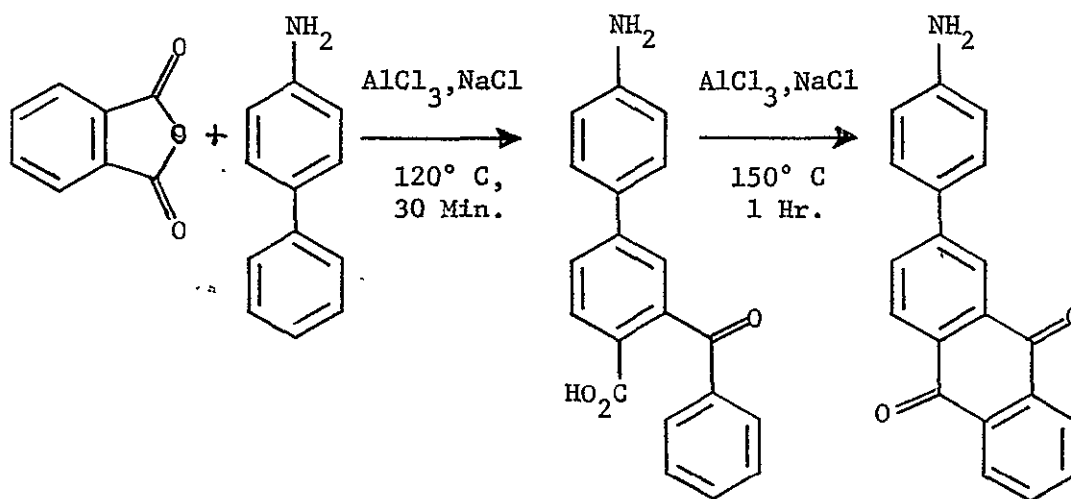
Other amines which were found to undergo at least the first step
of the condensation reaction were 3-methyl-4-aminobiphenyl, 3-amino-
phenanthrene, 2-aminofluorene, 2-aminochrysene and 3-aminopyrene.
However, similar condensations could not be effected with either
m-tolidine or benzidine probably because the 4,4'-positions of
these compounds are occupied.

Amides will also undergo condensation with phthalic anhydride.
When 1-acetamide-3-methyl-4-hydroxybenzene was heated with phthalic an-
hydride for ten minutes at 110°C in an $AlCl_3$,NaCl melt, a 64% yield of
2-acetamide-4-methyl-5-hydroxy-2-benzoylbenzoic acid was obtained[9].

A number of heterocyclic compounds have also been found to condense
with phthalic anhydride. The condensation of phthalic anhydride with
2-aminocarbazole or with 3-amino-9-ethyl-carbazole at 110°C in an
$AlCl_3$,NaCl melt gives 2-amino- and 3-amino-9-ethylphthalylcarbazole
in 65-70% and 52% yields, respectively[9]. Fusion of 3-aminodibenzo-

furan and phthalic anhydride with an $AlCl_3$,NaCl melt for 30 minutes at 115°C and then for 1.5 hours at 150°C leads to the production of the ring closed compound, 3-aminophthylbenzofuran in 40% yield[9]:
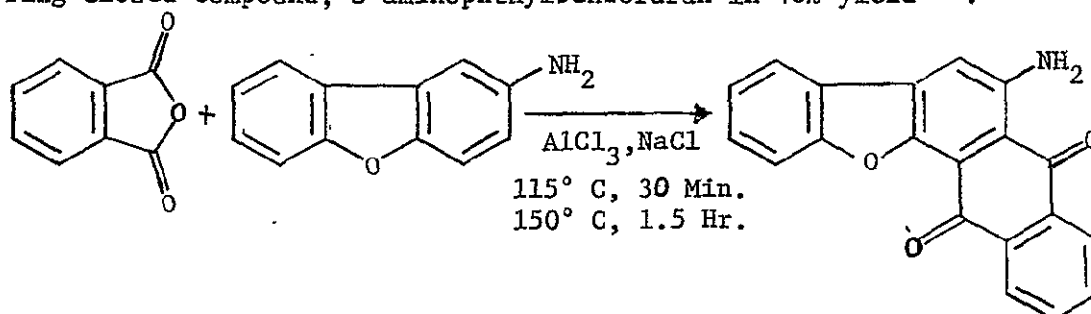
The compound, 2-(2,5-dimethyl-3-thenoyl)benzoic acid, upon heating in an $AlCl_3$,NaCl melt, is converted to the corresponding quinone[10]:
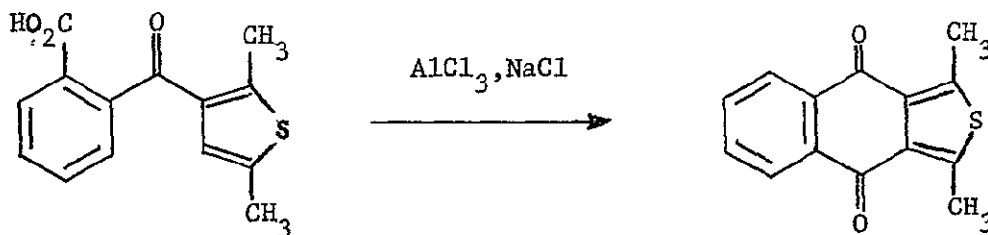
A few less reactive aromatic compounds have also been found to condense with phthalic anhydride. 2',5'-Dichloro-2-benzoylbenzoic had been prepared by heating 1 mole of phthalic anhydride with 0.5 moles of p-dichlorobenzene, and 1.5 moles of $AlCl_3$ at 110-120°C for about 4 hours[11].

Substituted phthalic anhydrides can also be used in the condensation reaction with aromatic compounds. For example, hydroquinone reacts with 3,6-dichlorophthalic anhydride at 200°C in an $AlCl_3$,NaCl melt to give an 84% yield of 5,8-dichloroquinezarin:
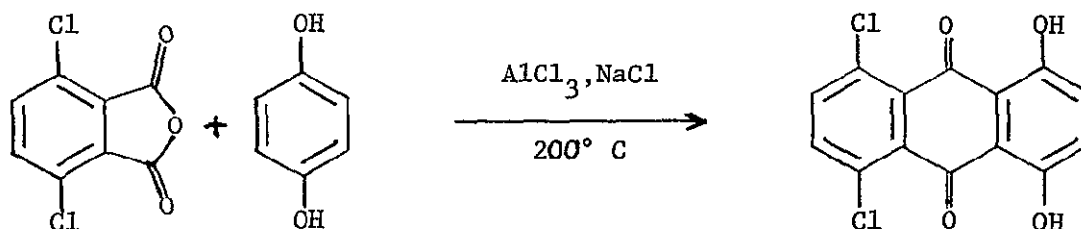
The 4;5-dichloro-acid anhydride similarly gave an 80% yield of 6,7-dichloroquinezarin[12].

Methylated phthalic anhydrides have been found to react with various hydroquinones in an $AlCl_3$,NaCl melt in the temperature range 180-190°C to give either the keto-acid or the anthraquinone derivatives[13].

A few investigators cite the use of acylated phthalic anhydrides in Friedel-Crafts type reactions. 4-Acetyl-phthalic anhydride has been condensed with hydroquinone in an $AlCl_3$, NaCl melt at 180°; heating for 45 minutes produces 5,8-dihydroxy-2-acetyl-anthraquinone:
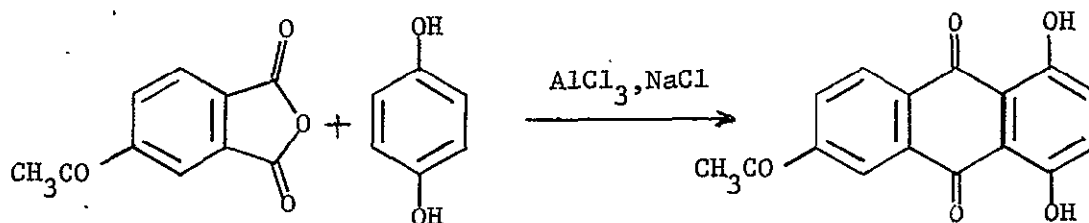
Like treatment of toluhydroquinone produced 2-acetyl-6(or 7)-methyl-5,8-dihydroxyanthraquinone, and analagous reaction with 1,4-naphtho-hydroquinone yields 2-acetyl-5,8-dihydroxy-6,7-benzoanthraquinone[14].

The anhydrides of other aromatic and heterocyclic dicarboxylic acids are also known to undergo Friedel-Crafts type condensation reactions. For example, phenols such as p-chlorophenol, p-cresol and p-naphthol have been condensed with naphthalene-2,3-dicarboxylic acid anhydride in an $AlCl_3$,NaCl melt at 200-210°C to yield the corresponding substituted benzanthraquinone[15]. Waldmann[16] using a 65:35 mole % $AlCl_3$:NaCl melt at 200-210°C for 3 hours found hydroxybenzanthraquinones from the interaction of naphthalene 1,2-dicarboxylic anhydride with

various phenols and hydroquinones. For example, with hydroquinone

the following occurs:
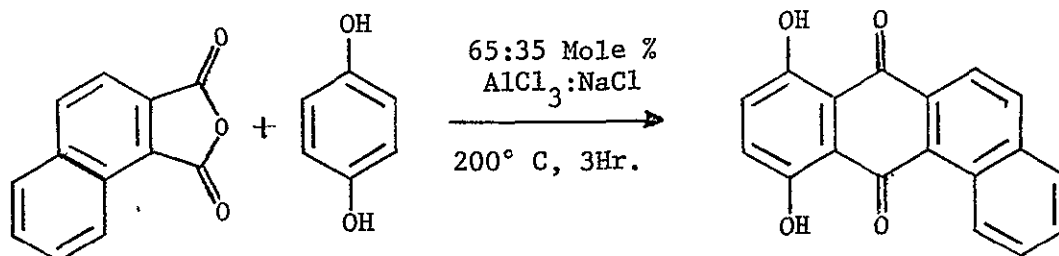
Mayer and his co-workers[17] have described the interaction of

thianaphthene-2,3-dicarboxylic anhydride and hydroquinone, in an

$AlCl_3$,NaCl melt to give a 76% yield of 7,10-dihydroxybenzothio-

phanthrenequinone. Friedel-Crafts' condensation of thianphthene-2,3-dicarbox-

ylic acid anhydride or its substitution products with aromatic hydrocarbons

and phenols in $AlCl_3$,NaCl melts is covered by several patents[18].

The condensation of aliphatic acid anhydrides with aromatic

substrates in $AlCl_3$ solvent systems has also been studied. Maleic

anhydride and hydroquinone in an $AlCl_3$,NaCl melt at temperatures

over 200°C yield naphthazarin[19]:
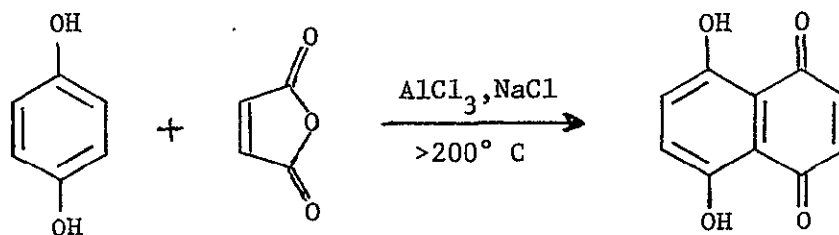
In the alkyl naphthazarins, the quinoid and benzenoid states of

both rings appear to be interchangeable. Hence, the condensation

of 3-alkylhydroquinones under the same conditions results in the

formation of naphthazarins in which the alkyl derivative is

substituted in the quinone nuclei[20]:
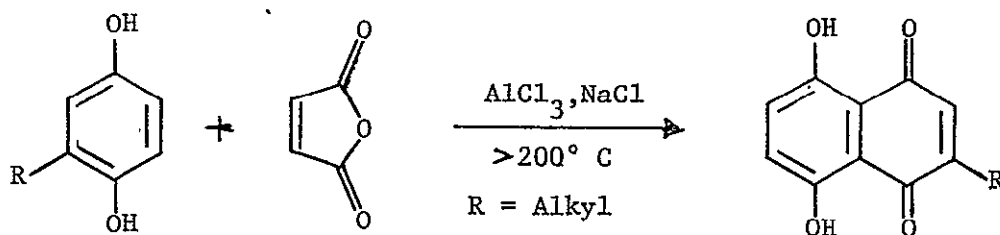
Brockman and Miller[21] have prepared alkylated naphthazins by reacting alkylated hydroquinone methyl ethers with maleic anhydride in an $AlCl_3$,NaCl melt. During the reaction, saponification of the methoxy group occurs. In the condensation of 3-isohexylhydroquinone-dimethyl ether under the above conditions, isohexylnaphthazarin was not obtained. Instead, the product was 1,1'-dimethyl-1,2,3,4-tetra-hydroquinizarin formed by ring closure of the intermediate alkyl naphthazarin:
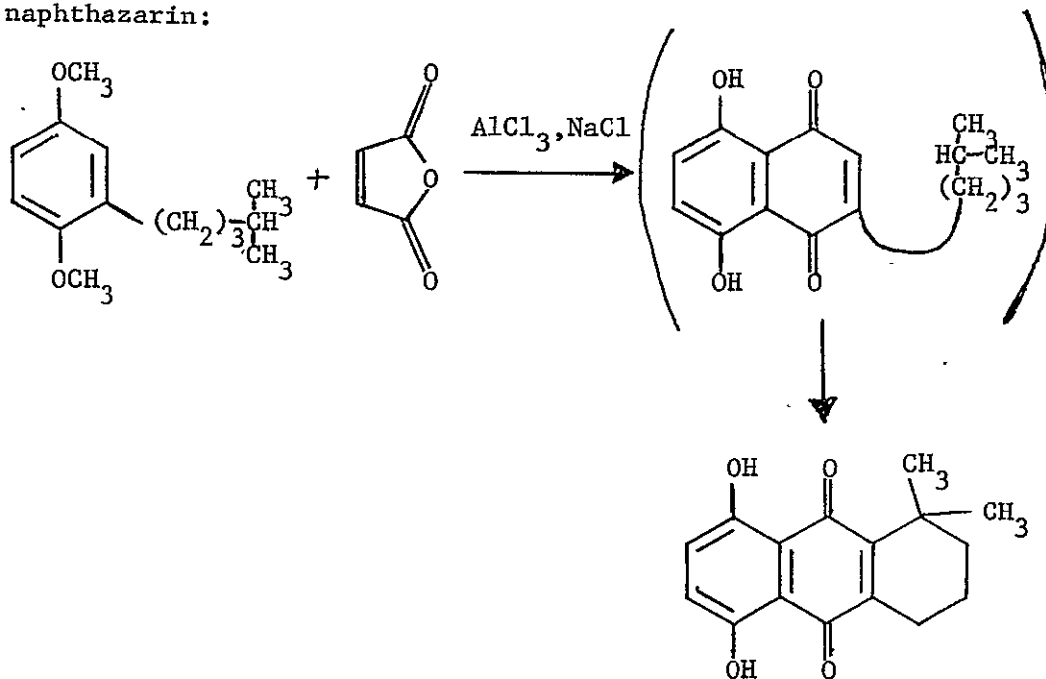
Substituted maleic anhydrides also undergo condensations. Citraconic anhydride and hydroxyhydroquinone in an $AlCl_3$,NaCl melt yields 6-(or 7)-hydroxy-2-methylnaphthazarin[22].

Dicarboxylic acids themselves are reported to undergo condensation with aromatic substrates in $AlCl_3$ solvent systems[23]. Succinic acid and hydroquinone in a 68:32 mole % $AlCl_3$:NaCl melt at 180-200°C for two minutes yields 1,2,3,4-tetrahydronaphthazarin, while under the same conditions adipic acid gives δ(2,5-dihydroxybenzoyl)-valeric acid.

Bruce, Sorrie, and Thomson[23] have also reported the condensation of lactones with hydroquinone under the above conditions. Upon reacting γ-butyrolactone with hydroquinone one obtains 4,7-dihydroxy-3-methyl-indane-1-one, the same product which one obtains from crotonic acid and hydroquinone:
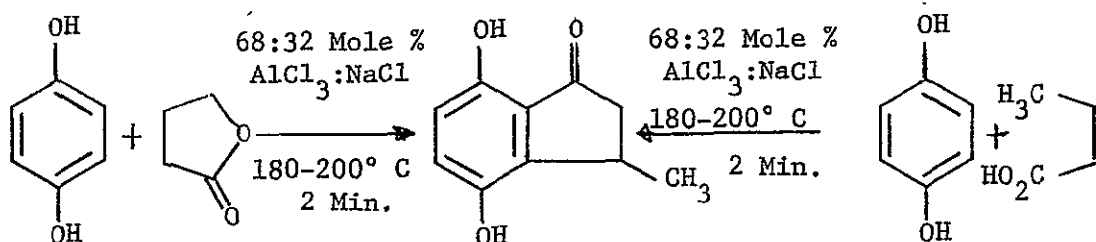
The product from the reaction of the lactone apparently arises by ring opening followed by elimination of hydroxide ion and a shift of the consequent double bond to form a vinyl ketone which, as we will see later, cyclizes to form the desired product. In a like manner, the product of the reaction between γ-valerolactone and hydroquinone under the same conditions, is 4,7-dihydroxy-3-ethylindan-1-one.

At the outset of this section we described the condensation reaction of an aromatic acid and phenolic derivatives as well as the intramolecular ring closure of keto-acids using the $AlCl_3$ solvent systems at temperatures below 150°C. The intramolecular cyclization of

aryl-substituted aliphatic acids has been described[23]. For

example, in a 68:32 mole % $AlCl_3$:NaCl melt at 180-200°C for two

minutes β-phenyl propionic acid yields 85% of indan-1-one:

CO$_2$H CH$_2$ CH$_2$ 68:32 Mole %
$AlCl_3$:NaCl
———————————→
180-200° C
2 Min.
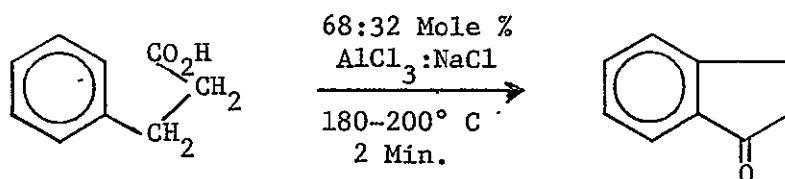
. while γ-phenylvaleric acid yields benzosuberone in 22% yield.

One other interesting example of the intermolecular ring

closure is the reaction of β-(3-acenaphthoyl)-propionic acid in an

$AlCl_3$,NaCl melt at 150°C to yield peri-succinoylacenaphthene[24]:

COCH$_2$CH$_2$CO$_2$H $AlCl_3$,NaCl
————————→
150° C

OC CO
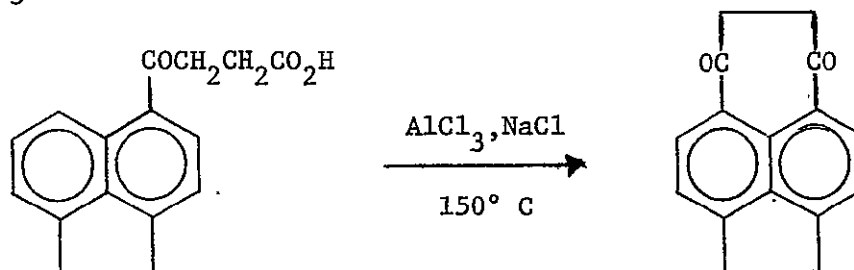
A thorough study of the intramolecular ring closure condensation

of derivatives of o-benzoylbenzoic acid in $AlCl_3$ solvents systems has

been carried out by Baddeley, Holt and Makar[25]. Some of the acids

were susceptible to isomerization and afforded anthraquinone after

migration of substituents. These isomerizations will be discussed

in a later section and it will be sufficient here to just illustrate

the course of the reaction. For example, when o(2,5-dimethylbenzoyl)-

benzoic acid is heated for 1 hour at 175°C in a 75:25 mole % $AlCl_3$:

NaCl melt, both 1,4-dimethyl- and 1,3-dimethylanthraquinone are obtained

while o(2,4-dimethylbenzoyl)benzoic acid under the same conditions

gives only 1,3-dimethylanthraquinone. This sequence is outlined

below:
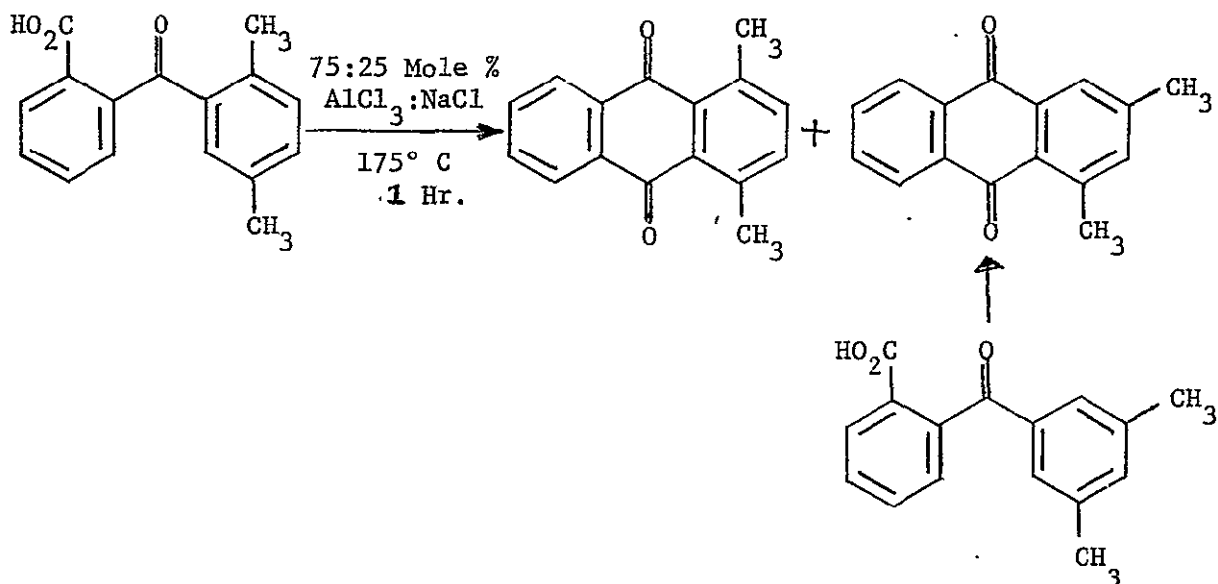
Similar examples are found with other alkyl derivatives of

o-benzoylbenzoic acid. It has been concluded by these workers

that products of fusion with $AlCl_3$ solvent systems are determined

by the relative rates of isomerization and of ring closure of

the o-aroylbenzoic acids.

One other class of acids which undergo intramolecular ring

closure in $AlCl_3$ solvent systems are the β-aroylacrylic acids which

yield 3-ketoindane-1-carboxylic acids[26]. This is not formerly

a condensation reaction as the acid function remains and therefore

this reaction will be discussed in a later section.

B. Molecular Rearrangements and Isomerizations

Rearrangement of the substituent groups in aromatic compounds is

frequently facilitated by the use of anhydrous aluminum chloride.

Nuclear bound alkyl may immigrate in either an intermolecular or an intramolecular manner. Acyl and sulfonyl substituents may also rearrange to new positions on the aromatic nucleus. These type reactions have been observed by many workers in $AlCl_3$ solvent systems.

The rearrangements of phenolic esters to hydroxy aromatic ketones, which is known as the Fries rearrangement, have been observed in 68:32 mole % $AlCl_3$:NaCl by Bruce, Sorrie, and Thomson[23]. For example, upon heating phenyl acetate for two minutes at 180-200°C in the above melt both o- and p-hydroxyacetophenone were obtained.
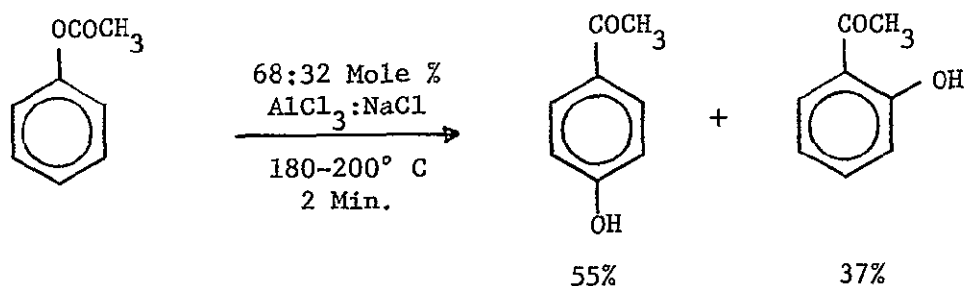
Similarly, quinol dibenzoate gave 2,5-dihydroxybenzophenone.
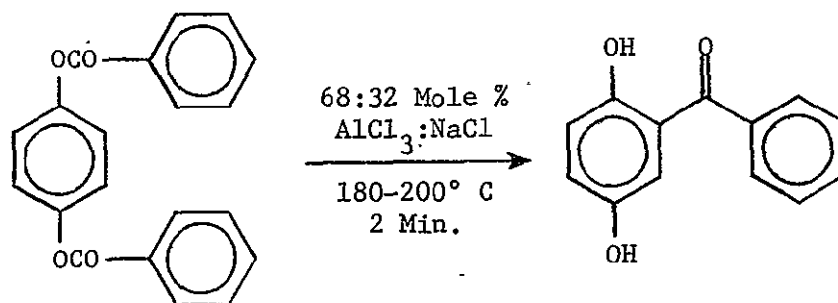
The fate of the second benzoyl group is unknown.

Auwers[27] has tabulated a number of instances in which the normal product of the Fries rearrangement was accompanied by an

isomeride, derived by displacement of an alkyl group from its original

position. Baddeley[27] later showed that the products depended on the

number of moles of $AlCl_3$ used. In particular, this author studied the

Fries rearrangement and subsequent isomerization of 3,5-dimethylphenyl

acetate at 140-150°C. The results are shown in the scheme below:
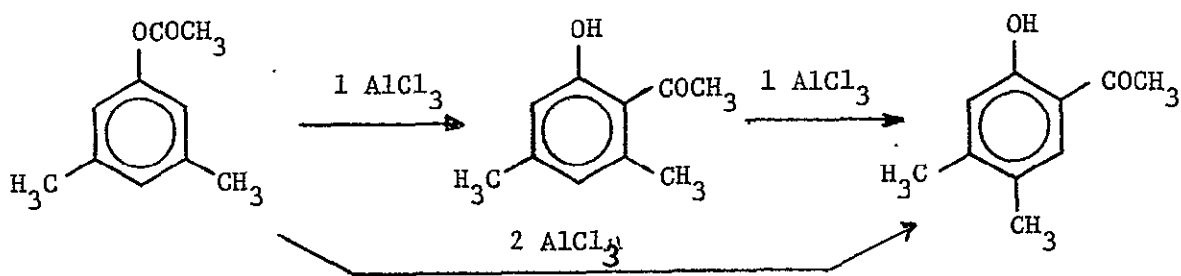
Baddeley also obtained kinetic data for the isomerization in a 83:17

mole % $AlCl_3$:NaCl melt at 140° and 150°C.

A reaction which is formerly analogous to the Fries rearrangement

is the isomerization of aryl sulfonates to hydroxyaryl sulfones. Upon

fusing phenyl benzenesulfonate with $AlCl_3$ at 150° for 1.5 hours,

o- and p-hydroxydiphenyl sulfone are obtained[29]:
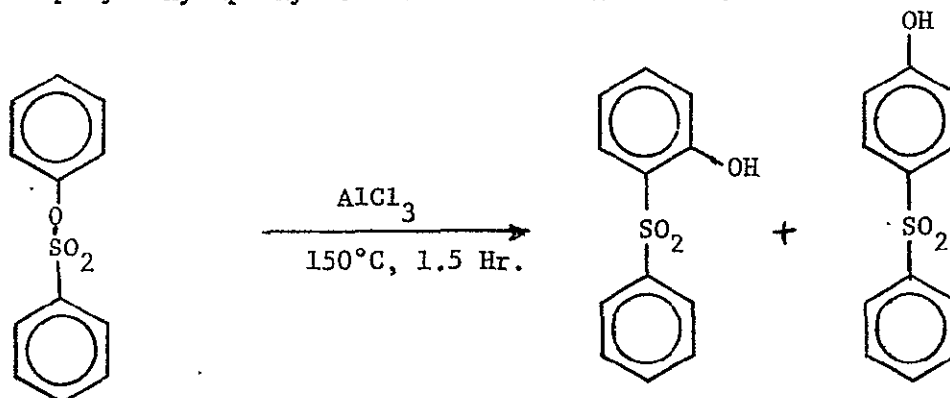
Similarly, p-chlorophenyl benzenesulfonate gave 2-hydroxy-5-chloro-

diphenylsulfone and p-toluyl benzenesulfonate gave 2-hydroxy-5-methyl

diphenylsulfone.

A number of isomerizations in which ring closure occurs are also known to occur in $AlCl_3$ melts[23,25]. As we mentioned before, β-aroyl-acrylic acids in a 75:25 mole % $AlCl_3$:NaCl melt at 135°C for 1 hour yields 5-ketoindane-1-carboxylic acids, e.g., the following reaction is observed:
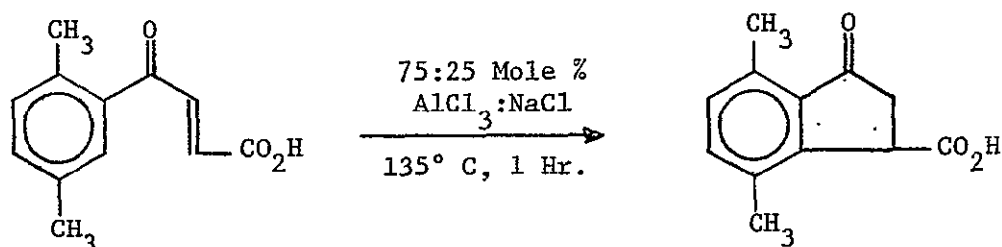
Similarly, aryl vinyl ketones are found to cyclize in a 68:32 mole % $AlCl_3$:NaCl melt. For example:
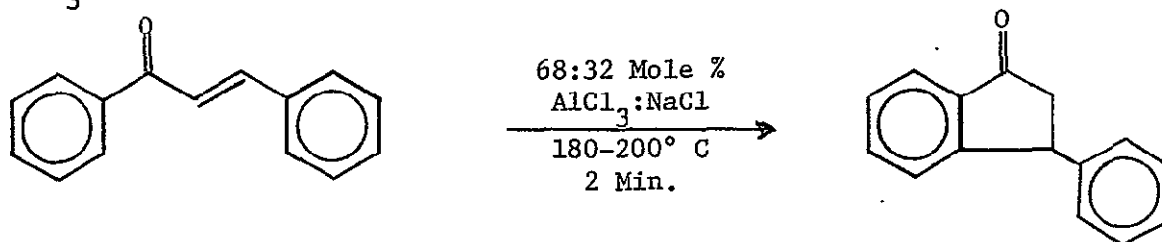
Ring closure is probably effected through formation of an oxonium complex and one of its resonance structures.
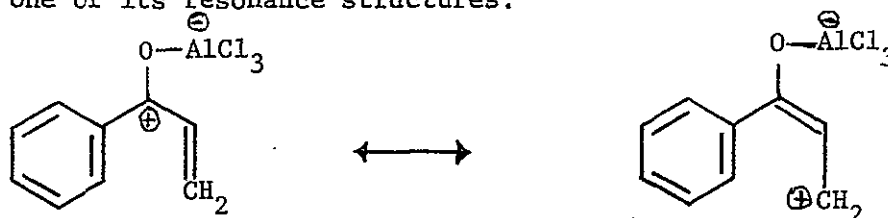
A number of other rearrangements have been observed in $AlCl_3$ solvent systems. Loudon and Razdan[30] found that chromanones and 3,4-dihydrocoumarins are rearranged to hydroxyindanones. Some typical examples are shown below:
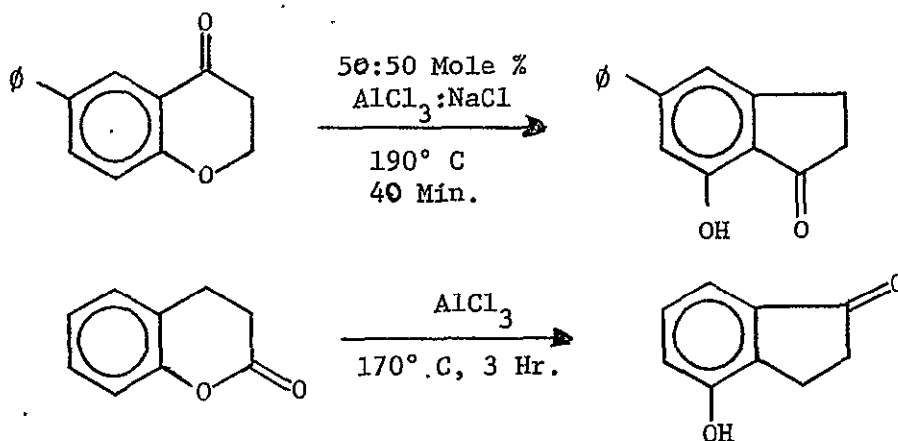
Similarly, 2,3-dihydro-4-methyl-3-oxobenz-1-oxazine was rearranged to give two oxindole derivatives when fused with AlCl$_3$[31]:
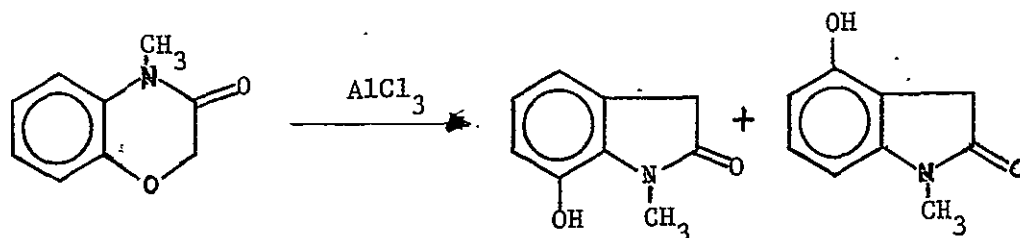
N-arylphthalimides are transformed into lactams upon heating with an AlCl$_3$,NaCl melt[32]. N-phenylphthalimide is converted to the lactam of 2-(2'-aminobenzoyl) benzoic acid:
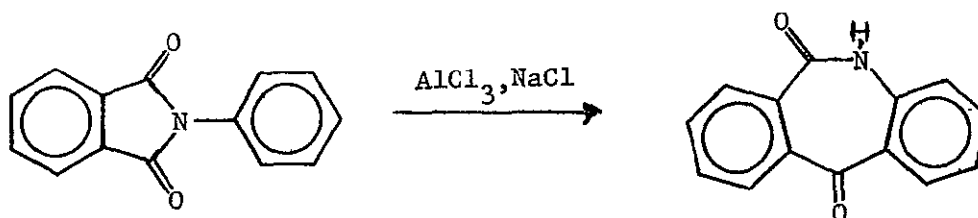
About 25 patents have been granted for methods of isomerizing n-paraffins to branched-chain compounds. Aluminum chloride/alkali metal melts containing an excess of AlCl$_3$ have been used[33]. The reaction is generally carried out below 200°C. The longer the carbon chain of the n-paraffin, the lower is the temperature chosen, since

otherwise undesireable cracking occurs. It has been found useful
to add small quantities of hydrogen chloride[34]; for example, the-
isomerization of n-butane to isobutane then proceeds at 141°C with
a 50% conversion. This process is of interest for increasing the
octane rating of petroleum fractions.

In a series of papers, Baddeley and his co-workers[25,26,28,35]
have made a thorough study of the isomerization that takes place in a
variety of aromatic ketones and alkylated phenols and benzenes in
$AlCl_3$ solvent systems. A few representative examples are illustrated
below:

OH

COCH₃

H₃C CH₃

AlCl₃
140-180° C
3 Hr.

→

OH

COCH₃

H₃C

CH₃

COCH₃

H₃C CH₃

H₃C CH₃

87:13
Mole %

AlCl₃:
NaCl
100° C

→

COCH₃

H₃C CH₃

H₃C CH₃

COCH₃

+

H₃C CH₃

H₃C CH₃

+

COCH₃

H₃C

H₃C CH₃

CH₃

150° C

↓

COCH₃

H₃C CH₃

CH₃

+

CH₃

H₃C CH₃

H₃C CH₃

CH₃
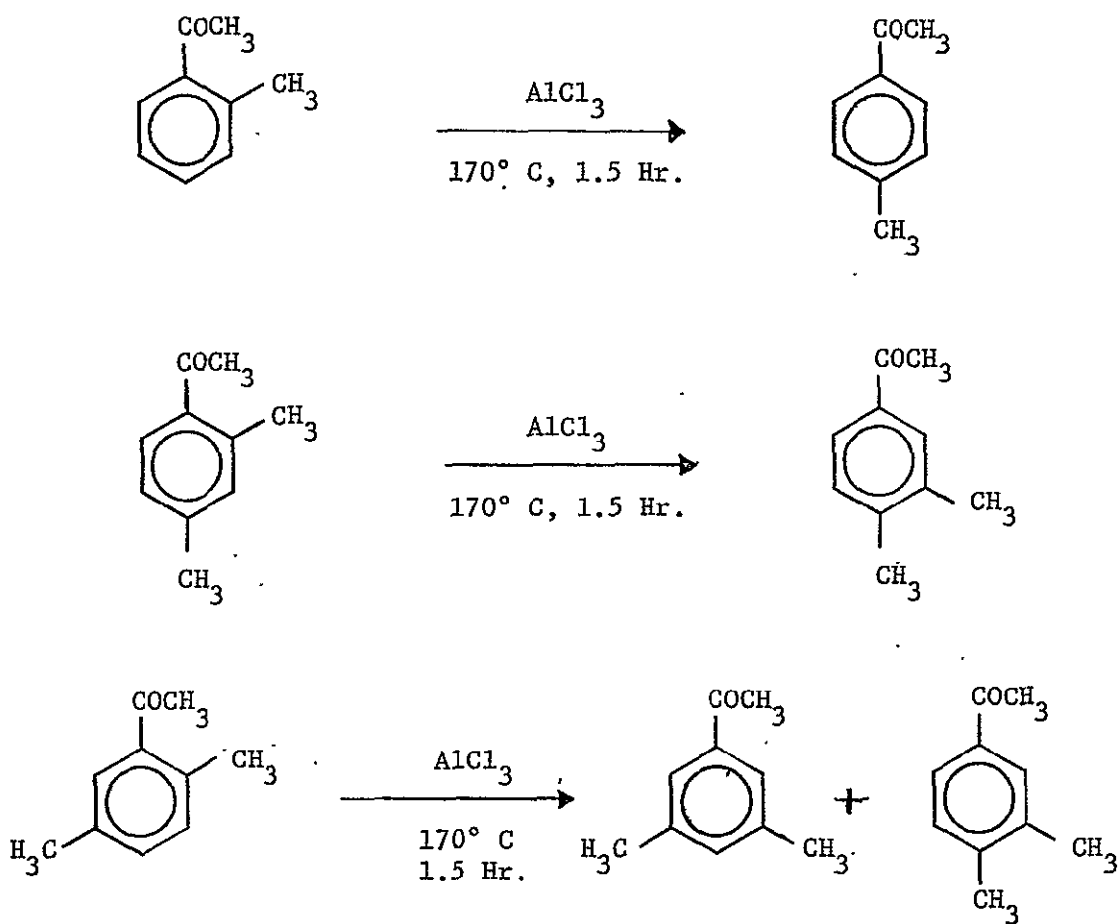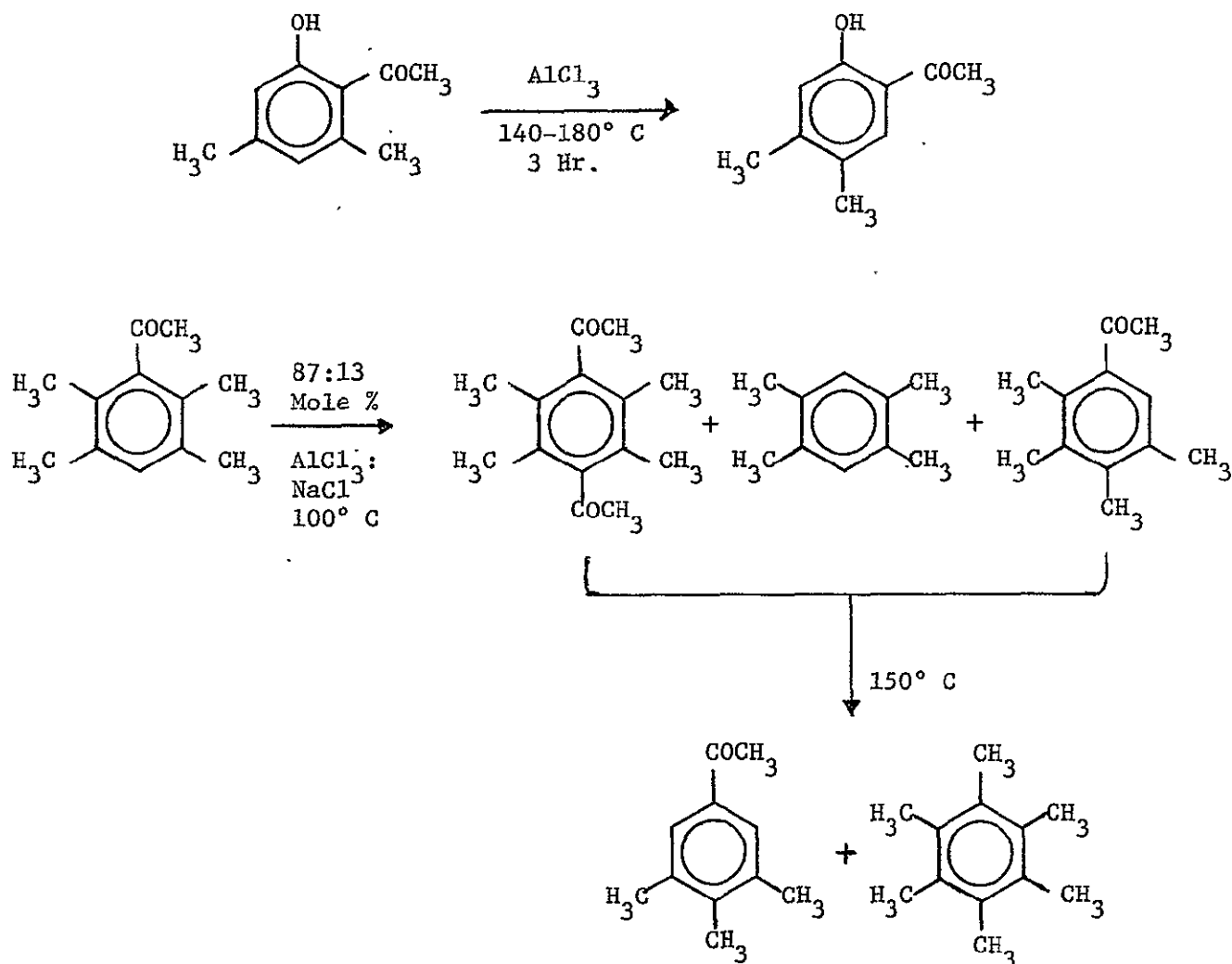
Without going into detail, a summary of the reaction mechanism can be given. The following points are known:

1. In the case of ketones, one molecular proportion of AlCl₃ combines with the carbonyl group to form an oxonium complex and an additional mole of AlCl₃ is needed to effect isomerization.

2. The presence of hydrogen halide is necessary.

3. The products are determined by the relative rates of (i)

deacylation followed by reacylation, and (ii) intramolecular

migration of the o-alkyl group to the adjacent meta-position.

4. As homologs of benzonitrile are not isomerized, it appears

   that steric factors determine the various isomerizations

   that take place. This is also seen in the case of methylated

   anthraquinones which also do not undergo isomerization.

5. The ease of alkyl migrations or mobility is in the order

   propyl >ethyl >methyl.

Similar migrations have been shown to occur with some o-alkylbenzene-

sulfonic acids and o-alkyldiphenyl sulfones[36]. For example, in an 81:19

mole % $AlCl_3$:NaCl melt at 200°C for 10 hours, the following isomerizations

were observed:
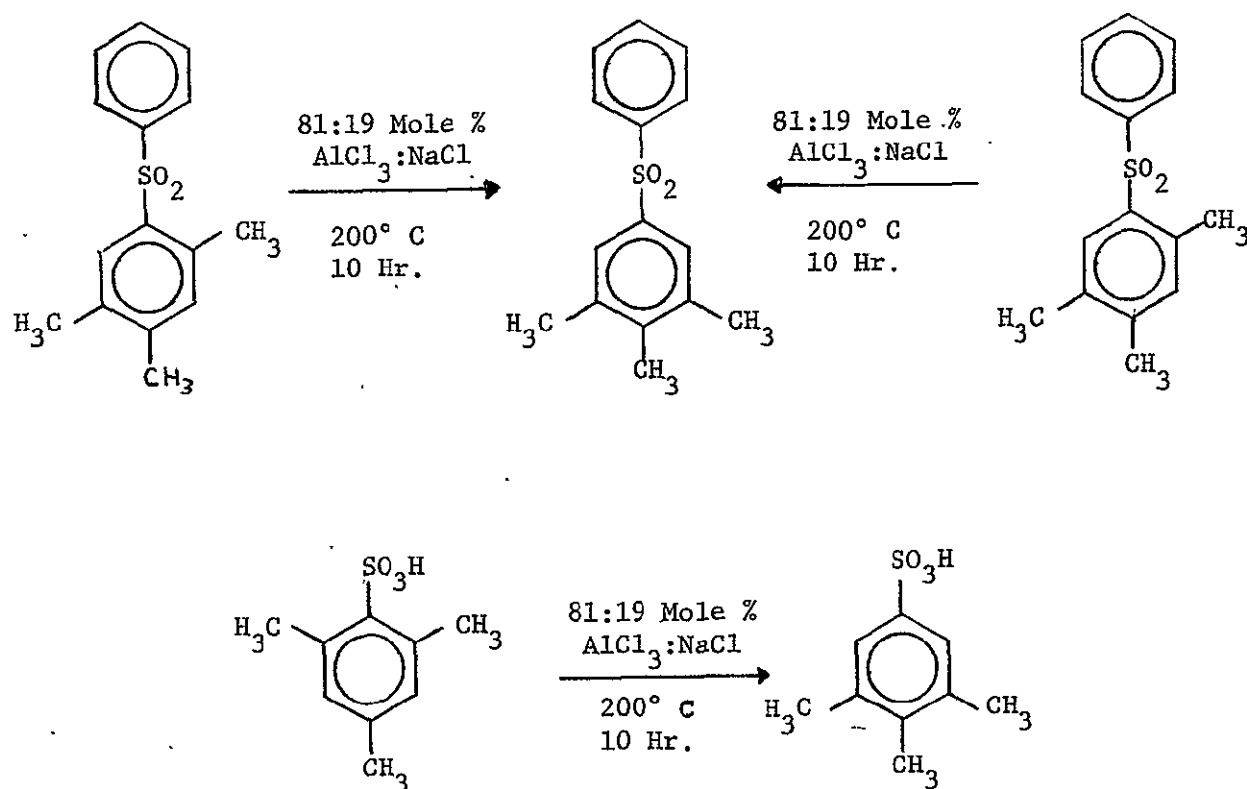
The greater mobility of ethyl groups over methyl groups was also

observed in several cases. The explanation for these reactions is no doubt identical to that for the aromatic ketone isomerizations.

C. Dehydrogenation-Condensation Reactions

Aluminum chloride is known to catalyze nuclear dehydrogenation condensation of aromatic hydrocarbons, with formation of higher ring compounds. The reaction may be intramolecular or intermolecular. Thus 1,1'-binaphthyl yields perylene[37] and two moles of chrysene yield 2,2'-bichrysenyl[38]. Since the application of the dehydrogenating activity of aluminum chloride to the synthesis of polynuclear ring systems has been largely worked out by Scholl, who has extended it primarily to the synthesis of a wide range of oxygenated derivatives, condensations of this type are known as the Scholl reactions. Although the Scholl reaction has been carried out in other solvents, in the many cases the use of $AlCl_3$ solvent systems was found to remove hydrogen (the byproduct of the reaction) more effectively.

In the original reports of the Scholl reaction, fused $AlCl_3$ itself was used as the solvent. For example, upon refluxing naphthalene with $AlCl_3$ at 180°C for 1 hour, perylene was obtained[39].

$$2 \text{ (naphthalene)} \xrightarrow[180°\text{ C, 1 Hr.}]{AlCl_3} \text{(perylene)} + 2H_2$$
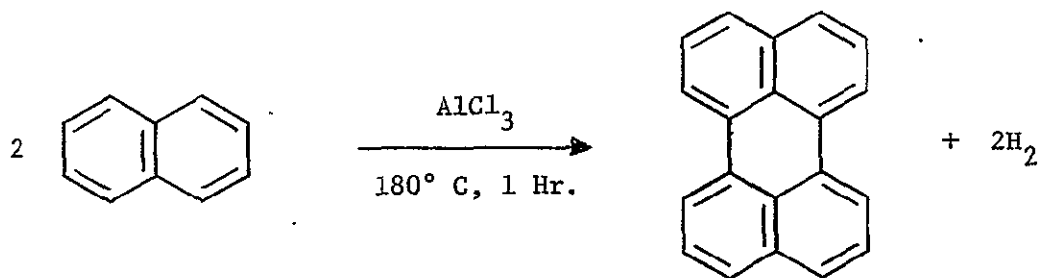
More recently, $AlCl_3 \cdot NaCl$ melts have been used in the synthesis of polynuclear hydrocarbons. The preparation of 1.12;4.5; 8.9- tribenzo-

perylene, I,[40] and 2.3; 10.11-dibenzoperylene, II, are illustrated

below: ·

80:20 Mole %
AlCl$_3$:NaCl
$\xrightarrow{\hspace{2cm}}$
130° C, 2Hr.

+ H$_2$

I

65:35 Mole %
AlCl$_3$:NaCl
$\xrightarrow{\hspace{2cm}}$
130° C
30 Min.

+ H$_2$

II
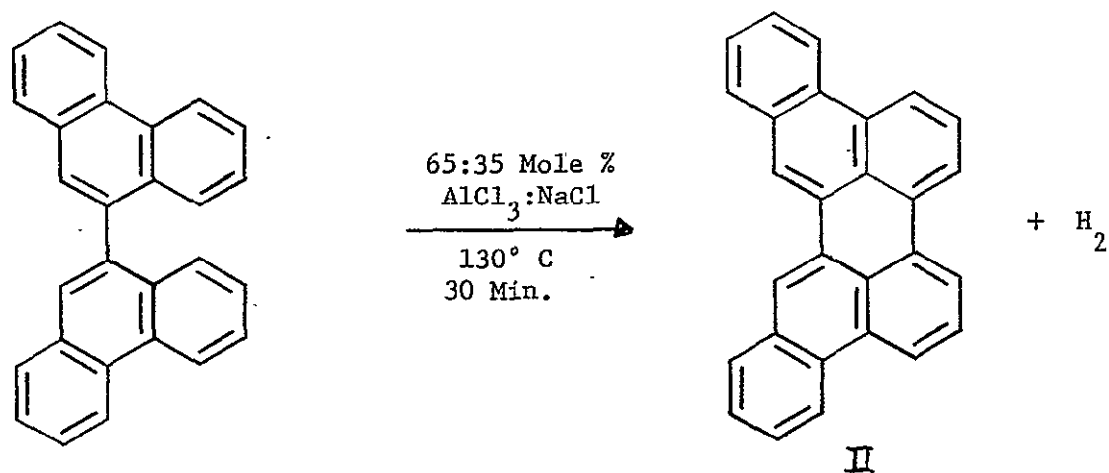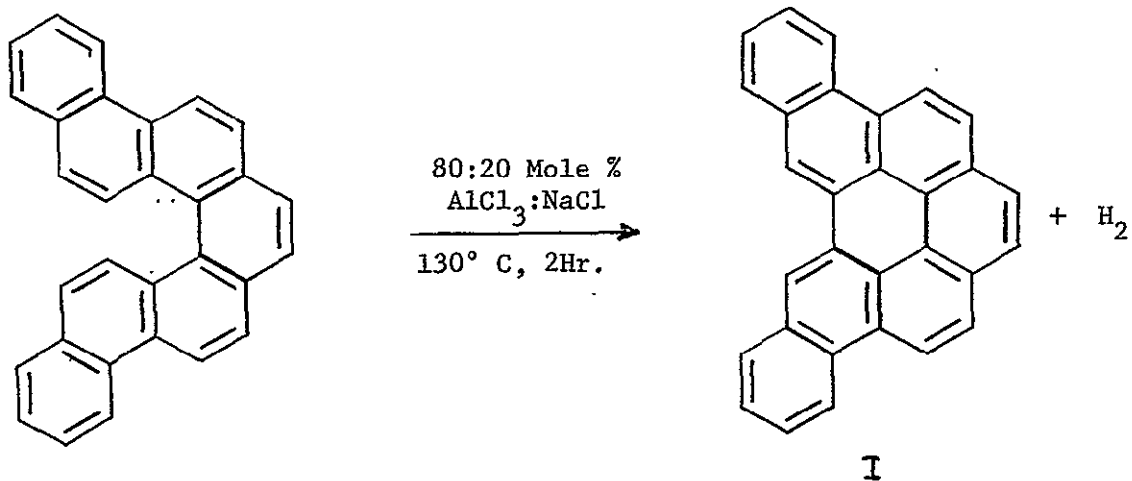
The Scholl reaction has more commonly been carried out on poly-

nuclear ketones. Scholl and Seer [42] prepared 1,9-benzanthrane from

phenyl 1-naphthyl ketone in 75% yield by heating the ketone with 5

parts of AlCl$_3$ at 150°C for 2.5 hours:
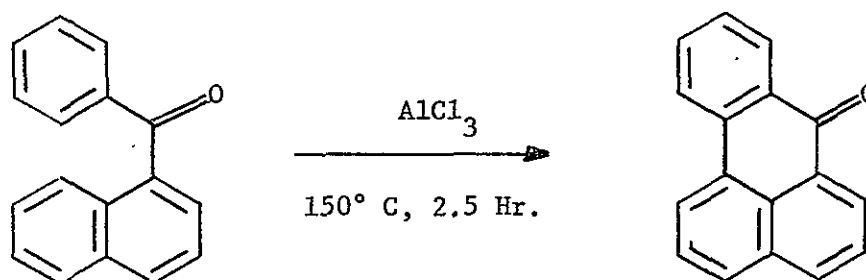
These investigators applied analogous procedures for the intermolecular ring closure of a miscellany of polynuclear ketones. However, fluorene could not be prepared by heating benzophenone with aluminum chloride. Polynuclear hydrogen is obviously more readily set free than is benzenoid hydrogen[43].

Since the Scholl reaction is one of dehydrogenation, the use of an oxidateve mixture of fused salts, or of an oxidizing agent together with aluminum chloride, has been found effective in accelerating condensation. The aroyl hydrocarbons used in these syntheses are ordinarily prepared by reaction of an aroyl chloride with the appropriate aromatic compound in the presence of $AlCl_3$. When reaction is effected in an $AlCl_3$,NaCl melt, ring closure may occur during the preparation of the ketone. Dibenzopyrenequinone and its derivatives are thus secured from α-aroylnaphthalenes and aroyl chlorides[44]. Polynuclear products from mixed diketones can also be formed by oxidative ring closure[45]. Thus, methylpyranthrone is formed by adding benzoyl-pyrene and p-toluyl chloride to an $AlCl_3$,NaCl melt at 110-120°C, raising the temperature quickly to 165°C, and passing in oxygen until the reaction is complete, the fused mass becoming blue. The reaction probably occurs according to the following scheme:
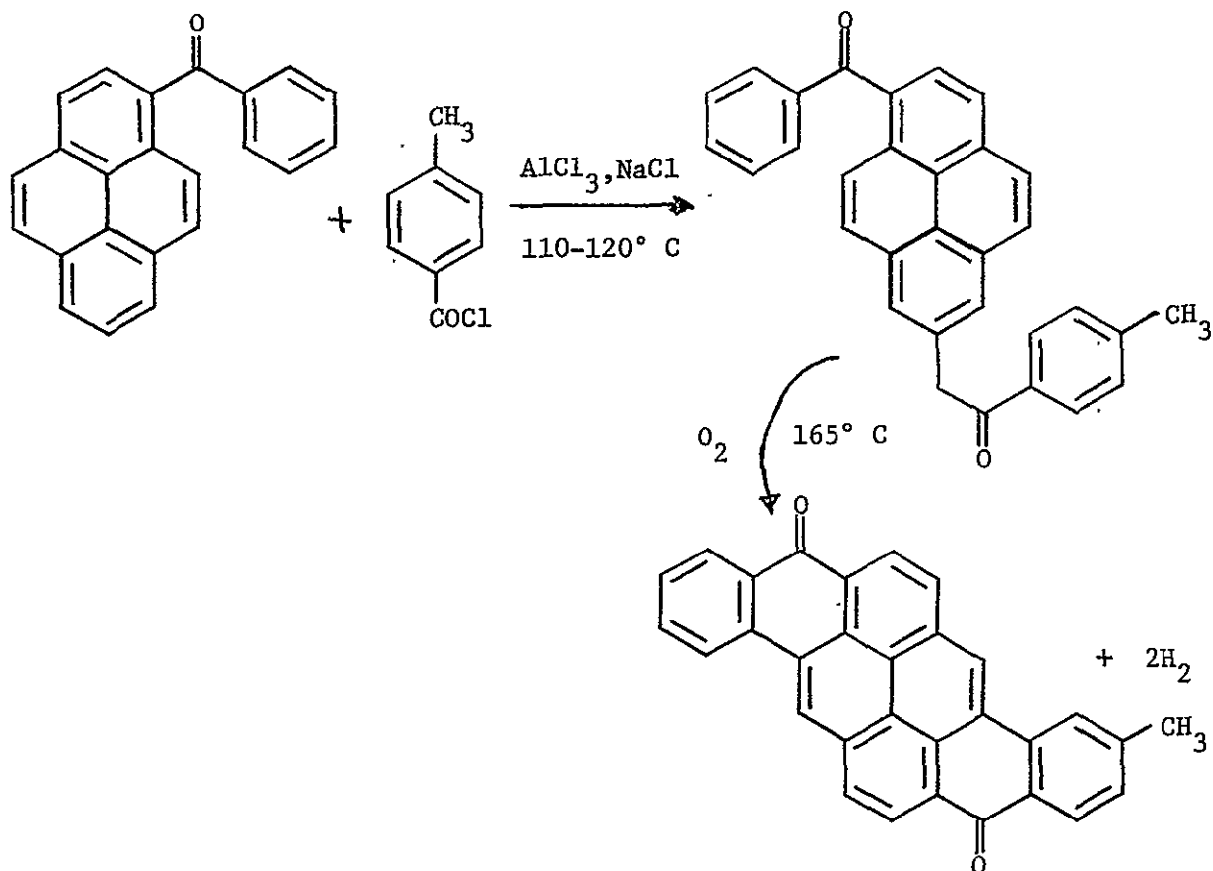
Other examples of ring closures of polynuclear ketones are summarized by Thomas[46].

Several other examples of the Scholl type reaction are illustrated below:

(Ref. 47)

$$\text{AlCl}_3, \quad 140°\text{C, 1.5 Hr.} \longrightarrow \quad + \text{H}_2 \quad \text{(Ref. 48)}$$

$$\text{AlCl}_3 \longrightarrow \quad + \text{H}_2 \quad \text{(Ref. 49)}$$
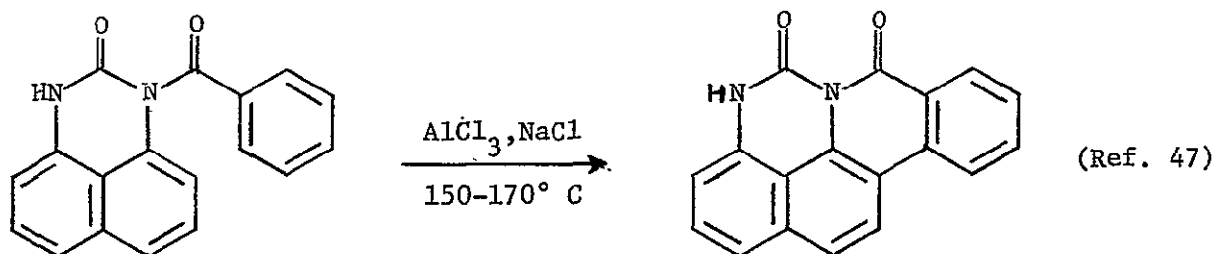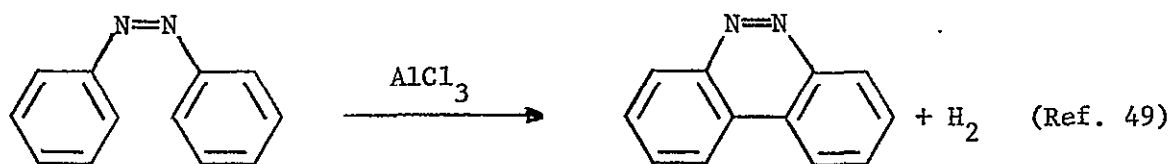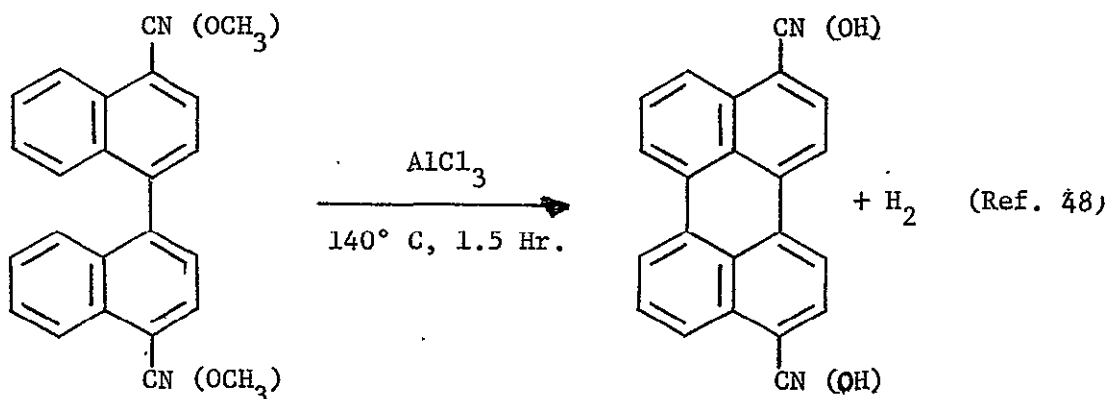
The by-product of the Scholl reaction is hydrogen gas. The fate of the hydrogen evolved is of interest. Various examples of reduction of compounds containing hydrogen acceptors confirm the evolution of hydrogen. When phenyl-1-naphthylphthalide is heated with 4 parts of AlCl$_3$ at 130-160°C, conversion to 1,2,3,4-dibenzopyrene occurs[50].

A similar dehydrogenation and reduction was shown in the conversion of meso-diphenyldihydroxy-dihydro-1,2-benzanthracene to 5-phenyl-1,2,3,4-dibenzopyrene. Condensation of 1,1'-binaphthyl-3,4,3',4'-tetraquinone yields 2,11-dihydroxyperylene-3,10-quinone[51].

$$\text{AlCl}_3 \longrightarrow$$
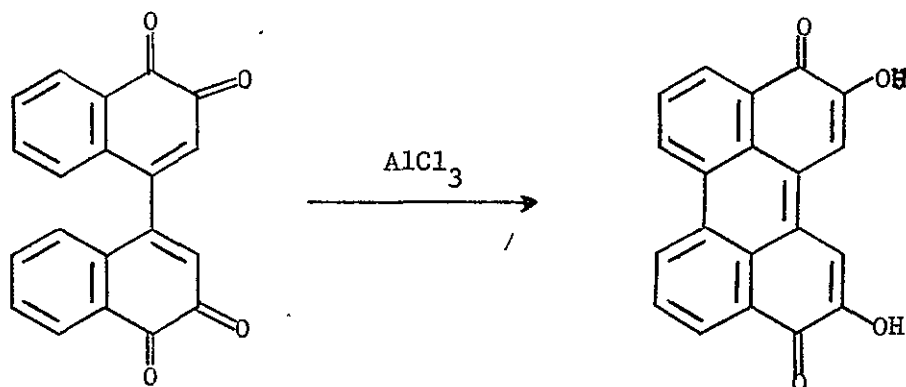
Here the fate of the hydrogen which is evolved is seen in the production of the hydroxy-derivative.

One further comment regarding the Scholl reaction is worthy. We have seen above that for the rearrangement and isomerization reactions studied by Baddeley[35] HCl was necessary as a catalyst for the reaction to proceed. This author also claims that HCl is necessary in the Scholl reaction. For example, 1-benzoyl-naphthalene is converted in 70% yield into benzanthrone by fusion with more than two molecular proportions of aluminum chloride at each 125°C in the presence of hydrogen chloride; however, the reaction did not occur when dry oxygen or nitrogen was passed through the molten mixture. Addition of sodium chloride and consequent formation of $NaAlCl_4$ did not promote the reaction. These observations indicate that the presence of HCl is essential for the occurence of the Scholl reaction, and also that a stream of dry nitrogen or oxygen can effectively remove hydrogen chloride from liquid mixtures containing $AlCl_3$.

D. Miscellaneous Reactions

Although the following reactions are included under the general heading of miscellaneous reactions, they are of some importance. We have classified them as dehydration, exchange, and reduction-chlorination reactions where possible.

(i) Dehydration reactions

One of the simplest dehydration reactions which has been

observed is the formation of benzonitrile in 84% yield from
benzamide[52]:
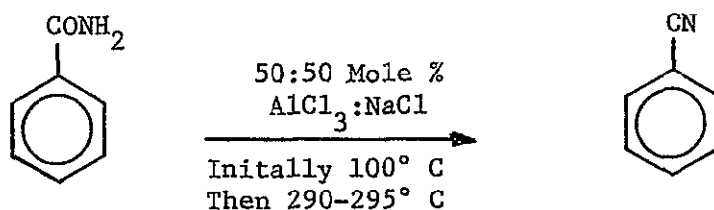
The reaction is carried out by initially heating the amide
at approximately 100°C with preformed sodium tetrachloro-
aluminate, then raising the temperature to 290-295°C where-
upon the product usually distills out. Similar treatment
of ammonium benzoate, using two molecular equivalents of
$AlCl_3$, gives a 50% yield of benzonitrile. The reaction
has also been applied to chloro- and nitro-derivatives of
benzamide and to 1- or 2-naphthamide.

Recently an interesting dehydration reaction involving
ring closure has been observed by Arient and Slavik[53].
When 1-arylamino-anthraquinones are heated in a 64:36 mole %
$AlCl_3$:NaCl melt at 150-160°C for 15 minutes ceramidonines,
III, are obtained and in some cases small amounts of
1,2-phthaloylcarbazol derivates:
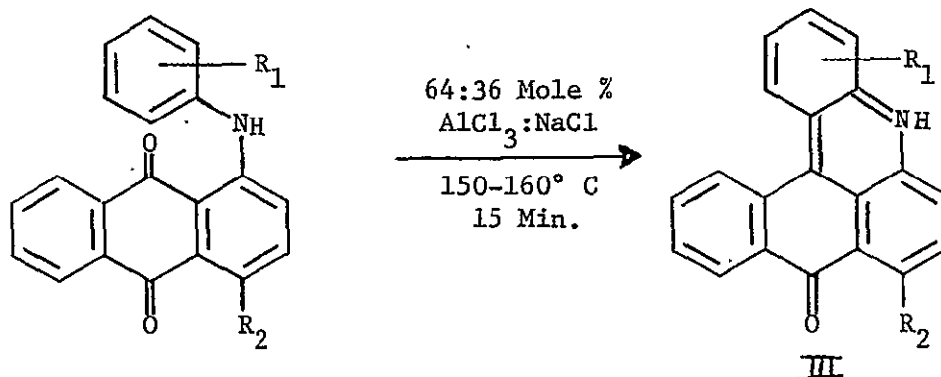
A similar reaction to that above was found when 2,2'-di-
phthalimidobiphenyl was heated in an $AlCl_3$,NaCl melt at
160-250°C for 10 hours to yield flavanthrene[54]:
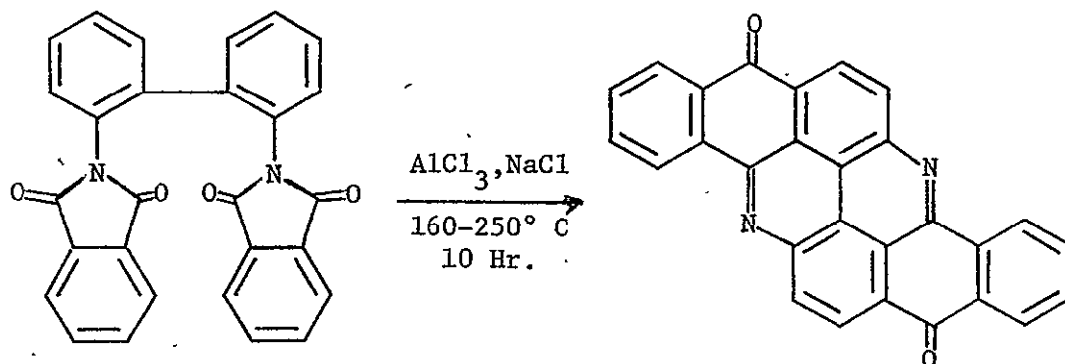
(ii) Exchange reactions

Several interesting exchange reactions have been ob-
served in $AlCl_3$ solvent systems. A very useful example is
the preparation of chlorosilanes. When a 1:1 mixture of
silane and hydrogen chloride is led into either an
$AlCl_3$:NaCl or $AlCl_3$:LiCl melt at 120°C, 80% of monochloro-
silane is obtained together with other chlorosilanes[55]:

$$SiH_4 + HCl \xrightarrow[120°C]{AlCl_3:NaCl} H_3SiCl + H_2$$
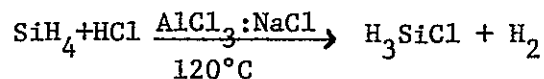
To avoid evolution of hydrogen from the valuable Si-H compounds,
the commutation under otherwise identical conditions is preferable:

$$SiH_4 + SiCl_4 \xrightarrow[120°C]{AlCl_3:NaCl} 2\ H_2SiCl_2$$
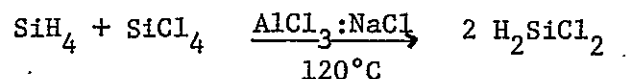
Alkylated silanes can also be prepared in this way using the

same type melts. This provides a simple and extremely

favorable method of preparing dimethylchlorosilane, which

is used for the synthesis of α,ω-hydridopolysiloxanes[56]:

$$(CH_3)_2 \, SiH_2 \; + \; (CH_3)_2 SiCl_2 \longrightarrow \; 2(CH_3)_2 SiHCl$$
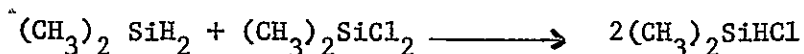
Recently, a new method has been developed for the preparation

of methyl metal compounds from methyl chloride and the chlorides of

boron, aluminum, silicon, tin, phosphorus, antimony, and mercury in

$AlCl_3$ solvent systems[57]. Metals are suspended in the melts to

act as halogen acceptors. The reaction is illustrated for tetramethyl-

silane:

$$3 \; SiCl_4 \; + \; 12 \; CH_3Cl \; + \; 8 \; Al \; \xrightarrow[180°C]{AlCl_3, NaCl} \; 3(CH_3)_4 Si \; + \; 8 \; AlCl_3$$
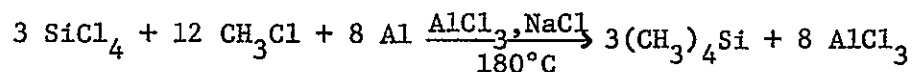
The difference between this reaction and the usual Wurtz synthesis

is that the acceptor metal is not an alkali metal, and that the metal

halide formed is soluble in the melt. Thus a free metal surface is

always available until the metal has been completely consumed. Moreover,

if the system is chosen correctly, more solvent (in the above case,

$AlCl_3$) is formed in the course of the reaction. Another important ad-

vantage is that the acceptor metal halide can be reconverted into the

acceptor metal (Al) and the halogen (Cl_2) by electrolysis of the melt.

The recovered chlorine can be used either for preparation of fresh silicon tetrachloride or for the oxychlorination of methane.

Another interesting exchange reaction which has been observed is the selective substitution of α-fluorine atoms by chlorine in perfluoro ethers. When, for example, perfluoro-2-methyl-tetrahydrofuran is heated with $AlCl_3$ at 180°C for 14 hours α,α,α'-trichloroperfluoro-2-methyltetrahydrofuran[58]:

$$\text{(ring structure)} \xrightarrow[\text{180° C, 14 Hr.}]{AlCl_3} \text{(chlorinated ring structure)}$$
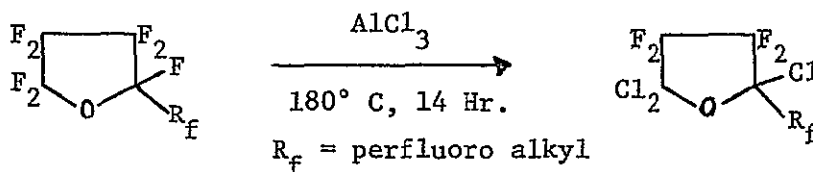
R_f = perfluoro alkyl

Several other perfluorotetrahydrofurans and tetrahydropyrans bearing a single perfluoroalkyl substituent in the α-position also undergo the above reaction. However, in the absence of an α-perfluoroalkyl substituent perfluoro ethers undergo cleavages as illustrated:

$$R_fCF_2OCF_2R_f \xrightarrow[\text{175° C, 16 Hr.}]{AlCl_3} (R_fCCl_2OCCl_2R_f) \longrightarrow R_fCOCl + R_fCCl_3$$

$$\text{(ring structure)} \xrightarrow[\substack{\text{175° C} \\ \text{13 Hr.}}]{AlCl_3} \left(\text{(ring structure)} \right) \longrightarrow Cl_3C(CF_2)_2COCl$$
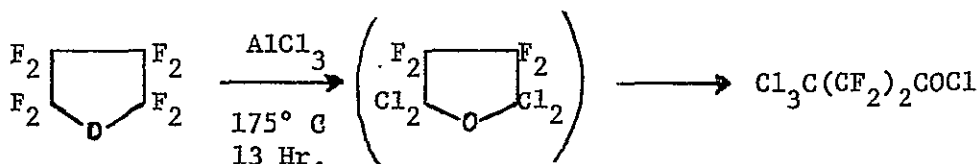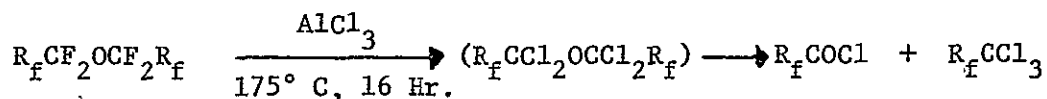
It is interesting to note that when α-alkyl substituted perfluoro ethers were heated at 230° for 15 hours in a 50:50 mole % $AlCl_3$:NaCl melt no reaction was observed. The authors attribute this observation to the speculated lower Lewis acidity of the binary system.

We see that simultaneous reduction of the nitro compound and

nuclear chlorination has occurred, the necessary hydrogen atoms

being supplied by the starting material itself. A similar reaction

occurs with the 3-nitrophenyl isomer.

A similar reaction has been observed by Russian workers[61].

When either m-dinitrobenzene or 2,4-dinitrochlorobenzene were

heated in a 72:28 mole % $AlCl_3$:NaCl melt at 125-150°C and treated

with a reducing agent such as stannous chloride and hydrogen

chloride for 3-4 hours, 2,4,6-dichloro-1,3-diaminobenzene resulted:
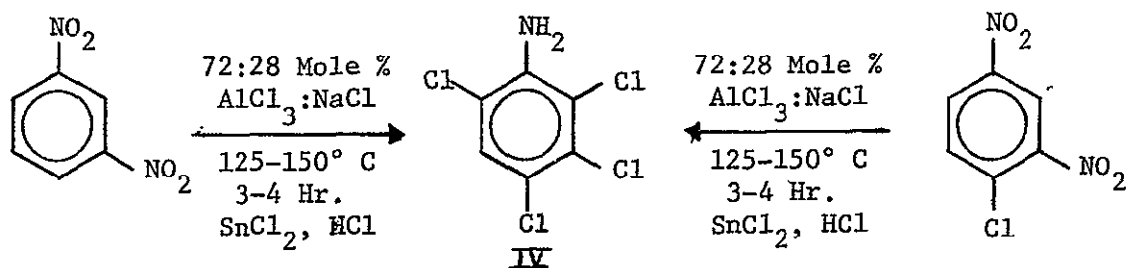
When m-dinitrobenzene and 1,5-benzoylnaphthalene are treated in the

same manner, one obtains IV and 3,4,8,9-dibenzpyrene-5,10-quinone.

In this, the hydrogen necessary for the reduction of the nitro

compound no doubt is supplied by the naphthalene derivative when

it simultaneously undergoes the Scholl reaction. One final point

to be noted is that the above nitro compounds themselves are

recovered unchanged on simple heating in an $AlCl_3$:NaCl melt.

Nuclear chlorination of unsubstituted aromatic compounds has also been found to occur in $AlCl_3$:NaCl melts. When a mixture of benzene and chlorine are passed into a 61:39 mole % $AlCl_3$:NaCl melt at 200°C, mono-, di-, tri-, and tetra-chloro benzenes are obtained[62].

Aliphatic chlorinations have also been carried out in $AlCl_3$ solvent systems. For example, 1,1,2-trichloroethane is prepared in 64% yield by passing chlorine and ethylene chloride, in the ratio of between 0.55 to 0.75 parts by weight of chlorine per part of ethylene chloride, through a 50:50 mole % $AlCl_3$:KCl melt at 350°C.[63]

E. Other $AlCl_3$ Containing Solvent Systems

So far in the above discussion, we have concerned ourselves with $AlCl_3$ solvent systems which consisted only of fused $AlCl_3$ or eutetics of $AlCl_3$ plus an alkali metal chloride. A number of other $AlCl_3$ solvent systems exist which contain as their second component an organic compound. These solvent systems have been used as organic reaction media and deserve comment. In one of these systems, the organic component serves also as a reactant.

The solvent system which is most like the ones so far discussed is the fused system aluminum chloride-pyridine. In an early British patent[64] it was suggested that the addition compound of pyridine (Py) with aluminum chloride would be an excellent condensing agent for effecting ring closure of dianthraquinonylamines. This type of reaction

has now been observed. In the earlier cited work of Arient and Slavik[53],

it was found that replacement of the $AlCl_3$:NaCl solvent media by a

67:33 mole %:Py melt the reaction of 1-phenylaminoanthraquinones led

to the formation of 1,2-phthaloylcarbazoles, the byproduct in the

former solvent, in approximately 30% yield.
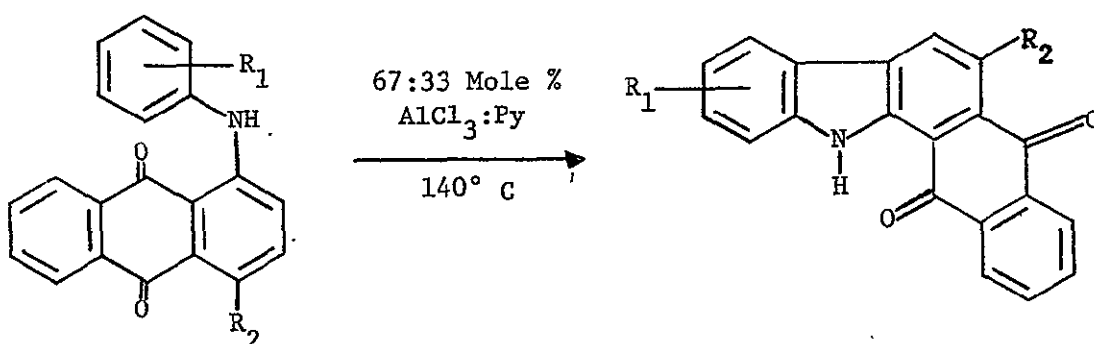
The Scholl reaction has also been carried out in the $AlCl_3$:Py

solvent system. When α-hydroxyanthraquinone is heated at 100–130°C

in an $AlCl_3$,Py melt 1,1'-dihydroxybianthraquinoyl is formed[65]:
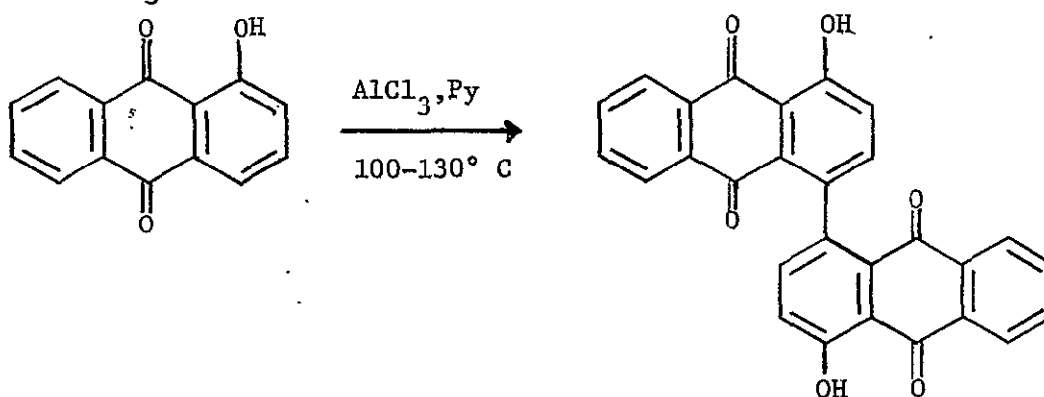
The phase diagram for the fused $AlCl_3$:Py system has recently

been determined by Wick[66].

The solvent system consisting of 66:32 mole % $AlCl_3$:Urea has been used as an organic reaction media[67]. The solvent is formed by adding urea to aluminum chloride under controlled conditions so that the temperature does not rise above 100°C, then the mixture is cooled to 25°C. The reactant is then added and the temperature raised to 70°C. In this manner, many substituted amides can be prepared from the appropriate aromatic
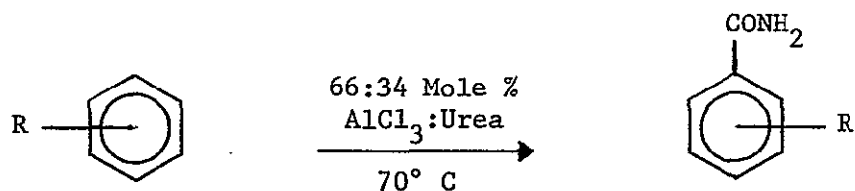
It is to be noted that one of the solvent components is also a reactant. Similar reactions occur[68] when mixtures of $AlCl_3$ and compounds of the general formula XCOX', where X denotes, hydrogen, halogen, alkyl or amino and X' is an amino or O-metal radical, if X is hydrogen, have been used as solvent systems and reactants.

F. Electroorganic Chemistry in $AlCl_3$ Containing Solvent Systems

Although a considerable number of papers have appeared on the electrochemistry of inorganic species in $AlCl_3$ containing solvent systems[69] to our knowledge only two reports on electro-organic chemistry have appeared. Fleischmann and Pletcher[70] have carried out a cyclic voltammetric study on a number of polynuclear hydrocarbons in a melt consisting of 50:36:14 mole % $AlCl_3$:NaCl:KCl at 150°C using a pyrolytic graphite electrode. They found that the large polynuclear hydrocarbons

show a series of electron transfers while the simple hydrocarbons

show a single wave. At sweep rates of 0.1 V/sec., pyrene, anthracene,

and diphenylanthracene gave peaks on the reverse sweep showing the

initial products of the first electron transfer to have some stability,

although it was clear from the peak size that they are not completely

stable. Furthermore, the reverse peaks occurred at a potential

close to that expected if the oxidation was electrochemically

reversible. In no case could evidence be found for the reduction

of the aromatic hydrocarbons. Their results are summarized in Table I.

TABLE I. Aromatic Hydrocarbon Oxidation Potentials in 50:36:14 Mole %
$AlCl_3$:NaCl:KCl (Volts vs Al)[70]

	$E_{p/2}$	Ratio of Wave Heights		$E_{p/2}$	Ratio of Wave Heights
benzene	2.09	–	chrysene	1.34	1
naphthalene	1.57	–		1.78	2
anthracene	1.24	1		2.10	4
	1.72	1	pyrene	1.19	1
	1.90	1		1.79	2
	2.30	2		2.03	4
phenanthrene	1.43	1	diphenyl-	1.25	1
	1.84	1	anthra-cene	1.75	2
chlorobenzene	2.48	–		2.20	4
			biphenyl	1.66	1
				2.03	1

The other known report on electro-organic chemistry in $AlCl_3$ solvent
systems concerns the electrochemical polymerization at a platinum

electrode of a variety of aromatic compounds[71]. The compounds

to be polymerized are dissolved in a ternary complex of an aromatic

hydrocarbon, a hydrohalogen acid and an aluminum halide with a mole

ratio 1:1:2 respectively, with electrolysis then being initiated.

Among the most interesting products are poly(p-phenylene) which is

formed from benzene and p-sexiphenyl, formed from biphenyl. The

relation between the current density, electrode potential, and

efficiency of formation of these products is very complex.

G. Summary

Let us briefly summarize the findings of the literature survey.

Many different organic reactions are found to proceed in $AlCl_3$ con-

taining solvent systems. Three major types of reactions, namely

condensation-addition, rearrangement and isomerization and dehydro-

genation-addition reactions have been studied extensively. Other

types of reactions which have been found to occur in these solvents

are dehydration, exchange and reduction-chlorination reactions.

$AlCl_3$ solvent systems having an organic compound as one of their com-

ponents have been studied. Only two reports have appeared on the

electrochemical behavior of organic compounds in $AlCl_3$ solvent systems.

Under the general category of condensation-addition reactions,

mono- and dibasic carboxylic acids, acid anhydrides and lactones were

found to react with a variety of aromatic and heterocyclic compounds,

most of which are activated by hydroxyl, amino and/or alkyl substituents.

The reactions are carried out in the temperature range of 100-220°C

with reaction times ranging from 2 minutes to hours. In the case of monobasic acids only keto products are obtained. With dibasic acids and acid anhydrides keto-acids are the initial products; however, if the reaction conditions are severe enough, ring closure of the keto-acid occurs yielding quinones. Lactones give rise to ring closed ketones. Intramolecular ring closure has been found in the case of aryl substituted aliphatic acid. In some cases, isomerization was observed to play an important role.

Numerous molecular rearrangements and isomerizations are found to occur in $AlCl_3$ solvent systems. In a few cases these reactions allow the synthesis of compounds which cannot be prepared by any other method. Of the rearrangements which have been studied, the Fries rearrangement is the most common. Phenolic esters and arylsulfonates undergo rearrangement to the respective hydroxy ketones and sulfones. Isomerization of alkyl groups is found to occur in some cases. β-Aroyl-acrylic acids and aryl vinyl ketones are found to rearrange to ring closed ketones, the acid function remaining in tact in the former case. Heterocyclic compounds such as chromanones and coumarins also rearrange to cyclic aromatic ketones. A thorough study was carried out by Baddeley and his co-workers on the isomerizations which take place in aromatic ketones and sulfones and in alkylated phenols and benzenes. The migration of an alkyl and/or acyl or sulfonyl group depends mainly on the relative rates of deacylation or desulfonation followed by re-acylation or resulfonation respectively and (ii) intermolecular migration of the o-alkyl group to the adjacent meta-position. Sufficient $AlCl_3$

together with some HCl is necessary for the reaction to occur.
Steric factors were also found to be of importance.

Dehydrogenation-addition reactions which are generally known
as the Scholl reaction have mainly been carried out with two classes
of organic compounds - unsubstituted and substituted polynuclear
hydrocarbons and diaryl ketones. Both intra- and intermolecular
reactions have been observed. Hydrogen chloride is claimed to be
needed as a catalyst for the reaction. The by-product of these
reactions is assumed to be hydrogen gas and the fate of this material
has been considered. In a few cases, reducible groups within the
starting materials have been found to be reduced during the course
of the reaction and this was offered as evidence for the existence
and fate of the hydrogen gas.

Several other types of organic reactions have been observed in
$AlCl_3$ solvent systems. Dehydration reactions have been carried out,
one example being the formation of benzonitriles from benzamides.
The ring closure dehydration of 1-arylamino-anthraquinones to cer-
amidonines has been extensively studied.

Exchange reactions involving a variety of starting materials have
been reported. Of technical importance are the exchange reaction
of the hydrogens attached to silicon for chlorines and the exchange
reaction forming methylmetal compounds from methyl chloride and the
chlorides of the metal. Chlorine has also been found to exchange with
fluorine in $AlCl_3$ solvent systems.

One final reaction of interest which has been reported to occur
in $AlCl_3$ solvent systems is the one involving aromatic nitro compounds.
In two instances, it has been reported that nitro-substituted aromatics

undergo simultaneous reduction of the nitro group and chlorination of the aromatic nucleus. The hydrogen necessary for the reduction probably comes from hydrogen chloride which is either added to the reaction mixture or formed during the course of the reaction.

$AlCl_3$ solvent systems having as one of their components an organic compound have been used as organic reaction media. In the fused $AlCl_3$-pyridine system reactions similar to those which occur in $AlCl_3$ solvent systems have been found. Reactions have also been reported to occur in which the organic component also acts as a reactant, e.g., the formation of benzamide from benzene in an $AlCl_3$:urea melt.

Only two reports on the electrochemical behavior of organic compounds in $AlCl_3$ solvent systems have appeared. In one case, the electro-oxida-.tion of polynuclear hydrocarbons was briefly studied. While in the second case the electro-initiated polymerization of several aromatic compounds was reported.

If one is to draw any conclusion from this literature survey, it certainly must be the observation that considering the known reactivity and catalytic behavior of $AlCl_3$, many different organic compounds are stable in $AlCl_3$ solvent systems. In particular, the stability of aromatic hydroxy and amino compounds in comparison to aromatic nitro compounds. The many rearrangements and isomerizations that occur together with the Scholl reaction emphasizes the need for caution when attempting to carry out physical chemical studies in $AlCl_3$ solvent systems. The need for catalytic amounts of hydrogen chloride for

many of these reactions to proceed is worthy of further study.

The possibility of bubbling dry oxygen through an $AlCl_3$:NaCl melt

is hard to believe as one can readily calculate the favourable heat

of formation of aluminum oxide. Finally, it would appear that many

of the reactions discussed could be subjected to an electrochemical

study both synthetically and mechanistically.

REFERENCES

(Section I)

(1) Cromwell, T.I. and Hillery, P., J. Org. Chem., 30, 1339 (1965).

(2) Sundermeyer, W., Angew. Chem. Internal. Edit., 4, 222 (1965).

(3) Gordon, J. E., Tech. Methods Org. Organometal Chem., 1, 51 (1969).

(4) Komagorov, A.M., Baeva, I.K. and Koptyug, V.A., Izu. Sibirsk. Otd. Akad. Nauk SSSR, Ser. Khim. Nauk, 147 (1966).

(5) Sundermeyer, W. and Glemser, O., Angew. Chem., 70 629 (1958); Glemser, O. and Kleine-Weischede, K., Ann., 659, 17 (1962).

(6) Waldman, H. and Sellner, P., J. Prakt. Chem., 150, 145 (1938).

(7) Raudnitz, H., Ber., 62, 509 (1929).

(8) German Pat. No. 660,220; c.f. C.A., 32, 6257.

(9) Kranzlein, P., Ber., 71 2328 (1938).

(10) Steinkopf, W., Barlag, T., and V. Petersdorff, H. J., Ann., 540, 7 (1939).

(11) Phillip, M., J. Am. Chem. Soc., 48, 3198 (1926); c.f. Dougherty, G. and Gleason, A. H., ibid., 52, 1024 (1930).

(12) Waldmann, H. and Mathiowetz, H., J. Prakt. Chem., 126, 250 (1930).

(13) Mayer, F. and Stark, O., Ber., 64, 2003 (1931).

(14) Mayer, F., Stark, O. and Schön, K., ibid., 65, 1333 (1932).

(15) Waldmann, H. and Mathiowetz, H., ibid., 64, 1713 (1931).

(16) Waldmann, H., J. prakt. Chem., 127, 195 (1930); ibid., 131, 71 (1931).

(17) Mayer, F., Mombour, A., Lassman, W., Werner, W., Landmann, P. and Schneider, E., Ann., 488, 259 (1931).

(18) British Pat. No. 261,383; c.f. Brit.Chem. Abs.-B, 635 (1928).

(19) Zahn, K. and Ochwat, P., Ann.; <u>462</u>, 72 (1928).

(20) Kuroda, C. and Wada, M., Proc. Imp. Acad. Tokyo; <u>12</u>, 239 (1936).

(21) Brockmann, H. and Müller, K. Ann. <u>540</u>, 51 (1939).

(22) Kuroda, C. and Wada, M., Sci. Papers Inst. Phys. Chem. Res., <u>34</u> 1740 (1938).

(23) Bruce, D.B., Sorrie, A.J.S. and Thomson, R.H., J. Chem. Soc., 2403, (1953).

(24) Fieser, L.F., Organic Synthesis, <u>20</u>, 1 (1940).

(25) Baddeley, G., Holt, G., and Makar, S. M., J. Chem. Soc., 2415 (1952)

(26) Ibid., 3289 (1952).

(27) Auwers, K., Ann., <u>460</u>, 254 (1928).

(28) Baddeley, G., J. Chem. Soc. 273 (1943).

(29) Aleykutty, A.A. and Baliah, V., J. Indian Chem. Soc., <u>31</u>, 513 (1954).

(30) Loudon, J. D. and Razdan, R. K., ibid., 4299 (1954).

(31) Cook, J. W., Loudon, J.D. and McCloskey, ibid., 3904 (1952).

(32) British Pat. No. 305,593; c.f., Brit. Chem. Abs. -B, 603 (1930).

(33) U.S. Pat. No. 2,342,073.

(34) U.S. Pat. No. 2,439,301.

(35) Baddeley, G., J. Chem. Soc., 527, (1943); ibid., 232 (1944); ibid., 994 (1950); Baddeley, G. and Pendleton, A.G., ibid, 807 (1952); Baddeley, G., Holt, G., Makar, S.M., and Ivinson, M.G., ibid.,3605 (1952); Baddeley, G., Holt, G., and Pickles, W., ibid., 4162 (1952).

(36) Holt, G. and Pagdin, B. ibid., 4514 (1961).

(37) Scholl, R., Seer, C., and Weitzenbock, R., Ber., <u>43</u>, 2202 (1910).

(38) French Pat. No. 795,447; cf.C.A., <u>30</u>, 5595.

(39) Scholl, R., Seer, C. and Weitzenbock, R., Ber., <u>43</u>, 2202 (1910).

(40) Reinlinger, H. and Overstraeter, A., Ber., <u>91</u>, 2151 (1958).

(41) Zinke, A. and Zeigler, E., ibid.; 74, 115 (1941).

(42) Scholl, R. and Seer, C., Monatsh.; 33, 1 (1912).

(43) Scholl, R. and Seer, C., Ann., 394, 111 (1921).

(44) German Pat. No. 483,229.

(45) Scholl, R., Meyer, K. and Donat, J., Ber.,70, 2180 (1937).

(46) Thomas, C. A., "Anhydrous Aluminum Chloride," ACS Monograph No. 87, Reinhold Publishing Corp., New York, N.Y., 1941, pp 653-655.

(47) U.S. Pat. No. 1,749,795; c.f. Brit. Chem., Abs. -B,809 (1930).

(48) Weitzenbock, R. and Seer, C., Ber., 46, 1994 (1913).

(49) German Pat. No. 513,206.

(50) Padowa, R., Ann. chim. phys., 19, 353 (1910).

(51) German Pat. No. 412,120.

(52) Norris, J.F. and Klemka, J., J. Am. Chem. Soc., 62, 1432 (1940).

(53) Arient, J. and Slavik, V., Collection Czechoslov. Chem. Comm., 34, 3576 (1969).

(54) Krepelka, V. and Stefee, R. ibid., 9,29 (1937).

(55) Sundermeyer, W. and Glemser, O., Angew. Chem., 70,628 (1958).

(56) Sundermeyer, W., Lecture, IUPAC Congress, London, September, 1963.

(57) Sundermeyer, W. and Verbeek, W., Angew. Chem. Internat. Edit.,5, 1 (1966).

(58) Tiers, G. V.D., J. Am. Chem. Soc.,77, 4837 (1965).

(59) Tiers, G.V.D., ibid., 77, 6703, 6704 (1955).

(60) Kobrina, L.S.; Furin, G.G. and Yakobson, G.G., Izv. Sib. Otd. Akad. Nauk SSSR, Ser. Khem. Nauk, 98 (1968).

(61) Dokunikhin, N.C. and Sergeeva, M.M., Doklady Akad. Nauk SSSR, 88 987 (1953).

(62) Glemser, O. and Cleine-Weischede, K., Ann., 659, 17 (1962).

(63) U.S. Patent No. 2,140,549.

(64) British Pat. No. 297,133; c.f. Brit. Chem. Abs.-B, 949 (1928).

(65) British Pat. No. 310,353; c.f. Brit. Chem. Abs.-B, 637 (1929).

(66) Wick, A.K., Helv. Chim. Acta, 51, 85 (1968).

(67) Wiley, J.C., Jr. and Linn, C. B., J. Org. Chem., 35, 2104 (1970).

(68) German Pat. No. 878,467; c.f., C.A., 55, 16940.

(69) Hames, D.A. and Plambeck, J.A., Can. J. Chem., 46, 1727 (1968);
Anders, U. and Plambeck, J.A., ibid., 47, 3055 (1969).

(70) Fleischmann, M. and Pletcher, D., J. Electroanal. Chem., 25, 449
(1970).

(71) Wisdom, N.E., Abstracts, 135th. Meeting, The Electrochemical
Society, New York, May 1969, Abs. No. 138.

II

ACID-BASE EQUILIBRIUM IN NaAlCl$_4$ MELTS

AND EXPERIMENTAL WORK

A. Chemical Equilibrium

The NaAlCl$_4$ melt can be considered as an acid-base system in which

an acid is defined as an acceptor of a chloride ion. Similarly a base

is defined as a chloride ion donor.

$$2AlCl_4^- = Al_2Cl_7^- + Cl^- \qquad (1)$$
$$\text{base} \qquad\quad \text{acid}$$

The electrode reaction at an aluminum electrode in this melt can be

written as

$$AlCl_4^- + 3e = Al\downarrow + 4Cl^- \qquad (2)$$

and the electrode potential is given by

$$E = E^\circ - \frac{RT}{3F} \ell n \frac{[Cl^-]^4}{[AlCl_4^-]} \qquad (3)$$

Several other electrode reactions can be written for this electrode.

The internal thermodynamic equilibria which must be satisfied at all

times will reduce all of these Nernst equations to equation 3 by the

inclusion of the appropriate equilibrium constants in the E°. For a

large portion of the AlCl$_3$ concentration range the AlCl$_4^-$ concentration

will remain constant and the aluminum electrode becomes an acid-base

indicating electrode.

Two separate groups of workers [1, 2] used AlCl$_3$ to titrate an

NaAlCl$_4$ melt saturated with sodium chloride. The object of their work

was to determine the equilibrium constant for the dissociation

$$2AlCl_4^- = Cl^- + Al_2Cl_7^- \qquad K_M \qquad (4)$$

The electrochemical cell used to make the potentiometric measurements was

$$Al/AlCl_3, \; NaCl_{saturated} \; // \; AlCl_3, \; NaCl_I/Al \qquad (5)$$
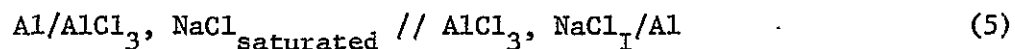
and the cell potential is given by

$$\Delta E = \frac{4RT}{3F} \ln \frac{[Cl^-_{sat}]}{[Cl^-_I]} \qquad (6)$$

since the ratio between the two $AlCl_4^-$ concentrations is near unity. At higher $AlCl_3$ mole percentages this approximation is no longer justified.

The first assumption made in their calculations was that any $AlCl_3$ added to the system reacted <u>completely</u> by one of the following reactions:

$$(1) \quad AlCl_3 + Cl^- \rightarrow AlCl_4^- \qquad \text{(in basic melts)} \qquad (7)$$

or

$$(2) \quad AlCl_3 + AlCl_4^- \rightarrow Al_2Cl_7^- \qquad \text{(in acidic melts)} \qquad (8)$$

The titration produced the typical S-shaped acid-base titration curve. At the inflection point of the curve the melt is neutral and from equation 4 the following can be stated:

$$[Cl^-]_{eq.} = [Al_2Cl_7^-]_{eq.} = K_M^{\frac{1}{2}} \qquad (9)$$

At 175° C., ΔE was about 180 mv for cell (1) and the amount of $AlCl_3$ added was supposedly equal to the amount of excess chloride ion in the saturated melt.

$$X_{AlCl_3} = [Cl^-]_{sat.} - [Cl^-]_{eq.} \qquad (10)$$

Therefore,

$$\Delta E = \frac{4RT}{3F} \ln \frac{X + [Cl^-]_{eq.}}{[Cl^-]_{eq.}} \qquad (11)$$

and the $[Cl^-]_{eq.}$ and K_M can be easily calculated. Torsi and Mamantov[1] attempted to fit their data at higher $AlCl_3$ concentrations using K_M and found that the deviations at compositions beyond 55 mole percent $AlCl_3$ indicated that the above assumptions are not justified. The potential between an aluminum half cell containing a 50:50 mole percent $AlCl_3$:NaCl melt and a similar cell containing a 66:34 mole percent $AlCl_3$:NaCl melt at 175° C. was 480 mv. Anders,[2] in a crudely designed cell, measured only about 110 mv for the same cell. King[4] reports a value of 220 mv for the same measurement. The latter two values are suspect due to the inexact experimental conditions under which the measurements were made.

From vapor pressure measurements King and Seemiller[5] have reported on the thermodynamic equilibria for the $NaAlCl_4$ system as follows:

$$Cl^- + AlCl_3 = AlCl_4^- \qquad\qquad K_1 = 6 \times 10^4 \qquad (12)$$

$$AlCl_4^- + AlCl_3 = Al_2Cl_7^- \qquad\qquad K_2 = 2 \times 10^4 \qquad (13)$$

$$2AlCl_3 = Al_2Cl_6 \qquad\qquad K_D = 2 \times 10^6 \qquad (14)$$

$$Al_2Cl_6 + Cl^- = Al_2Cl_7^- \qquad\qquad K_3 = \frac{K_1 K_2}{K_D} = 6 \times 10^2 \qquad (15)$$

$$2AlCl_4^- = Cl^- + Al_2Cl_7^- \qquad\qquad K_4 = \frac{K_2}{K_1} = 0.33 \qquad (16)$$
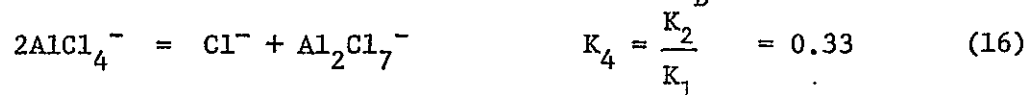
There is a glaring discrepancy between the K values obtained for equation 16 by this method ($K_4 = 0.33$) and the K_M value of 7.9×10^{-8} determined by the titration method.[1, 2] The K_4 value of 0.33 is unrealistic since it states a 50:50 mole percent mixture must contain very large portions of free chloride ion and if this were true, the titration of the melt with small amounts of $AlCl_3$ would have a very

small effect on the emf of the cell. King[4] has indicated these values were only preliminary and a revised value for the vapor pressure work would be forthcoming. There are probably several sets of K values which can be fitted to the data by a computer to give a local minimum deviation between the experimental and the calculated points. The equilibrium involving the dimer would explain the deviation between the calculated emfs and the observed values. As the $AlCl_3$ was added, only a small portion would be available to react with the Cl^- or $AlCl_4^-$ while the bulk of the addition would remain as the dimer. It appears that the emf data is reliable but the interpretation is in error, whereas from the vapor pressure measurements only the K_D is reliable. Using this as a starting point, it is proposed that with the aid of analytical techniques on a computer an attempt will be made to fit the emf data to equations 6, 12, 13 and 14. It is hoped that by the inclusion of the various equilibria a reasonable fit can be made over the entire composition range. The existence of the $AlCl_3$, $AlCl_4^-$, $Al_2Cl_7^-$ and Al_2Cl_6 species in the $NaAlCl_4$ melt has been confirmed recently by Raman spectroscopy.[6]

It has been reported that the difference between the E° value for the Ag(I)/Ag couple in the 50:50 and 66:34 mole percent $AlCl_3$:NaCl melts is about 546 mv at 200° C.[7] Combining this fact with the 480 mv[1] for the cell,

$$Al/AlCl_3, NaCl // AlCl_3, NaCl/Al \qquad\qquad (17)$$
$$50:50 \qquad\qquad 66:34$$
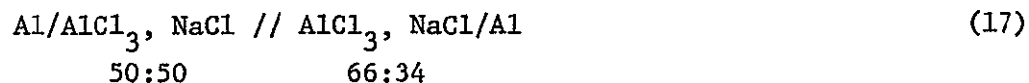
the following emf series can be set up based on the aluminum reference electrode in a 50:50 mixture.

TABLE I

ELECTRODE POTENTIALS IN NaAlCl$_4$ MELTS

Couple	E° (V.)	AlCl$_3$:NaCl
Al(III)/Al	0	50:50
Al(III)/Al	0.480	66:34
Ag(I)/Ag	1.290	66:34
Ag(I)/Ag	1.356	50:50

The 66 mv difference between the two Ag(I)/Ag potentials is insignifi-
cant since the E° for the couple in the 66:34 mole percent melt is an
extrapolated value and the sum of all the errors in the measurements
probably exceeds 66 mv. The significance of the two similar standard
potentials is that Ag(I) is unaffected by the Cl⁻ ion concentration in
the melt and the Ag(I)/Ag couple is a better reference electrode for these
melts than the aluminum electrode. The indifference of Ag(I) to the Cl⁻
concentration indicates that the Cl⁻ ion is more strongly complexed by
AlCl$_3$ than by Ag(I). · This approach can be easily applied to other metals
in these melts to study their chloride complexing ability.

B. Equipment Design and Experimental Procedures

The melt purification procedure reported previously[7] was used to
purify all of the melts. A new experimental cell was designed and sev-
eral new furnaces were built to facilitate the ease and rate at which
new electrode cells could be set up. The new cell (figure 1) consists
of a teflon biscuit (½" x 3") sealed to the top of a glass cell by means
of a tight fitting groove in the teflon. Several holes were drilled in

the teflon top and various sizes of ground joints were press-fitted in
these holes. The typical cell top contained a 6 mm hole for a thermo-
couple well, a 10/18 joint for a counter electrode, a 14/20 joint for
the reference electrode compartment and a 1" hole with an 0-ring groove
around the top for the working electrode compartment.

The normal procedure was to prepare a 100 ml melt in a cell placed
in a furnace containing a window so that the bottom of the cell could be
seen. After purification the 7 mm fine porosity sintered glass fritted
reference electrode compartment was placed into the melt. The aluminum
reference electrode consisted of a spiral of aluminum wire connected to
a short piece of tungsten wire sealed in the glass plug in the top of
the reference compartment. The counter electrode consisted of a large
tungsten wire spiral sealed into a 10/18 glass plug.

A second melt of about 250 ml was prepared in a second furnace.
About 10 ml of this melt was transferred by means of a preheated pipette
to a working electrode compartment in the smaller cell. This electrode
compartment consisted of a 20 mm medium porosity sintered glass frit at
one end, a 1" piece of glass tubing in the middle and a 14/20 ground
joint at the top. A tightly fitting 0-ring around the 1" glass barrel
of the compartment both supported and sealed it to the teflon top. Tef-
lon adapters purchased from Kontes of Illinois were used to seal the
electrodes into the compartment as well as adjust the level of the elec-
trode in the compartment. All of the compartments were adjusted so that
all of the melt levels in the cell were equal. It was necessary to blow
a small hole 2 to 3 inches above the melt level in each of the cell com-
partments to equalize any differences in the vapor pressures above the
various melts.

Small ring furnaces were built to fit around the teflon tops. By maintaining the tops between 175 and 200° C., the build-up of $AlCl_3$ in the cooler portions of the cell was eliminated. This feature will be of utmost importance when measurements are made in the $AlCl_3$ rich melts. Two temperature controllers purchased from ThermoElectric, Model 32422, were used to control the temperatures of the melts to ±0.5° C. It should be pointed out that the original (manufacturer's) controllers left 110 volts connected to the heating coils when it was in the off position. The two controllers have been rewired to eliminate this unsafe feature of the instrument.

It was noticed that in several of the melts a white salt-like precipitate remained in the bottom of the cell after the purification process. A 30 gram NaCl-$AlCl_3$ (Fluka reagent chemicals) sample was weighed out into an all-glass cell, evacuated for 5 minutes and then sealed. The cell was slowly heated to 180° C. and maintained at this temperature for 3 hours. A salt-like precipitate remained in the bottom of the cell (about 2 - 3 grams) and the melt was very dark in color. A small sample of the liquid phase was taken for analysis and then the temperature was increased to 425° C. There was no solid left in the cell at this elevated temperature. After about 1 hour the melt became light amber in color and a dark ring formed on the cooler portions of the glass at the top. Another sample was taken and then the melt was slowly cooled to 250° C. The melt turned cloudy at first and then a white salt-like precipitate settled out in the bottom. A third sample of the liquid was taken, the melt reheated to 425° C. for 48 hours and then cooled once again to 200° C. A much larger precipitate with a chunky appearance formed this time and a fourth sample of the melt was taken.

8-Hydroxy-quinoline in an acetic acid-ammonium acetate buffer was
used to precipitate the aluminum as $Al(C_9H_6NO)_3$. The analysis showed
that all the samples contained the same mole percent of $AlCl_3$ (53.6
±0.1%) regardless of whether there was a solid at the bottom of the
cell or not. These results indicated that the precipitate must have
had a composition of $NaAlCl_4$ and not NaCl as previously suspected. The
potential of the Al reference in the small electrochemical cell never
varied by more than 5 mv from an aluminum electrode immersed in the
melt which had been pipetted from the large bulk melt storage cell.
This provided another piece of evidence in support of the results from
the aluminum analysis. Additional work is required to determine exactly
what is occurring in these melts, even though the presence of this pre-
cipitate doesn't appear to affect any of the electrochemical measurements.

Chemical analysis of the NaCl and $AlCl_3$ found their purity to be
better than 99.5%. The NaCl was further dried at 450° C. under vacuum
for 3 hours before it was transferred to the dry box and weighed out
into the cells. The $AlCl_3$ was stored at all times in the dry box to
prevent any contamination.

Four different electrodes were used in the experimental measurements.
A pyrolite carbon button electrode (area = 0.0985 cm^2) was prepared by
press-fitting a short piece of carbon rod into a piece of ½" teflon rod.
The background current for the carbon electrode in a purified melt using
a linear sweep of 0.5 V/sec. is given in figure 2a. This electrode
proved to be useful for potentials in excess of 1.5 volts vs the aluminum
reference electrode. The tungsten electrodes tended to become fouled
at these excessively anodic potentials.

The background cyclic voltammogram using a platinum button electrode (area = 3.63×10^{-3} cm^2) exhibited a behavior similar to that previously reported;[7] however, at potentials more anodic than +1.3 volts the electrode appeared to be well behaved (figure 2b). Continued cyclic sweeps was observed to cause one peak couple to grow and the other to decrease in height. The sweep rate dictated which couple was going to decrease and which one to increase. As the sweep rate was increased, the growth phenomenon shifted from the couple at 1.1 volts to the one at 0.75 volts. The fact that stirring had no effect on the voltammogram and that none of the other electrode materials exhibited peaks in this region suggested one of two things: (1) the peaks may arise from some surface reaction involving a platinum chloride film, or (2) some impurity is strongly adsorbed and reaction is catalyzed on the platinum surface. Additional work will be required on this electrode before it can be classified as a reliable indicator electrode for the NaAlCl$_4$ melts.

Two tungsten button electrodes (areas = 6.28×10^{-3} cm^2 and 5.08×10^{-3} cm^2) and a tungsten wire electrode (area = 4.07×10^{-2} cm^2) were used for most of the experimental measurements (figures 2c and 2d). The useful potential range of these electrodes was from 0.3 to 1.7 volts. Beyond this range it appeared as if the electrode increased in area resulting in a background current of about 4 to 5 times the magnitude of the original values. No significant changes were observed in the shape of these enhanced voltammograms except for the increase in magnitude by a constant factor. It was noted that the tungsten wire tended to be very splintery due to longitudinal holes in the wire. Attempts will be made to make new tungsten electrodes after the wire has been sputtered to seal up the end of the wire. It is hoped that this procedure will reduce some of the

fouling observed on these electrodes. The background currents using the tungsten button electrode in integral pulse polarography over several potential ranges are given in figure 3.

An attempt will also be made to construct a gold electrode utilizing shrinkable teflon to seal the gold wire into the glass.

C. Preliminary Studies of Hydrogen Chloride Gas in NaAlCl$_4$ Melts

A preliminary experiment has been carried out to study the electroactivity of HCl or H$^+$ ion in the NaAlCl$_4$ melts. Figure 4 shows the voltammogram which was recorded at 175° C on a tungsten button (area = 6.28 x 10^{-3} cm^2) immediately after bubbling dry HCl gas through the melt for 5 minutes. The large nondescript peak at +0.55 volts decayed rapidly with time to give a steady state voltammogram in about 10 minutes (figure 5). The first cyclic sweep produces a trace which is considerably larger than the steady state trace which is reached after about 5 cycles. Stirring the melt had no appreciable effect on the shape or magnitude of the recording.

The rest potential of the tungsten electrode in the HCl system was 1.202 volts vs aluminum which is the same as the corresponding value in the pure melt. No anodic wave could be detected on the reverse sweep using the tungsten electrode. Bubbling nitrogen through the melt for about 5 minutes reduced the peak height by about a factor of 5. This is consistent with the efficiency that has been reported for the removal of HCl from the organic AlCl$_3$ systems. Without knowing the concentration of the active species, it is not possible to relate the peak potential of 950 mv to the E° value. If a nominal value of 200 mv is used for the shift from E° to E$_p$, the estimated E° value of 1.15 volts is in agreement

with the 1.15 volts obtained for HCl in the 66:34 mole percent system.[9]
The absence of the change in E° for HCl when going from the 50:50 to the
66:34 mole percent system can be explained by considering the following
reactions:

$$HCl = Cl^- + H^+ \tag{18}$$

$$(H^+) = \frac{P_{HCl}}{K_H(Cl^-)} \tag{19}$$

$$H^+ + e = \tfrac{1}{2}H_2 \tag{20}$$

$$E = E° + \frac{RT}{F} \ln \frac{(P_{H_2})^{\frac{1}{2}}}{(H^+)} \tag{21}$$

$$E = E° + \frac{RT}{F} \ln \frac{(P_{H_2})^{\frac{1}{2}} K_H}{(P_{HCl})} + \frac{RT}{F} \ln (Cl^-) \tag{22}$$

$$E = E°^* + \frac{RT}{F} \ln (Cl^-) \tag{23}$$

Equation 23 has the same form as the equation for the aluminum elec-
trode reaction except for a unity term versus a 4/3 term. The precision
of the current experiments is not great enough to detect the difference
between 1 and 1.33. If the assumptions above are valid, the chloride
ion dependency of the HCl reduction potential indicates that it is the
dissociated hydrogen ion that is being reduced and not the molecular
hydrogen chloride. The large peak at 0.55 volts may perhaps be attrib-
uted to the reduction of HCl gas and the rapid reduction in peak current
is due to the evolution of the HCl gas in excess of its solubility in
the melt.

In order to observe an oxidation peak for H_2 it is necessary to
maintain a good three-phase contact at the electrode as well as a reason-
ably large solubility product for H_2 in the melt. Most gases are only

sparingly soluble in fused salts at the best of times.

D. Ferric-Ferrous Chloride in NaAlCl₄ Melts

The electrochemistry of iron in the NaAlCl$_4$ melts is of primary importance as it has been argued that the common impurity in the melt is iron,[10] organic materials[11, 12] or dissolved silicon compounds.[13] Three different reductions ($Fe^{+3} \rightarrow Fe^{+2} \rightarrow Fe^{+1} \rightarrow Fe$) and two oxidations ($Fe \rightarrow Fe^{+2} \rightarrow Fe^{+3}$) have been reported for the iron system in the 0.66 AlCl$_3$, 0.14 KCl, 0.20 NaCl ternary melt.[10] According to Giner and Hollek[10] the unpurified melt background exhibits reasonably defined peaks at 1.0 (cathodic peak) and 1.1 (anodic peak) volts vs Al. Two ill-defined peaks at 0.3 and 0.4 volts (cathodic and anodic peaks, respectively) were also recorded. Upon the addition of FeCl$_3$ to the melt, the peaks at 1.0 and 1.1 volts were only marginally increased in magnitude; however, distinct peaks of a major size were created at 0.3 and 0.5 volts. The $Fe^{+3} \rightarrow Fe^{+2}$ reduction was assigned to the 1.0 volt peak, the $Fe^{+2} \rightarrow Fe^{+1}$ reduction to the 0.3 volt peak and the current beyond 0.1 volt was attributed to the $Fe^{+1} \rightarrow Fe$ reduction. Giner and Hollek reported that the reoxidation of $Fe \rightarrow Fe^{+2}$ occurs at 0.5 volts and the $Fe^{+2} \rightarrow Fe^{+3}$ oxidation occurs at 1.1 volts.

The deposition potential of Fe^{+2} in the ternary melt at 156° C. was reported to be 0.55 volts by Yntema et al.[7] They reported that only iron was depostied from 0.55 to 0.35 volts but at 0.13 volts a co-deposit of iron and aluminum was formed. The two reports on the reduction of iron do not seem to be reconcilable; thus it was decided to examine the system in our 50:50 NaAlCl$_4$ melt.

Our investigation has not been completed; the figures given in this report are preliminary and subject to change. All of the data have not been fully analyzed due to the lack of a sufficient quantity of measurements in certain areas, hence some conclusions are speculative. The system has been studied utilizing cyclic voltammetry, integral pulse polarography, chronoamperometry and chronopotentiometry. Once the computer programming and the required electronic construction for double potential step-chronocoulometry[14] has been completed, this technique will be used to study adsorption in the system.

A typical cyclic voltammiogram is given in figure 6 for a $NaAlCl_4$ system at 175° C. after $FeCl_3$ has been added. An attempt was made to anodize a piece of iron wire (0.2 cm^2) in the melt. At currents as low as 0.5 milliamps the iron wire rapidly became polarized and evolved Cl_2 at about 2 volts. A steady current of about 100 µamps could be realized by potentiostating the iron wire at +1.6 volts vs the aluminum reference electrode. The electrochemical results appeared to be independent of the method of addition. The behavior of the double anodic peak at 0.78 and 0.74 volts with increasing sweep rate (figure 7) is characteristic of moderate to strong adsorption of Fe^{+2}.[15] Increasing the sweep rate decreases the amount of Fe^{+2} that is reduced during the cathodic portion of the sweep; consequently, after the adsorption layer has been filled (at 0.74 volts) there is a decreasing amount left to form the iron to free ferrous ion peak. Increasing the sweep rate from 0.125 V/sec. to 0.5 V/sec. caused the two relative peak heights to be reversed.

Repeated scanning between 0.63 and 0.3 volts has the effect of showing how increasing the Fe^{+2} concentration affects the voltammogram

(figure 8). The rapid switching back to the cathodic scan just after the iron metal has been stripped from the electrode causes a local concentrating effect. Both the cathodic and anodic peaks exhibit an increase in magnitude with preference given to the more anodic peak of each doublet. This feature also confirms the presence of adsorption of the ferrous ion.[15] Figure 9 illustrates the effect of sweep rate on the Fe^{+3}/Fe^{+2} couple at 1.53 volts. The gradual increase in $i/v^{\frac{1}{2}}$ with sweep rate is indicative of weak adsorption of Fe^{+2} while the dramatic increase in the anodic peak current is the result of a local concentrating effect produced by the stripping of the iron metal from the electrode.

The dependency of peak heights on the adsorption makes the correlation of peak current with concentration almost useless for all the peaks save the Fe^{+3} to Fe^{+2} reduction at 1.48 volts (figure 10). The peak separation of 100 mv is slightly greater than the 84 mv for a completely reversible couple at 175° C. This increase in peak separation may be due to some irreversibility in the system or distortion of the anodic peak by the adsorption to more anodic potentials.[15] The $E_{\frac{1}{2}}$ for the ferric-ferrous couple by cyclic voltammetry is 1.53 volts and the $E_{\frac{1}{2}}$ for the reduction of ferrous to iron metal is 0.65 volts.

The equilibrium potential of an iron wire immersed in the $NaAlCl_4$ melt containing $FeCl_3$ was about .0.74 volts vs Al and the potential exhibited very little response to the $FeCl_3$ concentration. The equilibrium potential of a tungsten electrode was 1.53 volts at low ferric chloride concentrations (3.70 millimolar) and 1.62 volts in a 14.0 millimolar solution. Due to the uncertainty in the ferrous ion concentration, it was not possible to calculate the E° potential from this

data. These numbers are in agreement with the $E_{\frac{1}{2}}$'s determined from the cyclic voltammetry.

The substantial potential difference the Fe^{+3}/Fe^{+2} couple and the Fe^{+2}/Fe couple means that thermodynamically the ferric ion and iron wire will react spontaneously to form the ferrous ion. The partial passivation of the iron wire during its oxidation to the ferrous ion suggests there is a kinetically controlled step in the process. The Fe^{+3}/Fe reaction is thermodynamically feasible; however, the kinetics of the half reaction may prevent the formation of any substantial amount of ferrous ion in the melt. Chemical analysis for the total iron content in the $NaAlCl_4$ melts will tell us how much ferrous ion is produced by this reaction.

TABLE 2

PULSE POLAROGRAPHY IN A $NaAlCl_4$ MELT AT 175° C.

[FeCl$_3$] millimolar	$Fe^{+3} \rightarrow Fe^{+2}$		$Fe^{+2} \rightarrow Fe^{+3}$		$Fe^{+2} \rightarrow Fe$	
	i_d (μA)	$E_{\frac{1}{2}}$ (V)	i_d (μA)	$E_{\frac{1}{2}}$ (V)	i_d (μA)	$E_{\frac{1}{2}}$ (V)
2.59	10.6	1.525	11.8	1.538	21.2	0.628
5.28	20.5	1.525	23.2	1.534	41.0	0.637
8.58	34.0	1.540	37.0	1.534	70.0	0.656
14.00	54.0	1.540	64.0	1.540	116.0	0.628
Average		1.532		1.536		0.637

Three different pulse polarograms were run on the system at the various concentrations. Figure 11 shows a complete pulse polarogram going

from 1.7 to 0.3 volts using a tungsten micro-button electrode (area = 5.08

x 10^{+3} cm^2). The wave height of the second wave at 0.635 volts is twice

that of the wave at 1.530 volts; they represent the $Fe^{+2} \rightarrow Fe$ and the

$Fe^{+3} \rightarrow Fe^{+2}$ reductions respectively. The data for the other pulse polaro-

grams are summarized in Table 1 and the i_d versus concentration relation-

ships are plotted in figure 12. Once again the slope of the ferrous to iron

reduction (curve A) is twice that of the ferric to ferrous reduction (curve

C). The currents for the reoxidation of Fe^{+2} to Fe^{+3} (curve B) is slightly

larger than that observed for the reverse reaction.

The reversibility of an electrode can be characterized by the use of

reverse scan pulse polarography.[16] For a D.M.E. the $[i^c_{d(cathodic)}/$

$i^a_{d(anodic)}]$ current ratio is unity for a reversible process and approxi-

mately 7 for an irreversible process. Without resorting to the rigorous

mathematical formulation of the problem and by imposing several conditions,

it is possible to convert the published results for the D.M.E. into a

usable qualitative form for solid electrodes. The experimental procedure

consists of running two pulse polarograms on a system such as

$$0 + ne = R \tag{24}$$

with only 0 in the initial solution. The first polarogram is the simple

reduction polarogram utilizing a rest potential several hundred millivolts

anodic of the $E_{\frac{1}{2}}$ for the reaction. The pulse heights are slowly increased

until the electrode potential during the pulse is well along the cathodic

diffusion limiting plateau (200 to 300 mv cathodic from $E_{\frac{1}{2}}$). t_m is the

time interval between the application of the pulse and the current mea-

surement and t_1 is the time interval between pulses. In the case of the

forward scan (cathodic) the t_1 must be long enough to allow the system

to reach complete equilibrium between each pulse. A depletion effect

will result if t_1 is too short and a diminished diffusion current will result.[17] Increasing t_1 until the i_d remains constant will insure a t_1 of a sufficient magnitude. The cathodic diffusion limited current i_d^c will be given by the Cottrell equation,

$$i_d^c = nFAC_0^* \sqrt{\frac{D}{\pi t_m}} \tag{25}$$

where C_0^* is the bulk concentration of the oxidized species and the other terms have their usual meaning. Equation 25 applies whether the oxidation reaction is reversible or irreversible.

The reverse scan (anodic) consists of sitting out on the cathodic limiting plateau for a period of time, t_1, before pulsing backward to more anodic potentials. In the derivation of the equations for the i_d (oxidation) of the reverse scan, it was assumed that at the birth of each drop a uniform concentration of C_0^* exists throughout the system.[16] Hence, at time t_1 the cathodic current is given by the Ilkovic equation.

$$i_d^c = nFAC \sqrt{\frac{7D}{3\pi t_1}} \tag{26}$$

This assumption is not strictly correct since repeated pulsing from the rest potential will cause a depletion effect[17] of the oxidized species and result in a current less than that preducted by equation 26 at time t_1. If, on a first order approximation, we neglect this depletion effect, then the cathodic current at time t_1 for a solid electrode will be given by

$$i_d^c = nFAC_0^* \sqrt{\frac{D}{\pi t_1}} \tag{27}$$

The pulse polarogram records the difference between the cathodic current at t_1 and the anodic current at t_m. For an irreversible electroreduction the anodic current is zero, hence the recorded anodic

current is

$$i_d^a = nFAC_0^* \sqrt{\frac{D}{\pi t_1}} \tag{28}$$

The ratio of the limiting currents for the cathodic and anodic scans for an irreversible electroreduction is

$$\frac{|i_d^c|}{|i_d^c|} = \sqrt{\frac{t_1}{t_m}} \tag{29}$$

For our experimental conditions this ratio equals 2.24.

In the case of a reversible electrode the concentration profile of the reduced species must be considered. The results from the treatment of non-uniform solutions[18] plus the fact that at time t_m and a potential on the limiting anodic plateau the anodic current is given by

$$i_{(t_m)}^a = nAFC_0^* \sqrt{\frac{D}{\pi t_m}} \left[1 - \sqrt{\frac{t_m}{t_1 + t_m}} \right] \tag{30}$$

Once again the pulse method records the difference between the cathodic current at t_1 and the anodic current at t_m which is equal to

$$i_d^a = nFAC_0^* \sqrt{\frac{D}{\pi}} \left\{ \sqrt{\frac{1}{t_m}} \left[1 - \sqrt{\frac{t_m}{t_1 + t_m}} \right] + \sqrt{\frac{1}{t_1}} \right\} \tag{31}$$

Hence the ratio of the limiting currents for the cathodic and anodic scans of a reversible electroreduction is

$$\frac{|i_d^c|}{|i_d^a|} = \left| 1 - \sqrt{\frac{t_m}{t_1 + t_m}} + \sqrt{\frac{t_m}{t_1}} \right|^{-1} \tag{32}$$

When t_m is small compared to t_1, equation 32 reduces to

$$\frac{|i_d^c|}{|i_d^a|} \sim 1 \tag{33}$$

The values for t_m and t_1 used in the current experiments were 50 and 250 milliseconds, respectively; therefore, the anticipated ratio is

$$\frac{|i_d^c|}{|i_d^a|} = \left| 1 - \sqrt{\frac{50}{300}} + \sqrt{\frac{50}{250}} \right|^{-1} = 0.962 \qquad (34)$$

Errors introduced into the calculation by the assumption can be reduced by several methods. If it is convenient, a rotating electrode or a stirred solution can be used to enhance the recovery of the concentration of the oxidized species around the electrode. The diffusion layers next to the electrode are too small to be affected by the stirring motion. A second method is to use a double step procedure in which the electrode is held far out on the limiting anodic plateau until an uniform solution is realized before stepping to the potential on the limiting cathodic plateau for the t_1 delay time. The pulse and current measurements are then made as before. This procedure is similar to the double step potential chronocoulometry in that it insures an identical start for each delay period.

The cathodic and reverse anodic scans for the Fe^{+3}/Fe^{+2} couple are presented in figure 13. The cathodic $E_{1/2}$ differ by only 9 mv and the i_d^c/i_d^a ratio is 0.89 where the theoretical values for a completely reversible system are 0 mv and 0.962, respectively. The experimental current ratio taken from the i_d versus concentration curves is 0.91. This latter value of the current ratio is closer to the theoretical value (6% low) and represents the average of all the data.

The good fit of the experimental polarogram to the theoretical polarogram in figure 13 further indicates a high degree of reversibility in the Fe^{+3}/Fe^{+2} couple.

Several preliminary current reversal chronopotentiograms were recorded (figure 14) in an attempt to confirm the presence of adsorption.[19] The irreproducibility of the current data obtained did not warrant any further interpretation save that there is an apparent couple at 0.4 to 0.3 volts. This may be due to a co-deposition of iron and aluminum on the electrode which is in keeping with the results of Yntema et al.[9]

The relationship between the first transition time, T_1, and the second, T_2, for a two step electrode process is given by[20]

$$T_2 = T_1 [2 (\frac{n_2}{n_1}) + (\frac{n_2}{n_1})^2]$$
(35)

$n_1 = 1$, and $n_2 = 2$ for the $Fe^{+3} \rightarrow Fe^{+2} \rightarrow Fe$ electrode process; therefore,

$$T_2 = 8T_1$$
(36)

The time scale used in the recording of the experiment and the factor of eight prevents the observation of the T_1 transition.

An $it^{\frac{1}{2}}$ curve from chronoamperometry (figure 15) was also used to calculate a value for the diffusion coefficient for comparison with those obtained from the other electrochemical methods. Only the reduction of ferric ion to ferrous ion gave reproducible results. The results for the other scans were dependent upon the length of time between initial potential application and pulse application. This behavior was to be expected since the starting at any potential other than on the anodic side of the Fe^{+3}/Fe^{+2} couple results in the electrolysis of a non-uniform solution rather than a uniform solution. For a similar reason, D values cannot be calculated from the pulse data for the other scans and the cyclic voltammetric data at the other areas of interest are too scattered to warrant their use. The Fe^{+3} D values calculated from the three electrochemical methods are summarized in Table 3 along with the measured $E_{\frac{1}{2}}$ values.

TABLE 3

ELECTROCHEMICAL CONSTANTS FOR THE IRON SYSTEM IN NaAlCl$_4$ MELTS AT 175° C.

	Method		
	Integral Pulse	Chronoamperometry	Cyclic Voltammetry
$E_{\frac{1}{2}}$ (volts)			
Fe^{+3}/Fe^{+2}	1.534	––	1.53
Fe^{+2}/Fe	0.637	––	0.65
D (cm^2/sec)			
Fe^{+3}	9.9×10^{-6}	8.2×10^{-6}	6.9×10^{-6}

Of the three methods used to determine D, the cyclic voltammetry method is the least reliable;[21] the average D value from the other two methods is 8.8×10^{-6} cm^2/sec. The deposition potential for Fe^{+2} in the 66 mole percent AlCl$_3$ has been reported to be 0.47 volts. Combining this value, the $E_{\frac{1}{2}}$ values for the 50:50 melt and the values in Table 1 of the acid-base equilibrium discussion produces the following emf series for the aluminum chloride melts.

TABLE 4

ELECTRODE POTENTIALS IN NaAlCl$_4$ MELTS

Couple	E°	AlCl$_3$:NaCl
Al(III)/Al	0	50:50
Al(III)/Al	0.480	66:34
Fe(II)/Fe	0.64	50:50
Fe(II)/Fe	0.95	66:34
Ag(I)/Ag	1.290	66:34
Ag(I)/Ag	1.356	50:50
Fe(III)/Fe(II)	1.53	50:50

The shift in the Fe(II)/Fe potential going from the 50:50 to the 66:34 mole percent melt is 0.31 volts in the same direction as the shift in the Al(III)/Al electrode potentials. The fact that the iron shift is 2/3 the aluminum shift and the valency ratio between the two is 2/3 may be just fortuitous. The study of other metal ions in the two melts should illuminate the situation and it should be possible to set up a series of chloride complexing equilibrium constants for these various metals.

The iron system in the $NaAlCl_4$ melt appears to be a very well behaved reversible system with a moderate adsorption of the ferrous ion on the tungsten indicator electrode. It is not clear yet just why the anodization of an iron wire in these melts semi-passivates the iron electrode only during electrolysis. Once the current has been discontinued, the iron electrode rapidly returns to its original state. The electroreduction curves verify that any iron impurity in these melts can be easily and effectively removed by simple electrolysis or displacement by aluminum metal.

Our deposition potential for Fe^{+2} (0.64 volts) in the 50:50 mole percent $AlCl_3$:NaCl melt is 0.31 volts cathodic of the value reported by Yntema et al.[7] for the 66:34 mole percent melt after correcting for the different reference electrodes. The increased stability of the ferrous ion in the melt containing the higher chloride ion concentration illustrates that the ferrous ion is fairly strongly complexed by the chloride ion.

The potential of the cyclic voltammetric peak reported by Giner and Hollek[10] for the reduction of Fe^{+3} to Fe^{+2} in the 66:34 mole percent melt vs. the aluminum reference electrode in the 50:50 mole percent melt

is 1.5 volts. This value is surprisingly close to the value (1.48 volts)

we observed in our 50:50 mole percent melt. The cathodic peak that Giner

and Hollek assigned to the $Fe^{+2} \rightarrow Fe^{+1}$ reduction after correcting for the

different reference electrodes appears at 0.5 volts in our system. This

value is some 400 millivolts cathodic of the corresponding value reported

by Yntema et al.[7] The fact that the potential of the Fe^{+3}/Fe^{+2} couple

does not shift with a change in the chloride concentration in going from

the 66:34 to 50:50 mole percent melt is not consistent with the other

observations. Giner and Hollek's $FeCl_3$ may have been wet or contaminated

thus causing the discrepancies. In addition, the adding of 480 millivolts

for the change in aluminum reference electrodes represents a major portion

of the electrode potentials.

E. Electrochemical Oxidation of Ferrocene in $NaAlCl_4$ at 175° C.

In their investigation of the electrochemical oxidation of a series

of polynuclear hydrocarbons, Fleischmann and Pletcher[22] indicated that

these electro-oxidations were partially reversible. However, they found

several waves for most of the compounds investigated with no quantitative

data being given. These results together with the known reactivity of

polynuclear hydrocarbons in $AlCl_3$ containing melts (see above) suggest

that these compounds form a very complex system in such melts. We there-

fore searched for a simple organic type compound which would lend itself

to a simple quantitative electrochemical study on which we could base an

electrochemical investigation of other organic species in $AlCl_3$ melts.

Peover[23] has shown that ferrocene is such a compound which behaves very

well electrochemically in several solvent systems. We quickly established

that ferrocene was stable in a $NaAlCl_4$ melt and therefore decided to study

its electrochemical behavior in $AlCl_3$ containing melts.

Analogous to its behavior in aprotic solvents, ferrocene was expected to undergo a reversible one-electron oxidation in molten $NaAlCl_4$. A cyclic voltammogram of a 1.75 mM solution of ferrocene in $NaAlCl_4$ at 175° C. at a sweep rate of 0.25 V/sec. is shown in figure 16. It appears that ferrocene does indeed undergo a reversible electro-oxidation. The expected linear relationship between the peak current, i_p, and square root of sweep rate, $v^{\frac{1}{2}}$, and the ferrocene concentration are shown in figures 17 and 18, respectively. Comparison of the i_p values for ferrocene at the same sweep rate and concentration with those for the Fe(III)/Fe(II) couple (see above) indicated that ferrocene was undergoing a reversible one-electron oxidation.

However, upon carrying out further diagnostic tests,[21] small deviations from ideal behavior were found. With a peak potential, E_p, value of 680 mv, $E_{\frac{1}{2}}$ (85.17 % E_p) was calculated to be 625 mv. At 175° C. theory predicts a value for E_p (anodic) - $E_{\frac{1}{2}}$ of 42 mv, while we observed a consistent value of 50 mv. Also at 175° C. E_p(anodic) - E_p(cathodic) is expected to be 84 mv and we observed varying values from 70 to 95 mv, the lower values occuring with higher concentrations and sweep rates.

We have also calculated the peak voltammograms for the reversible one-electron oxidation of ferrocene. Using a diffusion coefficient value obtained from cyclic voltammetry (see below) and Randles-Sevcik constant calculated from a value of 2.69 x 10^5 at 25° C., the current as a function of applied potential is given by the following equation:

$$i = 491 \ n^{3/2} \ AD^{\frac{1}{2}} \ v^{\frac{1}{2}} \ C(X') \tag{37}$$

where (X') is the current function evaluated by Nicholson and Shain,[24]

the other terms having their usual meaning. Comparison of the calculated with recorded voltammograms showed good agreement with the rising part of the curve and slightly beyond the peak. However, in all cases small deviations were found at. potentials 25 ml anodic of E_p, the observed anodic currents always being larger than theory predicted.

Evaluation of the ratio i_p(cathodic) to i_p(anodic), i_{pc}/i_{pa}, also gave values different from unity, the expected value for a reversible one-electron change. Depending on the evaluation method used, i_{pc}/i_{pa} was less than or equal to unity at low sweep rates, while reaching values as large as 1.2 at our highest sweep rates.

Pulse polarographic and chronoamperometric techniques were also used to investigate the electrochemical behavior of ferrocene. Normal pulse polarography on a 3.23 mM ferrocene solution from 0.3 to 1.1 V with a delay time of 250 msec. and a pulse width of 50 msec. gave the pulse polarogram shown in figure 19a. The $E_{\frac{1}{2}}$ value of 625 mV taken from the polarogram is identical to that obtained from cyclic voltammetry. Comparison of the experimental with a calculated polarogram indicates that the experimental one is not ideal. With a starting potential of 450 mV the observed pulse polarogram was much more ideal (see figure 19b). The non-ideal shape of the polarogram obtained with a starting potential of 300 mV may be caused by aluminum dissolution while with more anodic starting potentials this process ceases. When one calculates the pulse polarographic limiting currents from i_p values we find that the observed pulse limiting currents are somewhat larger. This is probably to be expected since in cyclic voltammetry at potentials more anodic of E_p, the calculated currents are lower than those observed.

Reverse scan pulse polarograms were also obtained for the ferrocene system. A representative example is shown in figure 19c. Although in all cases the polarograms were quite drawn out, a value of 680 mV was obtained for $E_{\frac{1}{2}}$. This is very much different from the $E_{\frac{1}{2}}$ value of 625 mV obtained from the normal pulse polarogram or cyclic voltammogram. The ratio of the anodic to cathodic limiting currents were, as predicted, less than unity; however, the value varied for the three concentrations studied.

Computerized chronoamperometric studies were also carried out on the ferrocene system. From the observed current time curves, diffusion coefficient values ranging from 5.6×10^{-6} to 1.74×10^{-5} cm^2sec^{-1} were obtained for ferrocene. Using data from cyclic voltammetry, an average value of 5.74×10^{-6} cm^2sec^{-1} was obtained for D. The varying values of D obtained from the computerized current-time curves is probably due to an insufficient amount of data.

An explanation of the observed deviations from the predicted values for several of the electrochemical parameters is not readily available. The small deviations in potential parameters may be due to measuring accuracy. A possible explanation for the larger deviations is that the product of the oxidation of ferrocene (the ferrocenium cation radical) is adsorbed.[15] This would account for the ratio of i_{pc} to i_{pa} being greater than unity. Product adsorption would also cause a cathodic shift in E_p or $E_{\frac{1}{2}}$ and this would explain the varying values of $E_{pa} - E_{pc}$ as the anodic peak potential does remain constant. However, it is doubtful that shift would amount to the 50 mV difference observed in pulse polarography.

Although the electro-oxidation of ferrocene in $NaAlCl_4$ appears to be a reversible one-electron oxidation with possible product adsorption, the noted deviations make it obvious that further work must be done. Controlled potential coulommetry will be carried out. Cyclic voltammetry over a much greater sweep rate and concentration range will be performed. Refinements in the chronoamperometric measurements will be made.

APPENDIX I

N71-19565

SYSTEM FOR COMPUTERIZATION OF
ELECTROCHEMICAL MEASUREMENTS IN FUSED SALTS

A. Purpose

Many of the modern electrochemical techniques involve outputing a
complex time-based potential wave form to a potentiostat followed by a
rapid measurement of the resulting current at specific points in time.
Complex analysis of the raw data is often required before the experi-
mental data can be interpreted in order to optimize the experimental
parameters. The results from a computerized system can be plotted
directly onto an $8\frac{1}{2}$ x 11" sheet of paper and the numerical values for
each data point (before or after analysis) can be listed. The use of
a 12 bit A/D converter gives a resolution of one part in four thousand
which is better by a factor of 40 than what can be expected from an oscil-
lographic trace. The use of RC timing circuits in analog systems is a
much more tedious process than merely typing a numerical time value into
the computer program. The versatility of the computerized system is only
limited by the imagination of the computer programmer since through pro-
gram control switches can be opened or closed, any voltage wave form can
be created, and both rapid and accurate numerical measurements can be
made. In a more sophisticated system a continuous dialogue and response
between the computer and experiment can be used to optimize the experi-
mental conditions.

B. Construction and Calibration of Transmission Lines

As outlined in our previous report[7] a method of driving two 50 yard RG174/AU coaxial cables connecting the computer to the experimental set up has been perfected. This system consisted of a line driver (figure 20a) at the transmitting end of the line and a line receiver (figure 20b) at the other end. A 50 ohm terminator is inserted between the transmission line and the line receiver to match the line impedance. The common mode signal (4 volts, 60 cps) picked up by the transmission line is eliminated by the use of a differential amplifier in the line receiver.

Since the output from the D/A on our computer ranges from 0 to -10 volts, it was necessary to incorporate a DPDT switch (S_1, figure 20b) to facilitate the use of both anodic and cathodic signals in the experimental measurements. In addition, the use of this switch in the receiver at the computer eliminated the necessity to distinguish between cathodic and anodic signals in the computer programming.

The imperfections in the amplifier circuits used in the transmission lines necessitated the use of a line calibration program and the appropriate potential correction subroutines for all the potential I/O used in the computer programs. The bias in the operational amplifiers is compensated for by the variable "B" and the amplification error is corrected by the variable "F" when used in the equations

$$V'_{out} = (V_{out}/F_{out}) + B_{out} \tag{A-1}$$

$$V_{in} = (V'_{in} + B_{in})/F_{in} \tag{A-2}$$

The V' is either transmitted to the D/A or received from the A/D and V is the corrected value used in the program. A typical printout from the

Transmission Line Calibration Program is given in figure 21. The four

calibration figures obtained from this program are then entered during

the initialization period of each program utilizing the transmission

lines.

Past experience has shown that it is often advantageous to connect

the experimental cell to the potentiostat at a controlled interval before

the computer begins to make measurements. Two additional transmission

lines are being constructed so that the relays on the computer can be

used to activate the switches in the potentiostat. In addition, these

lines will also be used in the timing procedure contained in the Pulse

Polarography on a Dropping Mercury Electrode Program. A more detailed

description of this program will be given in a later section of this

report.

C. Modifications to the Pulse Polarography at a Stationary Electrode

   Program.

The original pulse polarography program has been modified to allow

for the storage of up to eight different base lines. The appropriate

base line can then be automatically subtracted from the experimental

results before they are plotted. Figure 22 shows how this procedure can

improve the detail of a plot when the base line represents a significant

portion of the total current.

Another minor modification has been the addition of a parameter

"start" to the input of the program. This parameter sets the height of

the first pulse in the "normal" and "difference" modes of the program

which effectively expands the potential scale on the plot to any desired

scale. The scale expansion is very helpful when performing wave analysis

by providing a short potential range spanned by a very high density of data points.

D. <u>Pulse Polarography on a Dropping Mercury Electrode</u>

Prolonged exposure of solid electrodes to the $NaCl-AlCl_3$ melt often poisons the electrode surface and makes it unreliable. Several workers have used a mercury electrode successfully in these melts over a voltage range of 0 to 1 vs. an aluminum reference electrode. Since experimental evidence has shown that several metals and some organics are electroactive in this region, it was decided to construct the required electronics and to modify the existing pulse polarography program to facilitate phasing of the computer clock with the dropping electrode.

The electronic circuitry (figure 23) allows the computer to start a birth detector by the use of a computer relay and a transmission line. The birth detector consists of a sine wave generator which imposes a small A.C. signal on the D.M.E. through the potentiostat. The release of the mercury drop causes a sudden change in the surface area in contact with the melt. The abrupt change in the A.C. capacitive current causes the differentiator to generate a pulse which is then amplified and transmitted to the remote start on the computer's clock. Once the computer program senses that the clock has started, the birth detector is automatically disconnected from the potentiostat by program control. After a given time delay to allow the mercury drop to grow to a mature age, a pulse is applied, data recorded and then the birth detector is reactivated for the next drop. The major portion of the circuitry has been tested and proven to work; however, due to the back-order of certain electronic components,

the final assemblage using the transmission lines has not as yet been tested.

The input parameters to the new pulse program are identical to those used in the previous program except for the meaning of the delay time. Instead of being the time between the pulses, it will now be the time the computer waits before applying the pulse to allow for the formation of a mature new drop of mercury at the electrode. The absence of a drop knocker will prevent excessive agitation in the cell as well as eliminate many of the problems inherent in drop knockers. The natural drop rate must be adjusted so that the drop time exceeds the sum of the delay time and pulse width by at least a few milliseconds. There is no real upper limit to the drop time except excessive values will prolong each experimental run.

The obvious application of this system to aqueous systems will eliminate the reservations that many people had in using pulse polarography on a hanging mercury electrode or some other electrode with an unrenewable surface.

E. $it^{\frac{1}{2}}$ Program-Chronoamperometry

The diffusion coefficients for the Ag(I)[7] and the Cd(II), Pb(II), Sn(II) and Cu(I) ions[8] in the $NaAlCl_4$ melt are approximately one order of magnitude smaller than the values reported for the alkali metal chloride and nitrate melts.[25] The small diffusion coefficients indicate that there may be a significant difference in the structure of the $NaAlCl_4$ melt when compared to the simpler alkali metal chloride melts. In order to effectively examine these diffusion coefficients as well as to accurately determine the electrochemically active area of the solid electrodes,

a program utilizing the following equation[21] has been written and de-bugged:

$$it^{\frac{1}{2}} = 54.5 \times 10^3 \, nAD^{\frac{1}{2}} \, C \qquad \qquad (A-3)$$

i = microamps

t = seconds

A = cm^2

D = cm^2/sec

C = bulk concentration in millimoles/liter

The $it^{\frac{1}{2}}$ program has the capability of storing eight different base lines with a maximum of 120 data points in each base line. The normal approach to using equation A-3 is to delay the measurement of the first data point until the charging of the double layer is completed. In low-viscosity solvents the $it^{\frac{1}{2}}$ product is by no means constant, but increases rapidly with time due to the stirring action of concentration density gradients. This problem is accentuated at elevated temperatures. The computer system allows the experiment to be carried out in the millisecond time scale instead of the normal second or tens of seconds time scale. The subtraction of the base line which represents the residual charging current and impurity faradaic currents eliminates the problems associated with the previous methods at short time periods.

The program is set up so that any of the three parameters (viz., Area, A; Concentration, C; Diffusion Coefficient, D) can be calculated provided the other two parameters are known. A block diagram of the program is given in Appendix III and a typical printout for the calculation of the area of an electrode is given in figure 24. A description of the input

parameters and how to run the program is given in Appendix II. Figure 25

is the plot for the determination of the area of a platinum button elec-

trode using a 2.77 millimolar potassium ferrocyanide solution in a 2 molar

KCl base electrolyte. The $it^{\frac{1}{2}}$ vs t plot for the same system without a

base line correction has also been included on the plot. The computed

electroactive area of the electrode is 0.202 cm^2 compared to the visually

measured area of 0.210 cm^2. All of the tungsten electrodes appeared to

be immediately passivated when attempts were made to measure their areas

in the ferrocyanide solution. Preliminary measurements made in the fused

salt system indicates that this measurement will prove to be useful in the

determination of diffusion coefficients in melts. It will be necessary to

use a different system and published D values to determine the area of the

tungsten electrodes before any work can be done in the $NaAlCl_4$ melts.

APPENDIX II

$it^{\frac{1}{2}}$ COMPUTER PROGRAM

A. Purpose and Introduction

This program applies a given pulse to an electrochemical system and then records the current at given time intervals. Utilizing the equation for linear diffusion, one of the following three parameters—area, concentration and diffusion coefficient—can be calculated provided the other two are known. A plot of i vs t and $it^{\frac{1}{2}}$ vs t, the least squares slope and intercept of $it^{\frac{1}{2}}$ vs t and the requested parameter make up the output from the program. A facility has been incorporated into the program to allow for the use of transmission lines. This facility requests four calibration figures which are obtained from the Transmission Line Calibration Program. The remainder of this report explains the loading, operation and meaning of the parameters used in the program.

B. Loading the Program

The program may be loaded from the disk or from a punched binary paper tape. The floating point package must be stored on the disk under some name, say FPK1.

Set 7600 in the switch registers, press "stop", press "load add", press "start". The following printout will be produced on the teletype where the underlined type is the output of the computer:

    . LOAD ⟩

    IN- S:FPK1,S:PROG ⟩

    *

*
—

OPT— 2

ST = 200 ʝ

↑ ↑ ↑ ↑ ↑ ↑

ʝ designates a carriage return and each ↑ is replied to by typing "control P". "PROG" is the name that the program is stored under on the disk or if a paper tape is used, replace "PROG" by "R". The paper tape is loaded in the high speed paper tape reader and it will be read twice during the loading procedure. The program will start automatically after the loading is completed.

C. Hardware Set-Up

Connect the transmission lines, set the clock switch to operate and activate the plotter.

D. Input Parameters and Operation

The input parameters are listed below in the order that they appear in the printout. Certain parameters can be changed during the operation of the program without having to reload the program. Each of these parameters has a switch number, SW1, SW2, etc., which will be explained later.

CLOCK INTERVAL =

This is the time in milliseconds between each clock tick.

This value can be obtained from the clock calibration program.

B(IN) =

B(OUT) =

F(IN) =

F(OUT) =

>These are the 4 transmission line calibration figures obtained
>from the Transmission Line Calibration Program for the current
>electronic set-up.

PULSE HEIGHT =

>SW0; the absolute magnitude in volts of the potential pulse to
>be applied to the cell.

INPUT TIME FOR 1ST PT, INTERVAL & NUMBER OF PTS

>SW1; the time in milliseconds after the beginning of the pulse
>at which the first data point is taken, the time in milliseconds
>between each point and the number of points to be taken ($\leq$ 120).

R(M) =

>SW2: the current measuring resistor in ohms.

FOR X

MIN & MAX =

>SW3; the minimum and maximum values for the time scale on the
>plotter in milliseconds.

FOR X

MIN TCK & SPACE =

>SW3; the value of the first tick mark and the spacing for each
>successive tick mark along the time axis in milliseconds.

FOR Y

MIN & MAX =

>SW3; same as for X except along the current scale in micro
>amps.

FOR Y

MIN TCK & SPACE =

SW3; same as above.

FULL SCALE PR KY

SW4; use zero control on plotter to set required location of

the upper right-hand corner of the plot, then press any key.

ZERO PR KY

.SW4; use the calibration control on the plotter to set the

required location of the lower left-hand corner of the plot,

then press any key.

VALENCE CHANGE =

SW5; the n value in the equation

CALC A, C OR D?

SW6; select the parameter to be calculated, reply with A for

area, C for concentration or D for diffusion coefficient.

MILLIMOLAR CONC =

SW6; concentration in millimoles per liter.

D =

SW6; value of the diffusion coefficient in units of cm^2/sec.

AREA =

SW6; area of electrode in cm^2.

At this point in the program zero volts is the output to the potentiostat

so that the bias on the potentiostat can be adjusted to apply the desired

initial potential to the cell. The direction of the pulse to be applied

is determined by setting the switches on the two line receivers to cathodic

or anodic.

SCALE FAC & AVERAGE =

The scale factor is used to increase the magnitude of the
current values so that they fill the entire plot. The factor
doesn't change the values being used in the calculations.
Average is the number of times the experiment is to be repeated
before averaging the current. This is used to improve the sig-
nal to noise ratio.

B OR S & BASE NO =

B indicates that this is a base line determination and the
values are to be stored under the given base number (1 to 8).
S stands for a system with an electroactive species in it and
that the given base number is to be subtracted from the data
to correct for double layer charging and other impurities in
the system. Care must be taken to see that the time scale,
number of points and pulse height are the same for the S run
and the stored base line. The program doesn't make any checks
for compatibility between the two sets of data.

DELAY =

This parameter request appears only when "AVERAGE" is greater
than unity and it is the time in milliseconds that the computer
waits for before repeating the experiment.

REPEAT THE EXPT?

Y for "yes" sends the program directly to the scale factor
input request and it is ready to repeat the experiment without
altering any of the parameters associated with the switches.
N for "no" sends the program to the following printout.

SET SWITCHES PRESS KEY

Turn all the switches off and then turn on only the switches associated with the parameters you wish to change. Press any key once all of the switches are set.

There are several self-explanatory error messages built into the parameter input portion of the program. The usual correction is to reenter the requested parameters.

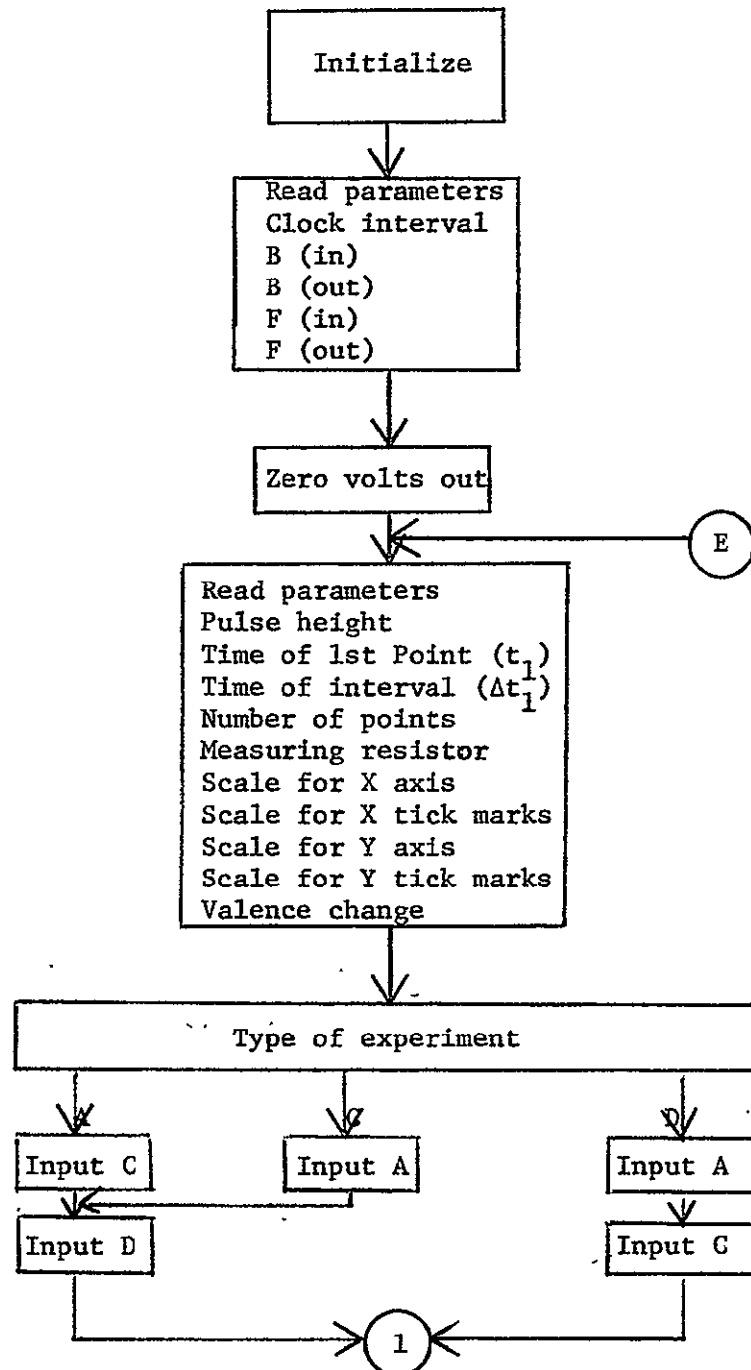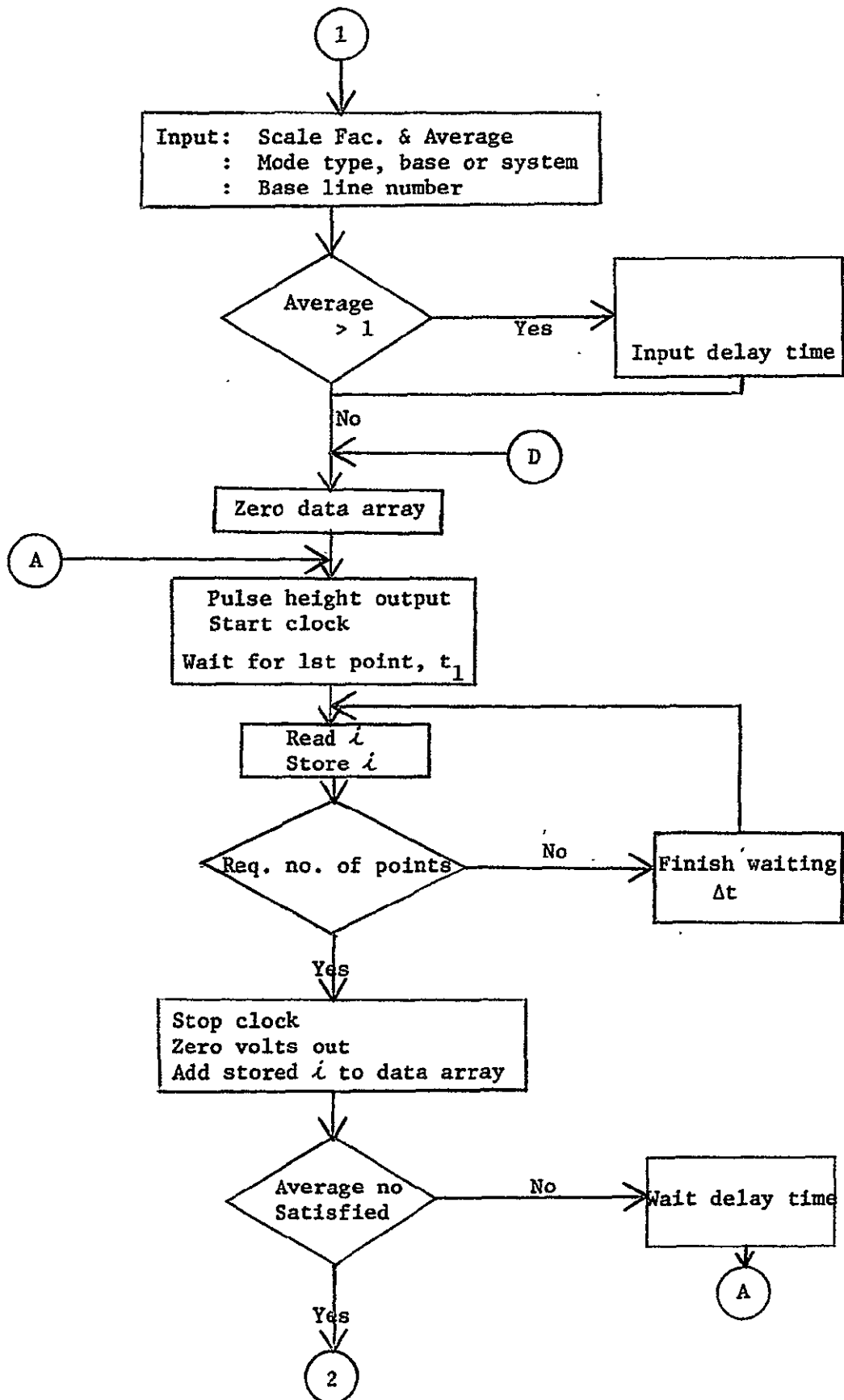SWITCH 11 CONTROLS THE AXIS DRAWING ROUTINE.

The routine isn't very fast and often the axes are not required on trial runs. The axes are only drawn when switch 11 is turned on.
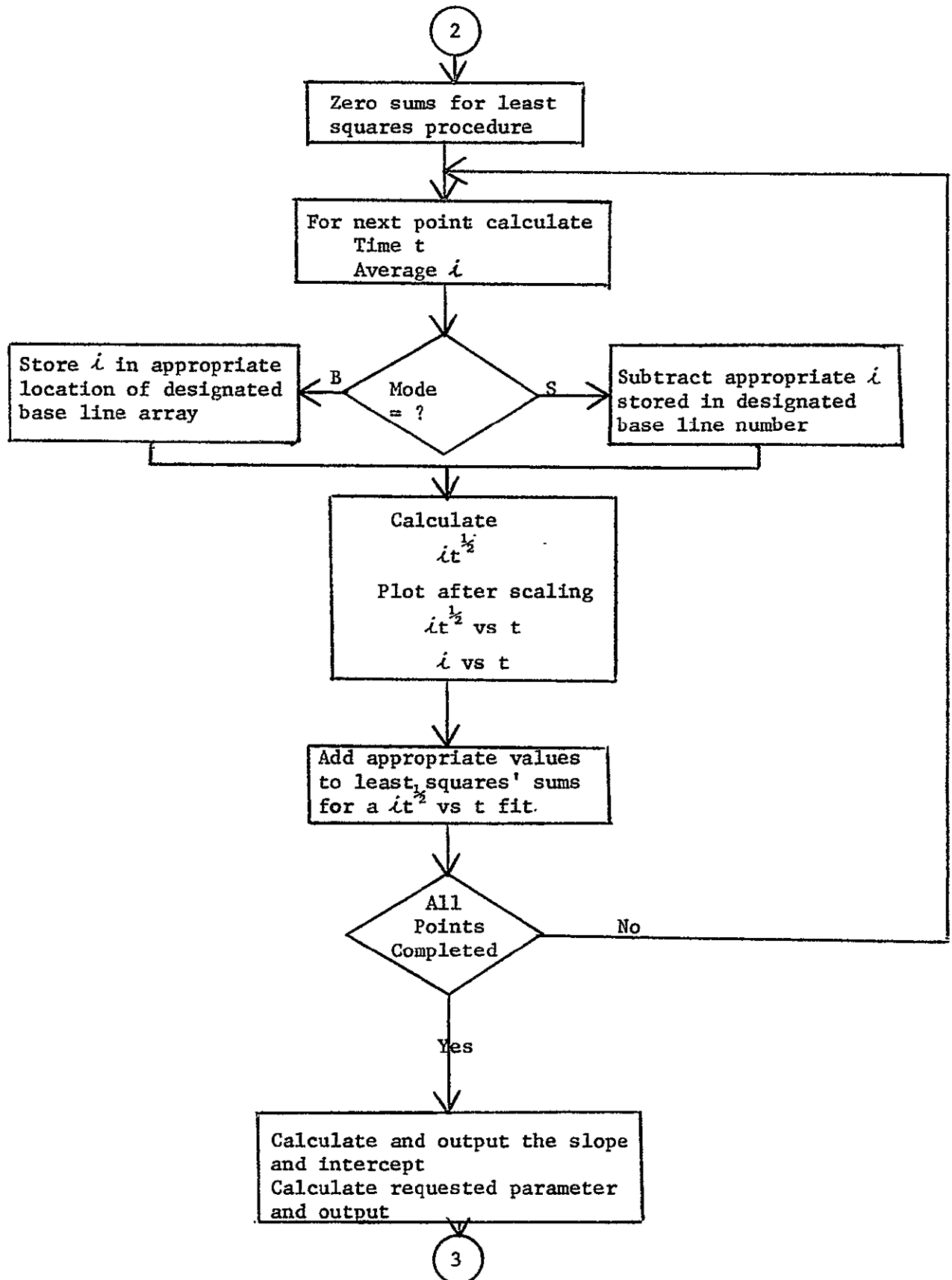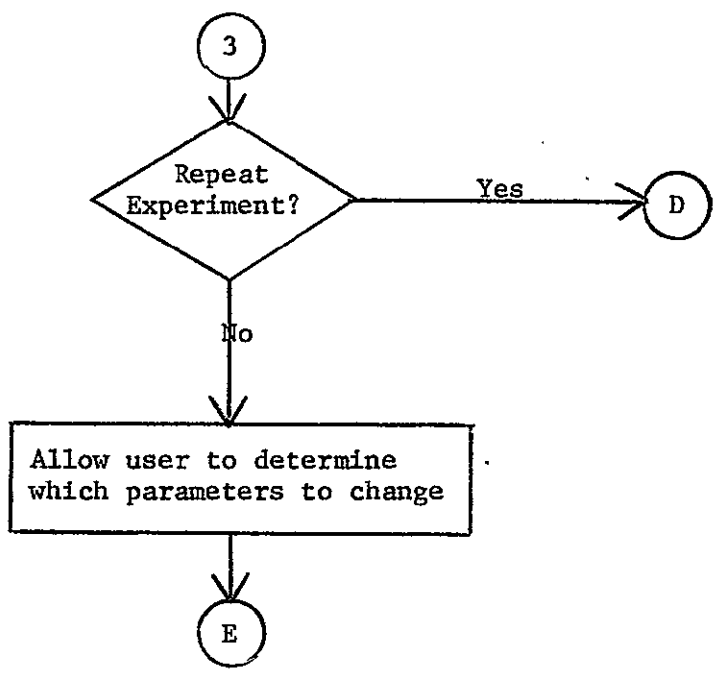
E. The Program

A description of the instruction mnemonics used can be found in the previous report on the Pulse Polarography Report.[7] The upper 4K of core storage is used strictly for data storage and no use is made of the disk.

APPENDIX III

Block Diagram for $it^{\frac{1}{2}}$ Program

```
                    ┌──────────────────┐
                    │    Initialize    │
                    └──────────────────┘
                              │
                              ▼
                    ┌──────────────────┐
                    │ Read parameters  │
                    │ Clock interval   │
                    │ B (in)           │
                    │ B (out)          │
                    │ F (in)           │
                    │ F (out)          │
                    └──────────────────┘
                              │
                              ▼
                    ┌──────────────────┐
                    │  Zero volts out  │
                    └──────────────────┘
                              │◄──────────────────( E )
                              ▼
            ┌────────────────────────────────┐
            │ Read parameters                │
            │ Pulse height                   │
            │ Time of 1st Point ($t_1$)      │
            │ Time of interval ($\Delta t_1$)│
            │ Number of points               │
            │ Measuring resistor             │
            │ Scale for X axis               │
            │ Scale for X tick marks         │
            │ Scale for Y axis               │
            │ Scale for Y tick marks         │
            │ Valence change                 │
            └────────────────────────────────┘
                              │
                              ▼
        ┌────────────────────────────────────────────┐
        │            Type of experiment              │
        └────────────────────────────────────────────┘
             │              │                  │
             ▼              ▼                  ▼
        ┌─────────┐   ┌─────────┐        ┌─────────┐
        │ Input C │   │ Input A │        │ Input A │
        └─────────┘   └─────────┘        └─────────┘
             │              │                  │
             ▼◄─────────────┘                  ▼
        ┌─────────┐                        ┌─────────┐
        │ Input D │                        │ Input C │
        └─────────┘                        └─────────┘
             │                                  │
             └────────────►( 1 )◄───────────────┘
```

```
                              ( 1 )
                                │
                                ▼
        ┌───────────────────────────────────────────┐
        │ Input:   Scale Fac. & Average              │
        │      :   Mode type, base or system         │
        │      :   Base line number                  │
        └───────────────────────────────────────────┘
                                │
                                ▼
                      ╱─────────────╲                          ┌──────────────────┐
                     ╱   Average      ╲          Yes           │                  │
                     ╲     > 1        ╱ ───────────────────────▶│  Input delay time│
                      ╲─────────────╱                          └──────────────────┘
                           │ No                                         │
                           │                                            │
                           ▼          ◀─────────────( D )               │
                  ┌──────────────────┐                                  │
                  │  Zero data array │                                  │
                  └──────────────────┘                                  │
                           │                                            │
    ( A )──────────────────▶│                                          │
                  ┌──────────────────────────┐                         │
                  │  Pulse height output     │                         │
                  │  Start clock             │                         │
                  │  Wait for 1st point, t₁  │                         │
                  └──────────────────────────┘                         │
                           │                     ◀────────────────────┐ │
                  ┌──────────────────┐                               │
                  │  Read i          │                               │
                  │  Store i         │                               │
                  └──────────────────┘                               │
                           │                                         │
                           ▼                                         │
                   ╱───────────────╲       No        ┌──────────────────┐
                  ╱ Req. no. of points╲ ────────────▶│  Finish waiting  │
                   ╲───────────────╱                 │       Δt         │
                           │ Yes                     └──────────────────┘
                           ▼
              ┌──────────────────────────────┐
              │  Stop clock                  │
              │  Zero volts out              │
              │  Add stored i to data array  │
              └──────────────────────────────┘
                           │
                           ▼
                   ╱───────────────╲       No        ┌──────────────────┐
                  ╱  Average no      ╲ ─────────────▶│ Wait delay time  │
                   ╲  Satisfied      ╱                └──────────────────┘
                   ╲───────────────╱                          │
                           │ Yes                              ▼
                           ▼                                ( A )
                         ( 2 )
```

t_1

Read i

Store i

Add stored i to data array

```
                                    ( 2 )
                                      │
                                      ▼
                          ┌───────────────────────┐
                          │ Zero sums for least   │
                          │ squares procedure     │
                          └───────────────────────┘
                                      │
                                      ▼
                          ┌───────────────────────┐
                          │ For next point calculate │
                          │      Time t           │
                          │      Average i        │
                          └───────────────────────┘
                                      │
                                      ▼
```

Store i in appropriate location of designated base line array

B ← Mode = ? → **S** Subtract appropriate i stored in designated base line number

```
                          ┌───────────────────────┐
                          │      Calculate        │
```

$$it^{\frac{1}{2}}$$

Plot after scaling

$$it^{\frac{1}{2}} \text{ vs } t$$

$$i \text{ vs } t$$

Add appropriate values to least squares' sums for a $it^{\frac{1}{2}}$ vs t fit.

```
                              All
                            Points          No
                          Completed
                              │
                             Yes
                              ▼
```

Calculate and output the slope and intercept
Calculate requested parameter and output

```
                                    ( 3 )
```

```
        ( 3 )
          │
          ▼
      ╱───────╲
     ╱  Repeat  ╲          Yes
    ╱ Experiment? ╲──────────────────▶ ( D )
     ╲           ╱
      ╲─────────╱
          │
          │ No
          ▼
  ┌─────────────────────────┐
  │ Allow user to determine │
  │ which parameters to change │
  └─────────────────────────┘
          │
          ▼
        ( E )
```

REFERENCES

(Section II and Appendices)

(1) Torsi, G. and Mamantov, G., preprint (1970).

(2) Tremillon, B. and Letisse, G., J. Electroanal. Chem. 17, 371 (1968).

(3) Anders, U., Ph.D. Thesis, Univ. of Alberta, Edmonton, Alberta, Canada, 1969.

(4) King, L.A., Department of Chemistry, U.S. Air Force Academy, Colorado Springs, Colo., private communication, 1970.

(5) King, L.A. and Seegmiller, D.W., Abstract 597, American Chem. Soc. Regional Meeting, New Orleans, Louisiana, Dec. 1970.

(6) Torsi, G., Mamantov, G. and Begun, G.M., Inorg. Nucl. Chem. Lett. 6, 553 (1970).

(7) Osteryoung, R.A., Electrochemical Studies in Aluminum Chloride Melts, Grant NCR 06-002-088, August 14, 1970.

(8) Francini, M., Martini, S. and Monfrini, C., Electtr. Metall. 1, 3 (1967).

(9) Wade, W.H., Twellmeyer, G.O. and Yntema, L.F., Trans. Electrochem. Soc. 78, 77 (1940).

(10) Giner, J. and Hollek, G. (Tyco Laboratories, Inc.), "Aluminum Chlorine Battery," Report to NASA, September 1969, Contract No. NAS-12-688.

(11) Frisch, M.A., Greenbaum, M.A. and Faber, M., J. Phys. Chem. 69, 300 (1965).

(12) Morrey, J.R., Inorg. Chem. 2, 163 (1963).

(13) Fischer, W. and Simon, A.L., A. Anorg. Allgem. Chem. 306, 10 (1960).

(14) Anson, F.C., Anal. Chem. 38, 54 (1966).

(15) Wopschall, R.H. and Shain, I., Anal. Chem. 39, 1514 (1967).

(16) Oldham, K.B. and Parry, E.P., Anal. Chem. 42, 229 (1970).

(17) Oldham, K.B. and Parry, E.P., Anal. Chem. 38, 867 (1966).

(18) Oldham, K.B., Anal. Chem. 40, 1024 (1968).

(19) Reinmuth, W.H., Anal. Chem. 33, 322 (1961).

(20) Delahay, P., New Instrumental Methods in Electrochemistry (New York: Interscience Publishers, Inc.), 1954, p. 192.

(21) Adams, R.N., Electrochemistry at Solid Electrodes (New York: Marcel Dekker, Inc.), 1969, pp. 214-23.

(22) Fleischmann, M. and Pletcher, D., J. Electroanal. Chem. 25, 449 (1970).

(23) Peover, M.S., J. Electroanal. Chem. 2, 1 (1967).

(24) Nicholson, R.S. and Shain, I., Anal. Chem. 36, 706 (1964).

(25) Janz, G.T., Molten Salts Handbook (New York: Academic Press), 1967, p. 334.

FIGURE TITLES

Figure

1 Experimental Electrochemical Cell

    A - Thermocouple well
    B - 19/22 ground joint for reference electrode
    C - 25 mm hole for working electrode compartment
    D - 14/20 ground joint for counter electrode
    E - Working electrode
    F - Teflon adaptor
    G - Working electrode compartment
    H - O-ring
    I - Teflon cell top
    J - Ring furnace
    K - Glass cell
    L - Furnace
    M - Melt
    N - Reference electrode compartment and Al electrode
    P - Tungsten counter electrode

2 Current Density vs Voltage Curves for $NaAlCl_4$ Melt at 175° C.

    A - Carbon electrode
    B - Platinum button electrode
    C - Tungsten button electrode
    D - Tungsten wire electrode

    Sweep rate = 0.5 V/sec
    Vertical lines represent a current density of 1 ma cm^{-2} for corresponding electrode.

3 Integral Pulse Polarography Background in a $NaAlCl_4$ Melt at 175° C.
    Area of tungsten electrode = 5.08×10^{-3} cm^2
    Pulse width = 50 msec
    Pulse delay time = 250 msec

4 Cyclic Voltammogram of HCl in a $NaAlCl_4$ Melt at 175° C.
    Area of tungsten electrode = 6.28×10^{-3} cm^2
    Sweep rate = 0.5 volts/sec
    Recorded immediately after bubbling HCl through the melt.
    Peaks decreased with time.

5 Cyclic Voltammogram of HCl in a $NaAlCl_4$ Melt at 175° C.
    Same as figure 4 except recorded 10 minutes later.

Figure

6 Cyclic Voltammogram of 5.28 millimolar $FeCl_3$ in a $NaAlCl_4$ Melt at 175° C.

   Area of tungsten electrode = 5.08 x 10^{-3} cm^2
   Sweep rate = 0.5 volts/sec
   S → 0.3 → 1.7 → 0.3

7 Anodic Portion of Cyclic Voltammogram of 8.58 millimolar $FeCl_3$ in a $NaAlCl_3$ Melt at 175° C.

   Area of tungsten electrode = 5.08 x 10^{-3} cm^2
   Range scanned: 1.7 → 0.3 → 1.7 volts vs Al

8 Cyclic Voltammogram of the Fe(II)/Fe Couple in a $NaAlCl_4$ Melt at 175° C.

   Area of tungsten electrode = 5.08 x 10^{-3} cm^2
   $[FeCl_3]$ = 8.58 mM
   Sweep rate = 0.5 volts/sec
   Repeated cycling increases both peaks.

9 Cyclic Voltammograms of the Fe(III)/Fe(II) Couple in a $NaAlCl_4$ Melt at 175° C.

   Area of tungsten electrode = 5.08 x 10^{-3} cm^2
   $[FeCl_3]$ = 14.0 mM

10 Cyclic Voltammetry Peak Currents vs $FeCl_3$ Concentration in a $NaAlCl_4$ Melt at 175° C.

   Area of tungsten electrode = 5.08 x 10^{-3} cm^2
   Sweep rate = 0.5 volts/sec

11 Integral Pulse Polarogram of 14.0 millimolar $FeCl_3$ in a $NaAlCl_4$ at 175° C.

   Area of tungsten electrode = 5.08 x 10^{-3} cm^2
   Pulse width = 50 msec
   Pulse delay time = 250 msec

12 Integral Pulse Diffusion Currents vs $FeCl_3$ Concentration in a $NaAlCl_4$ Melt at 175° C.

   Area of tungsten electrode = 5.08 x 10^{-3} cm^2
   Pulse width = 50 msec
   Pulse delay time = 250 msec

13 Integral Pulse Polarograms of the Fe(III)/Fe(II) Couple in a $NaAlCl_4$ Melt at 175° C.

   Area of tungsten electrode = 5.08 x 10^{-3} cm^2
   Pulse width = 50 msec
   Pulse delay time = 250 msec
   $[FeCl_3]$ = 5.28 mM

Figure

Figure

25 Chronoamperometric Curve with and without Correction for Base Line

$[K_4Fe(CN)_6]$ in 2M KCl = 2.28 mM
Temperature = 25° C
Platinum button electrode
Potential step from 0 to +0.7 volts vs S.C.E.
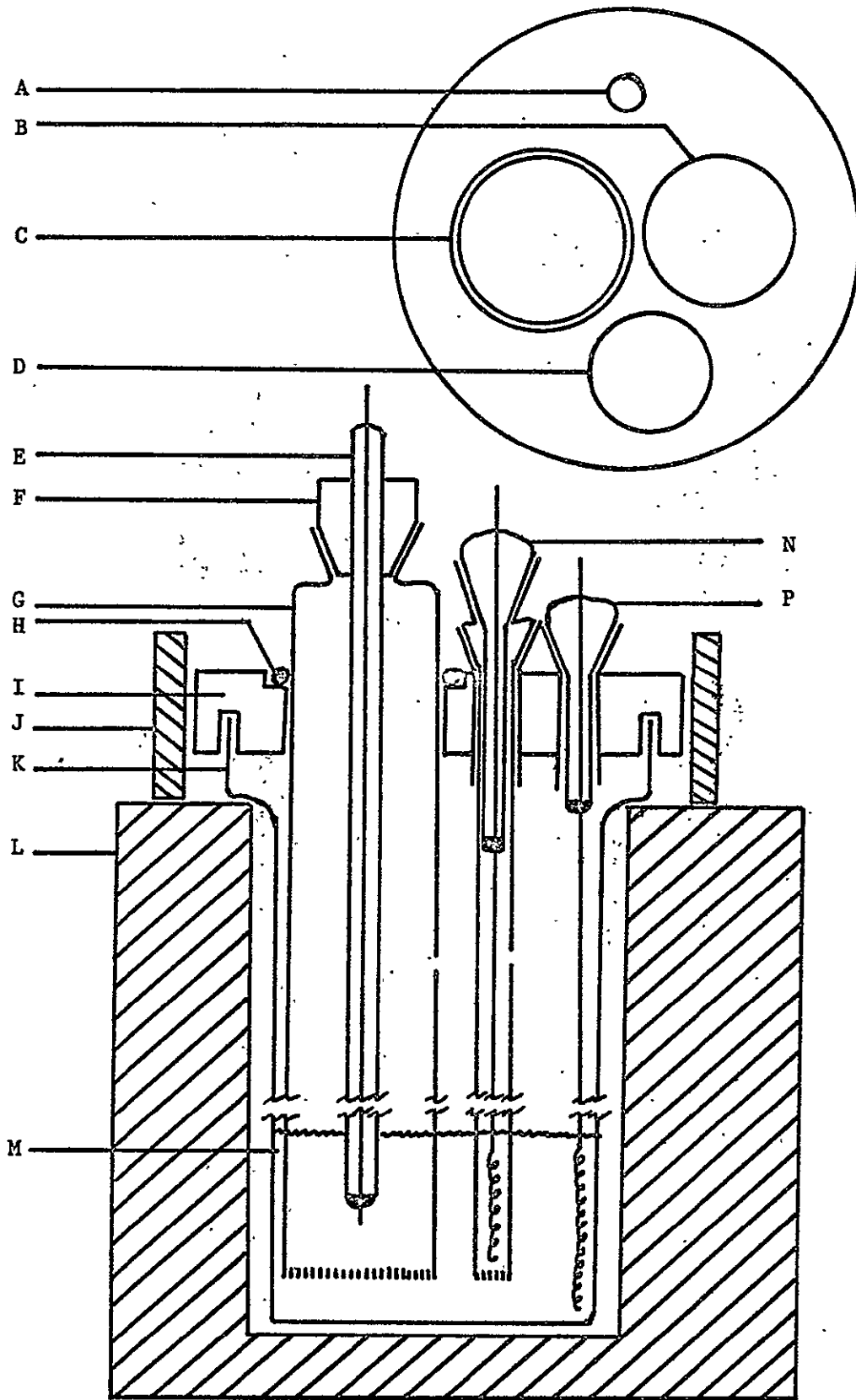
Figure 1

Figure 2

Figure 3

Figure 4
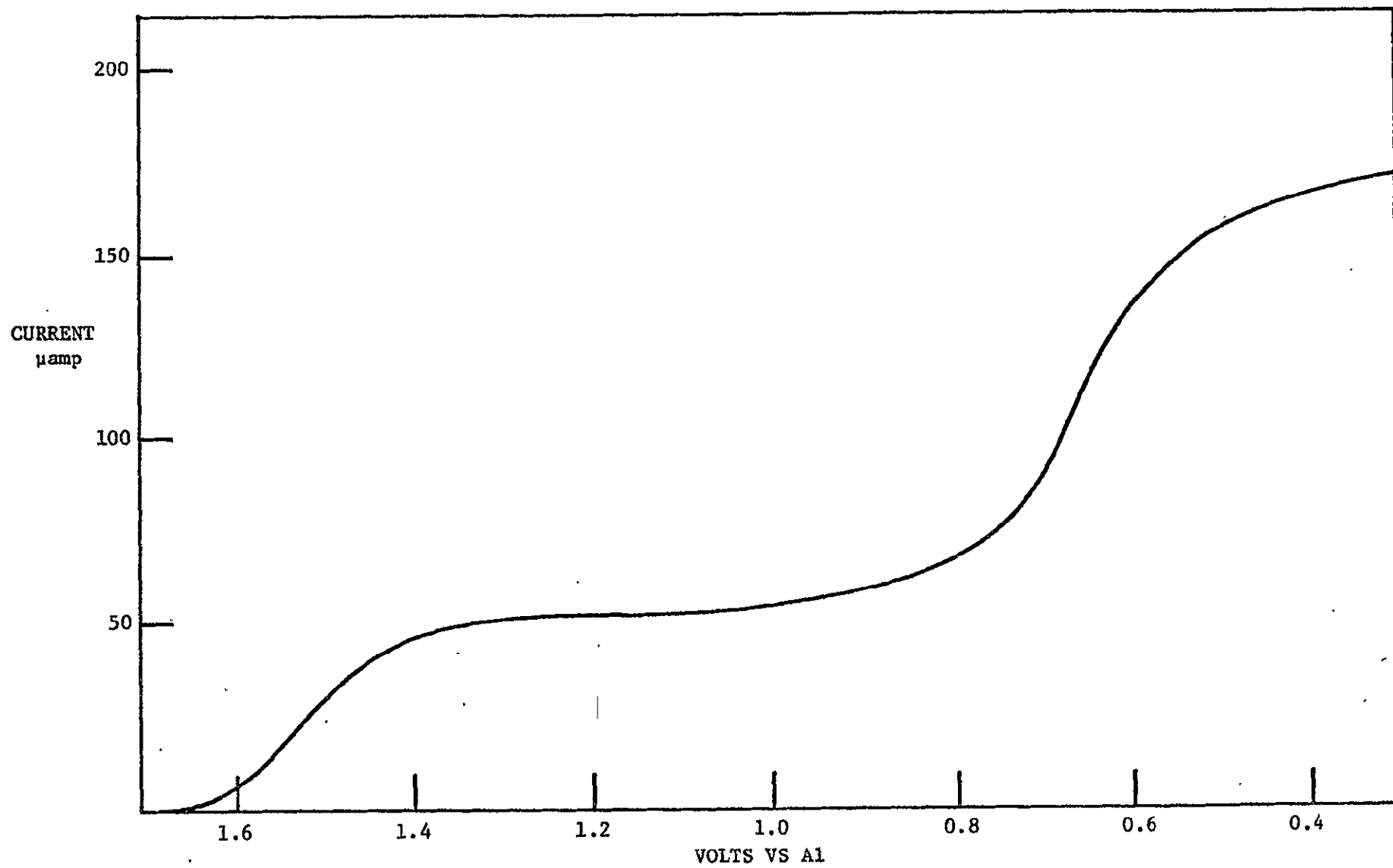
Figure 5

CURRENT
μA

VOLTS VS Al
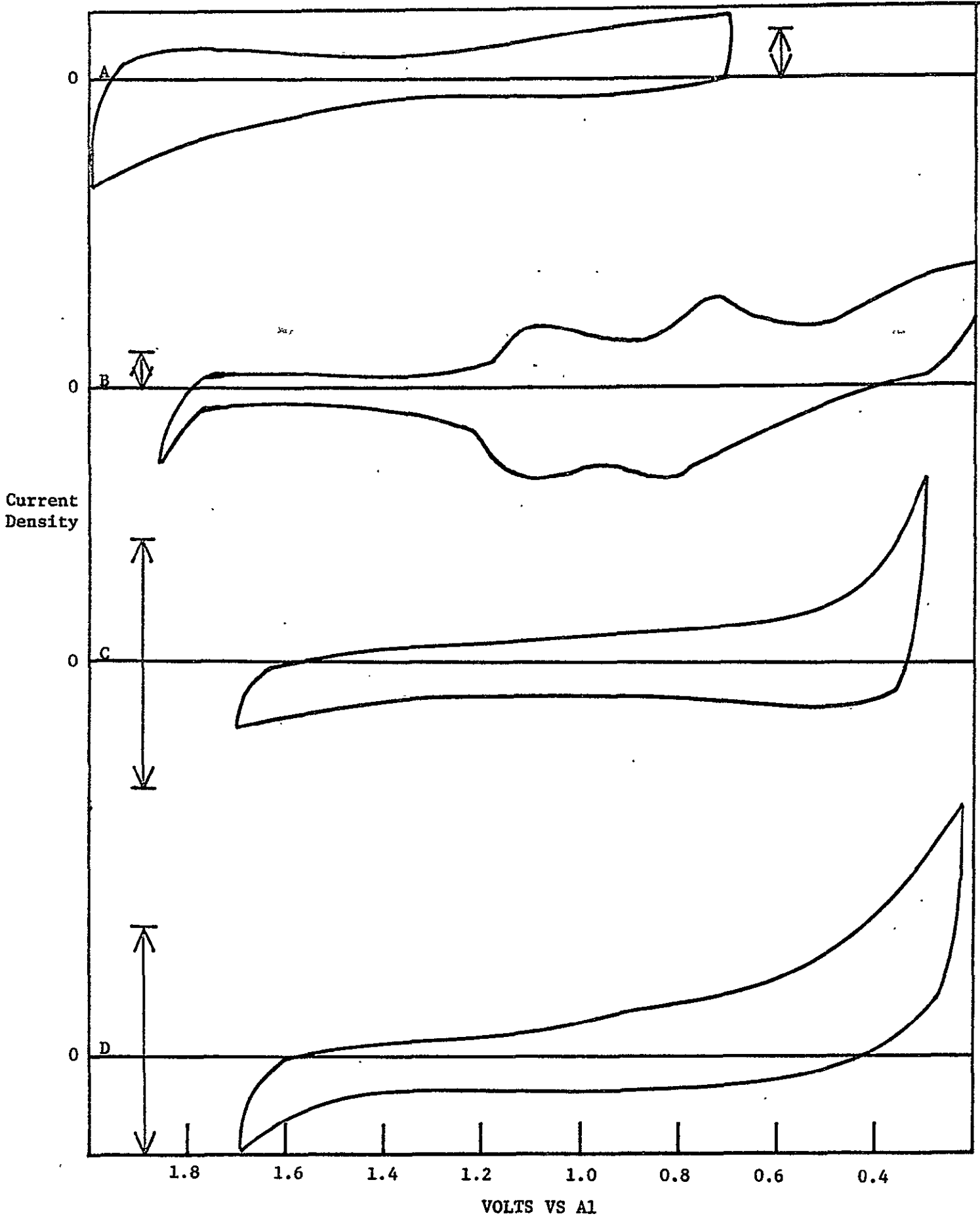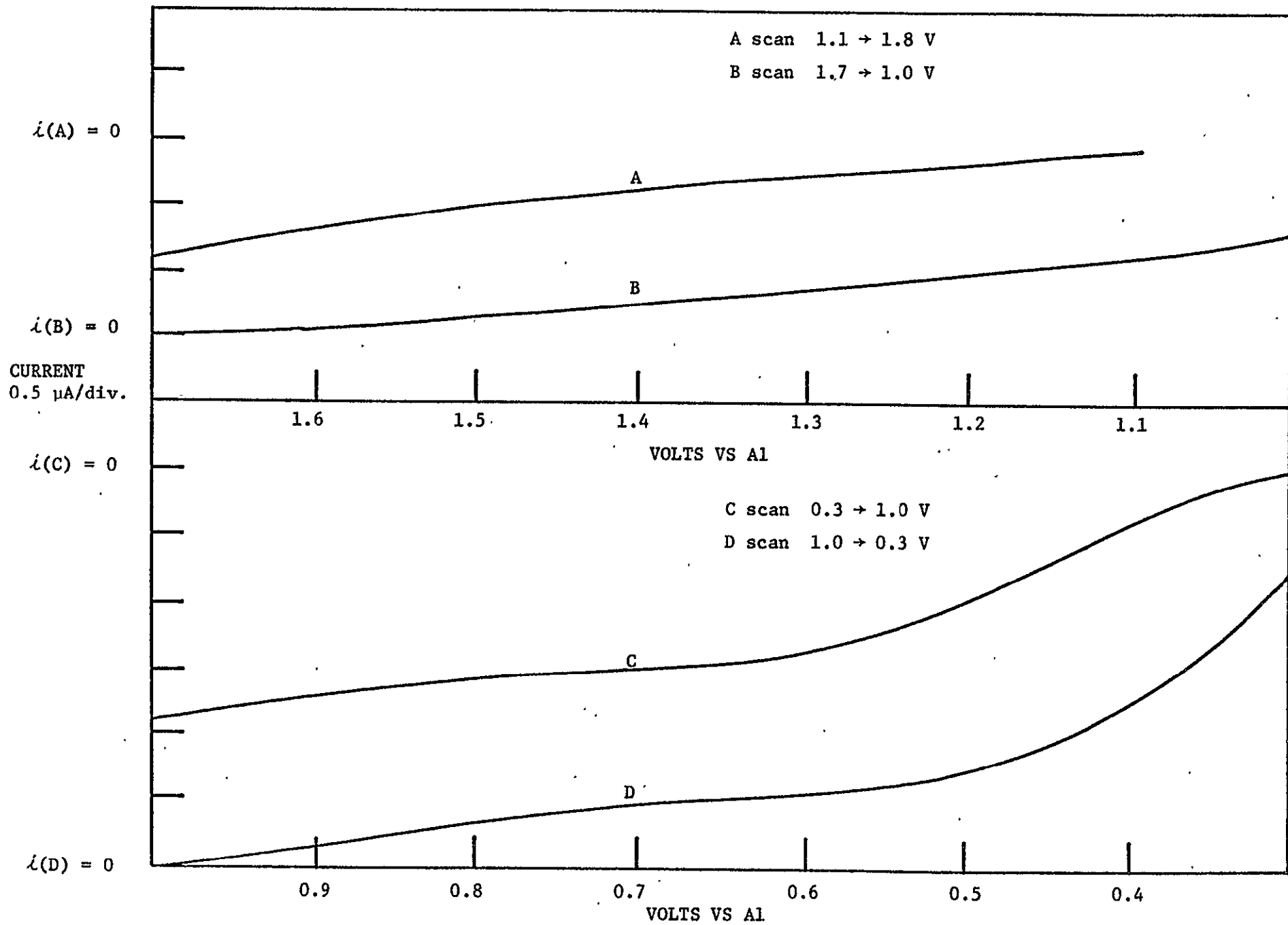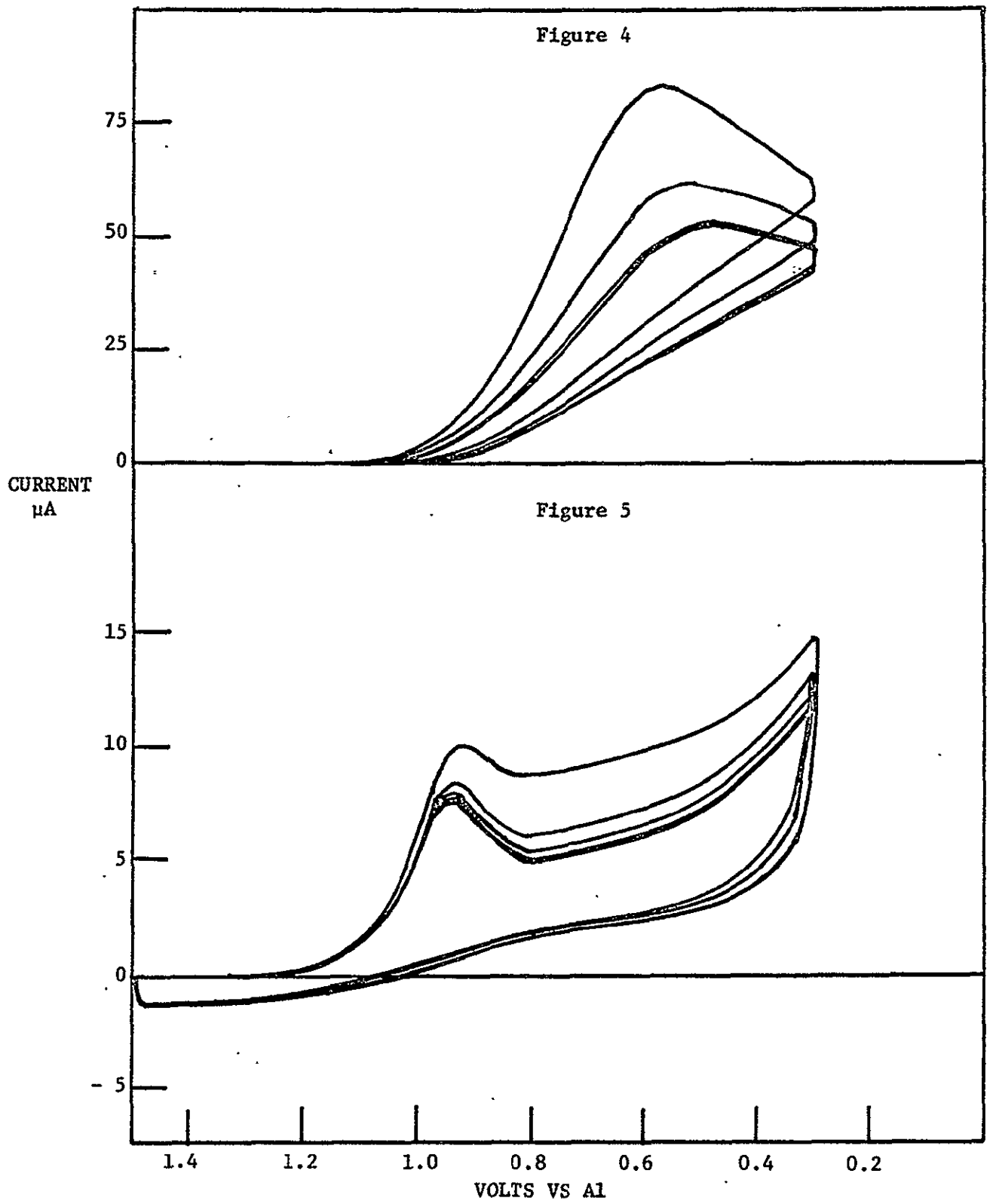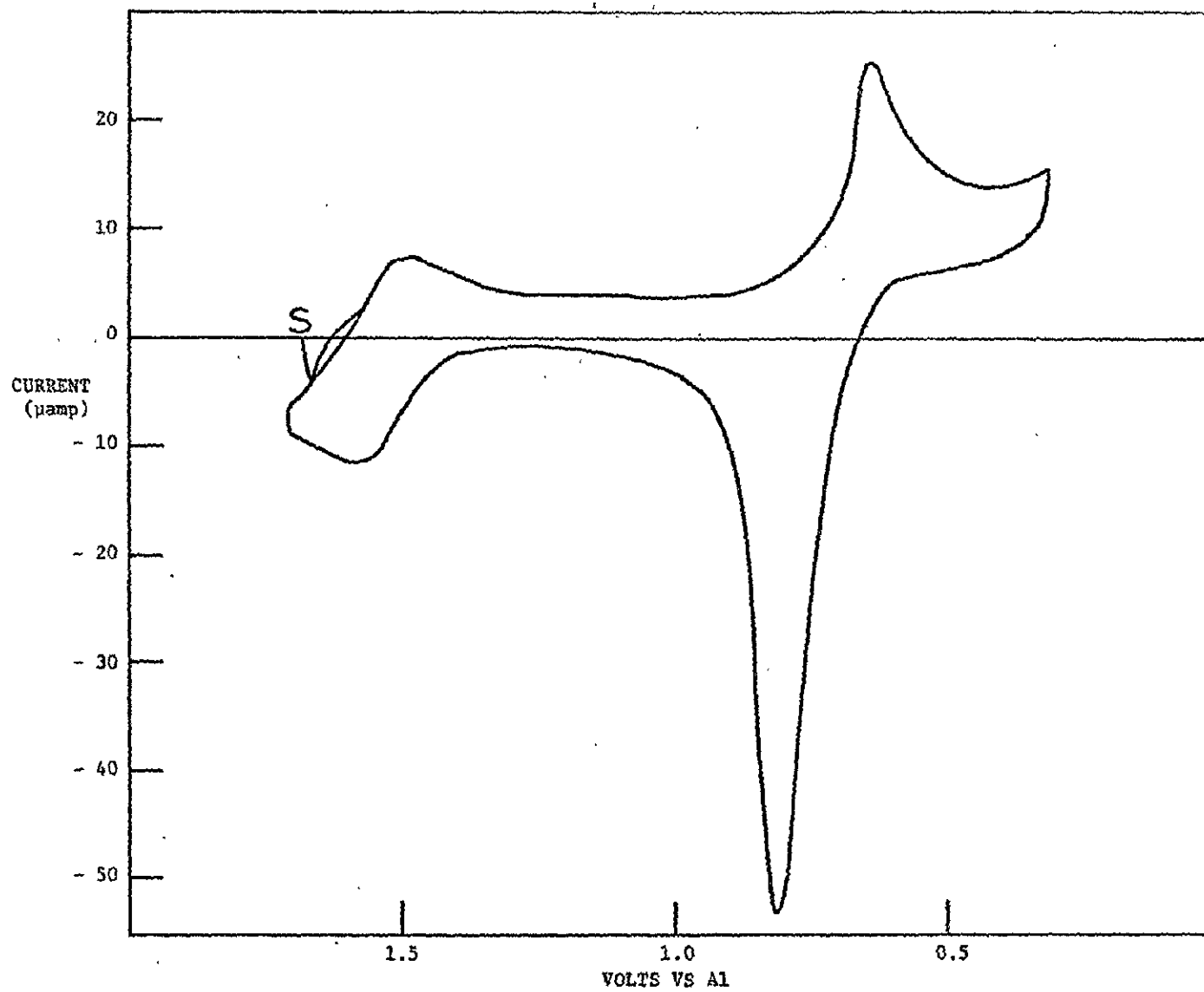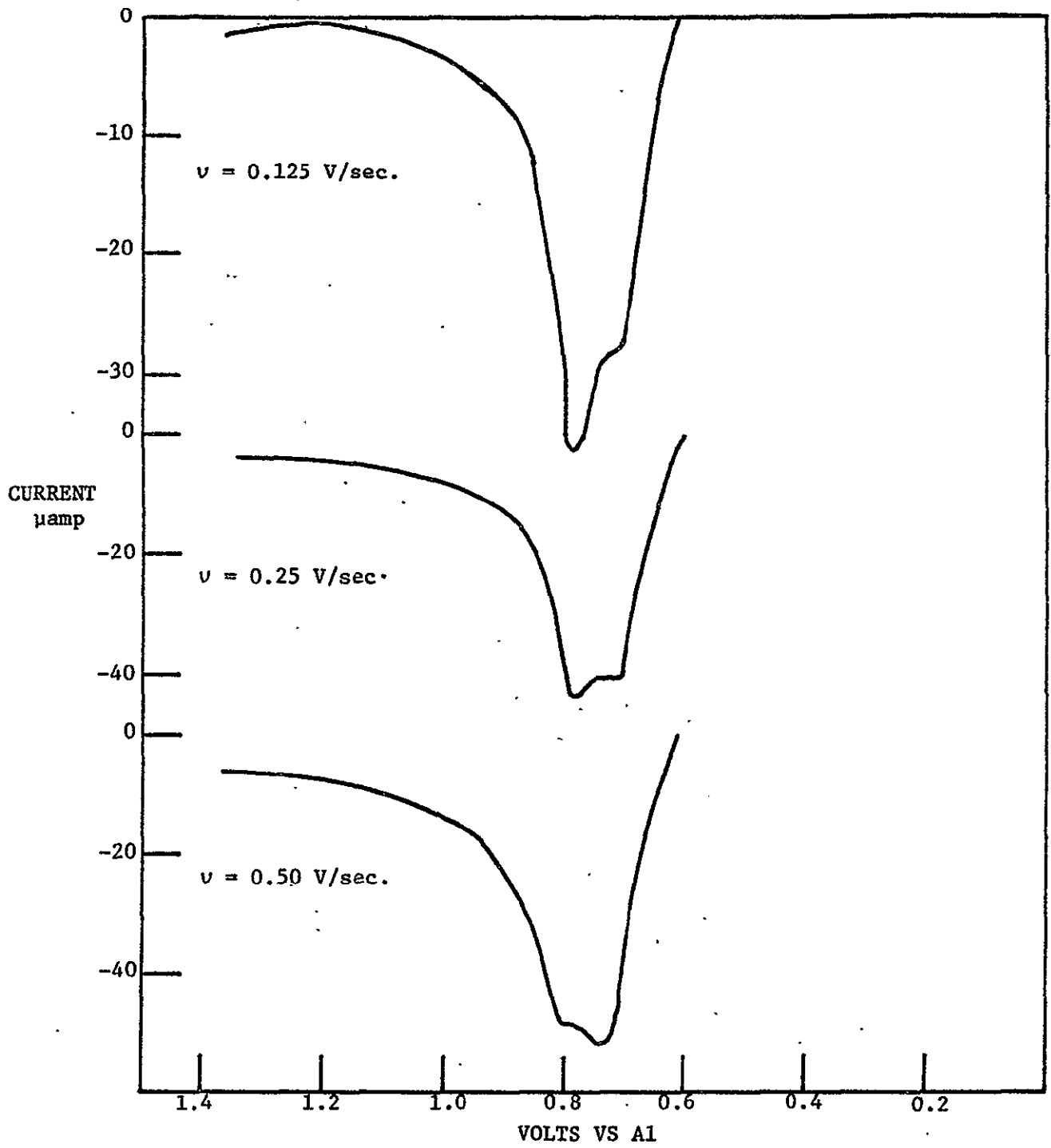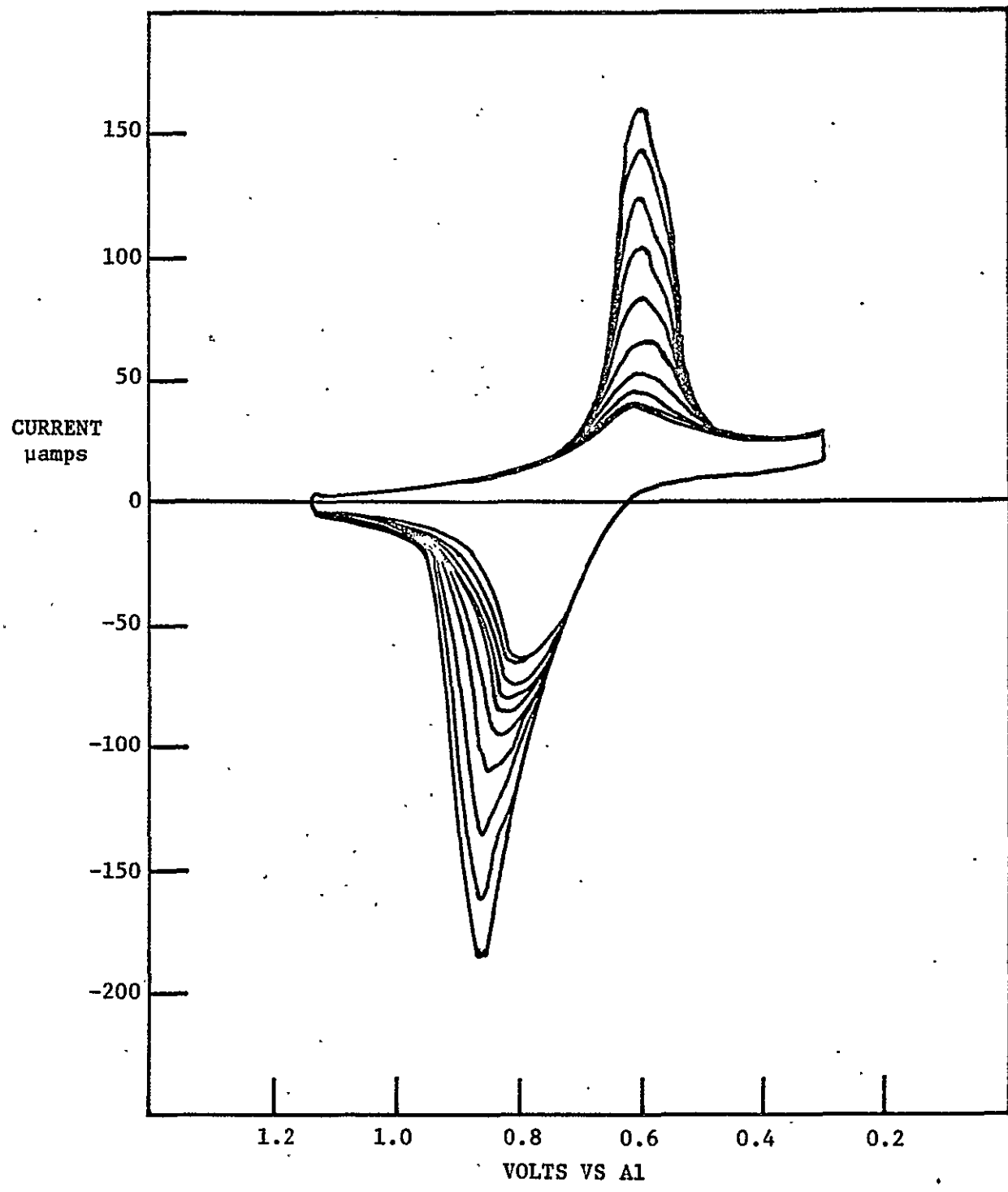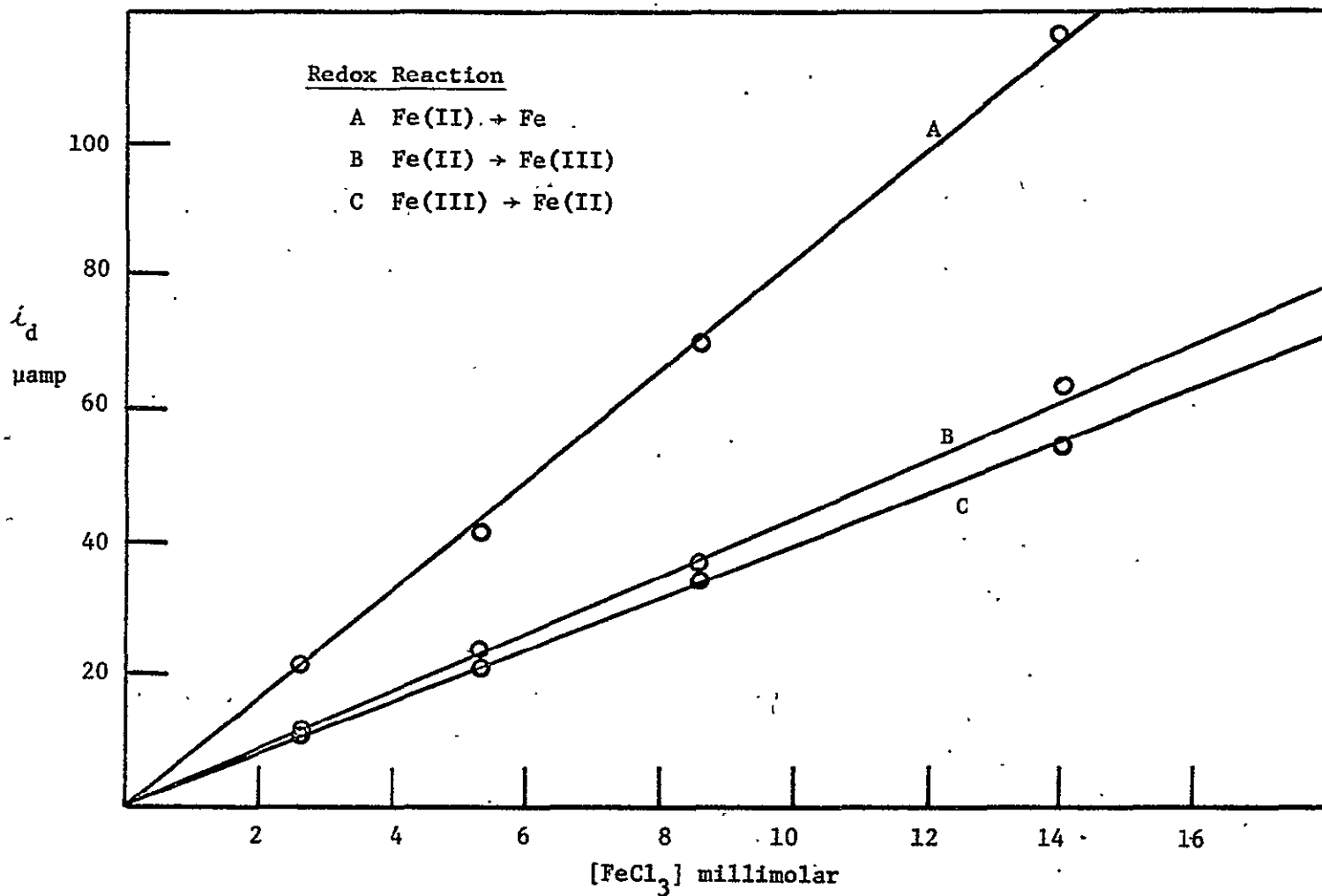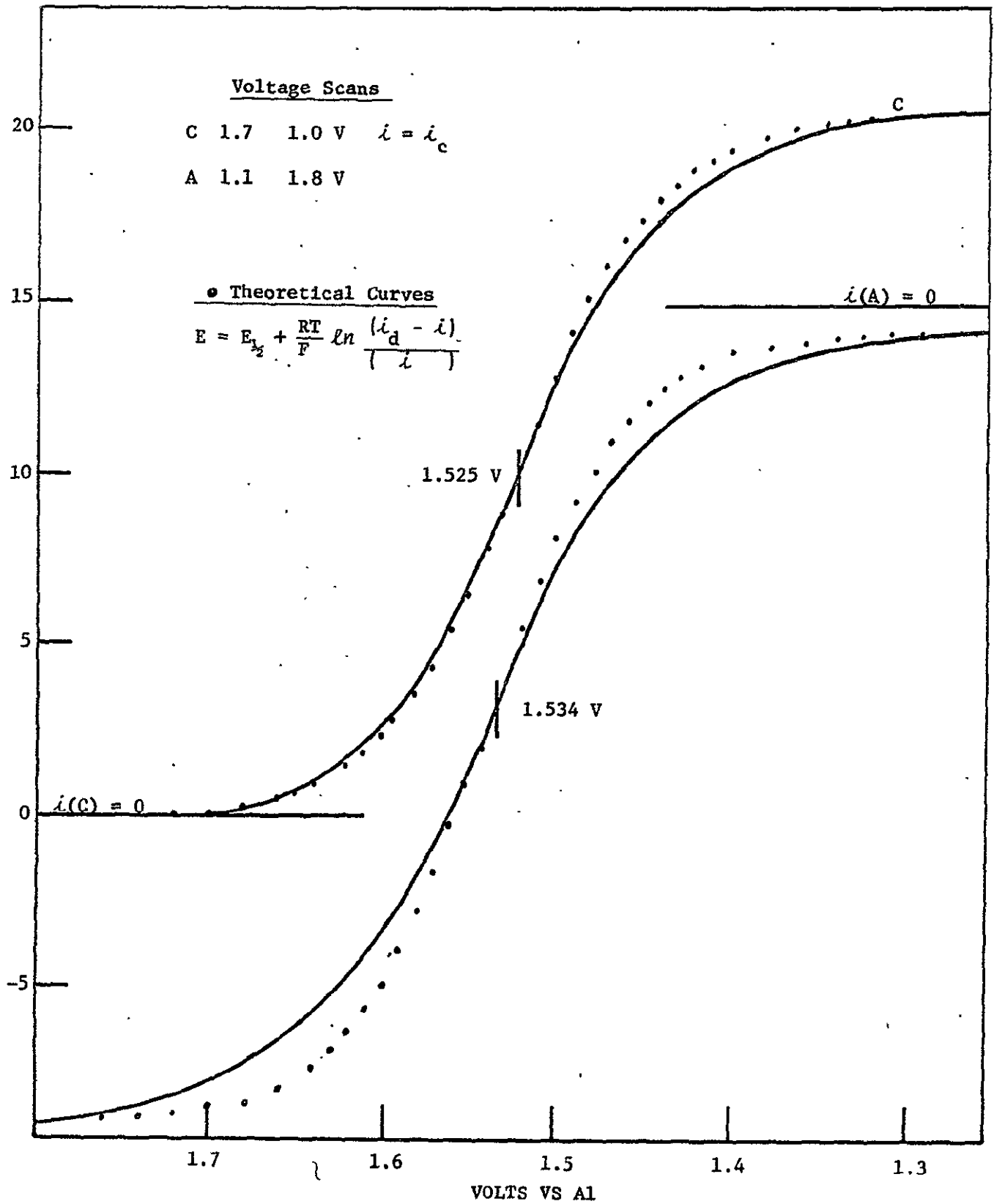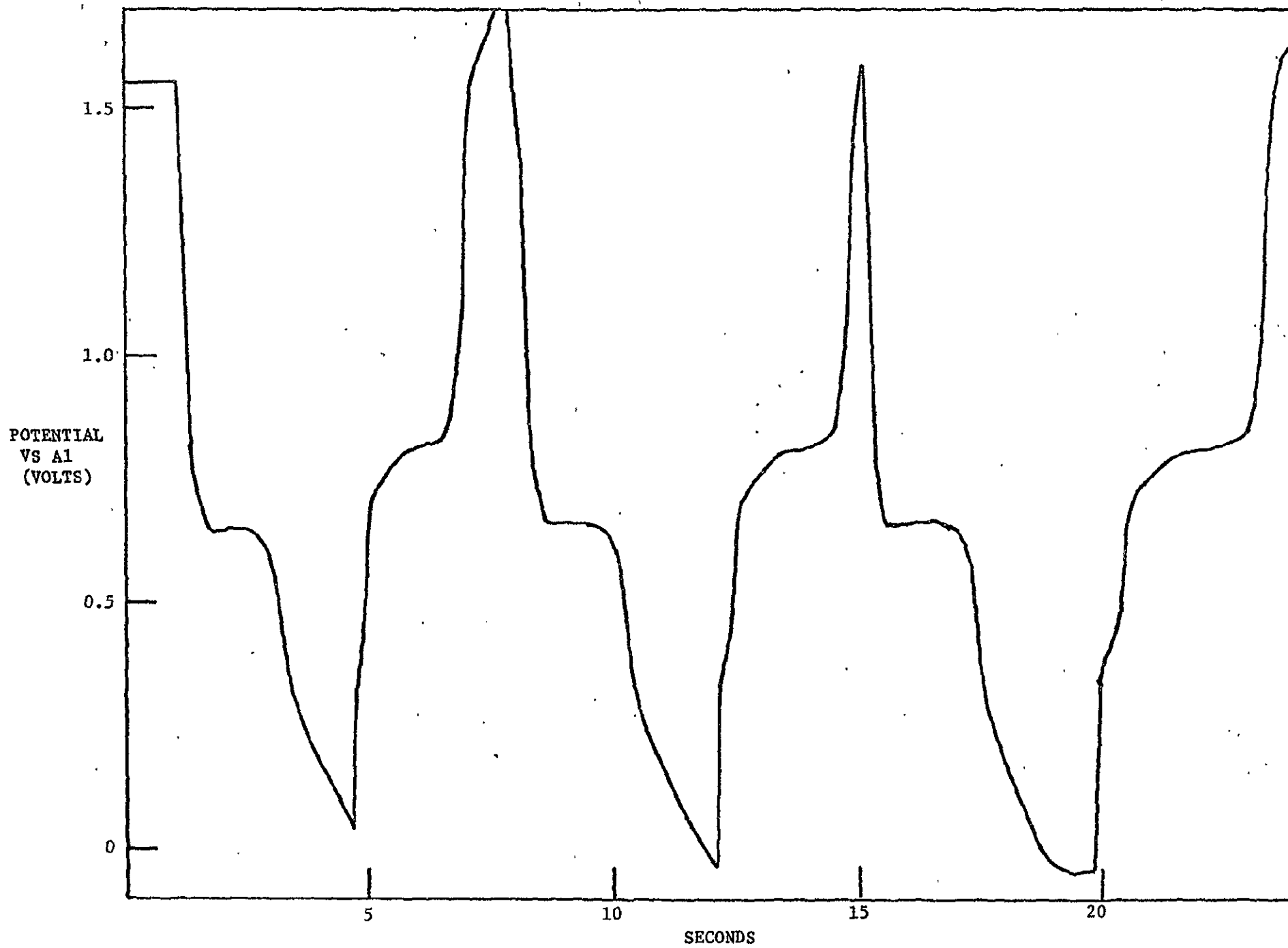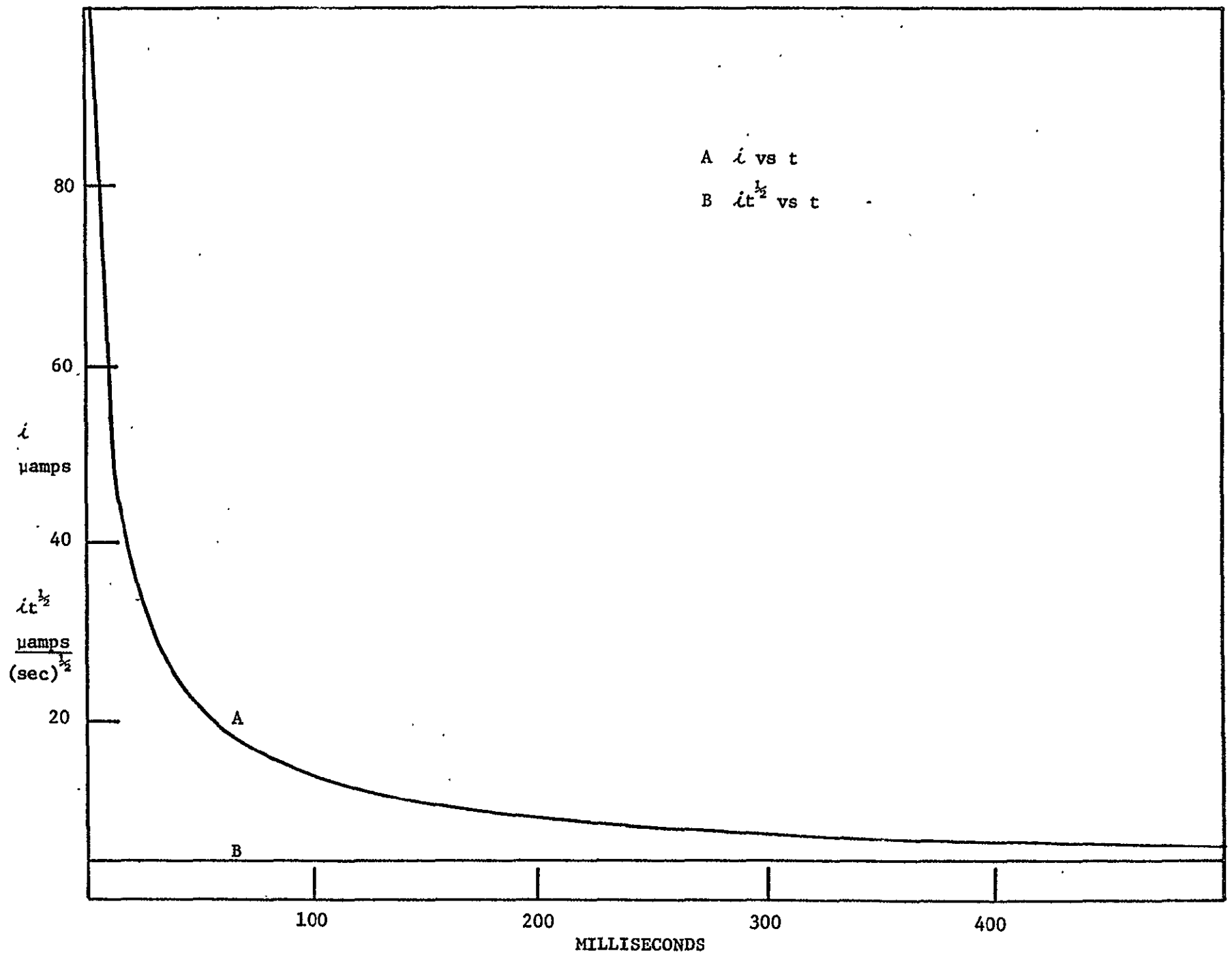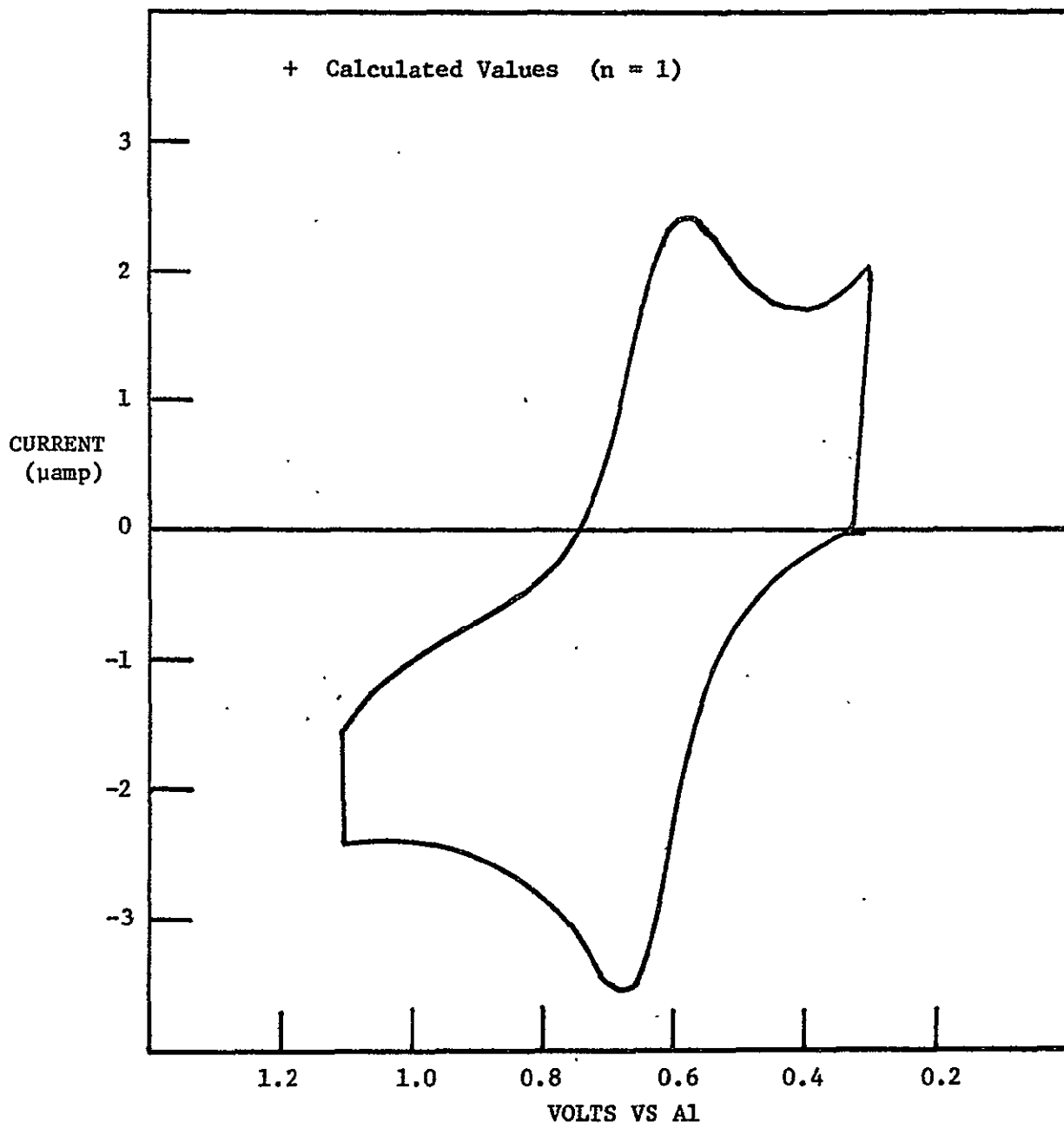
Figure 6

Figure 7

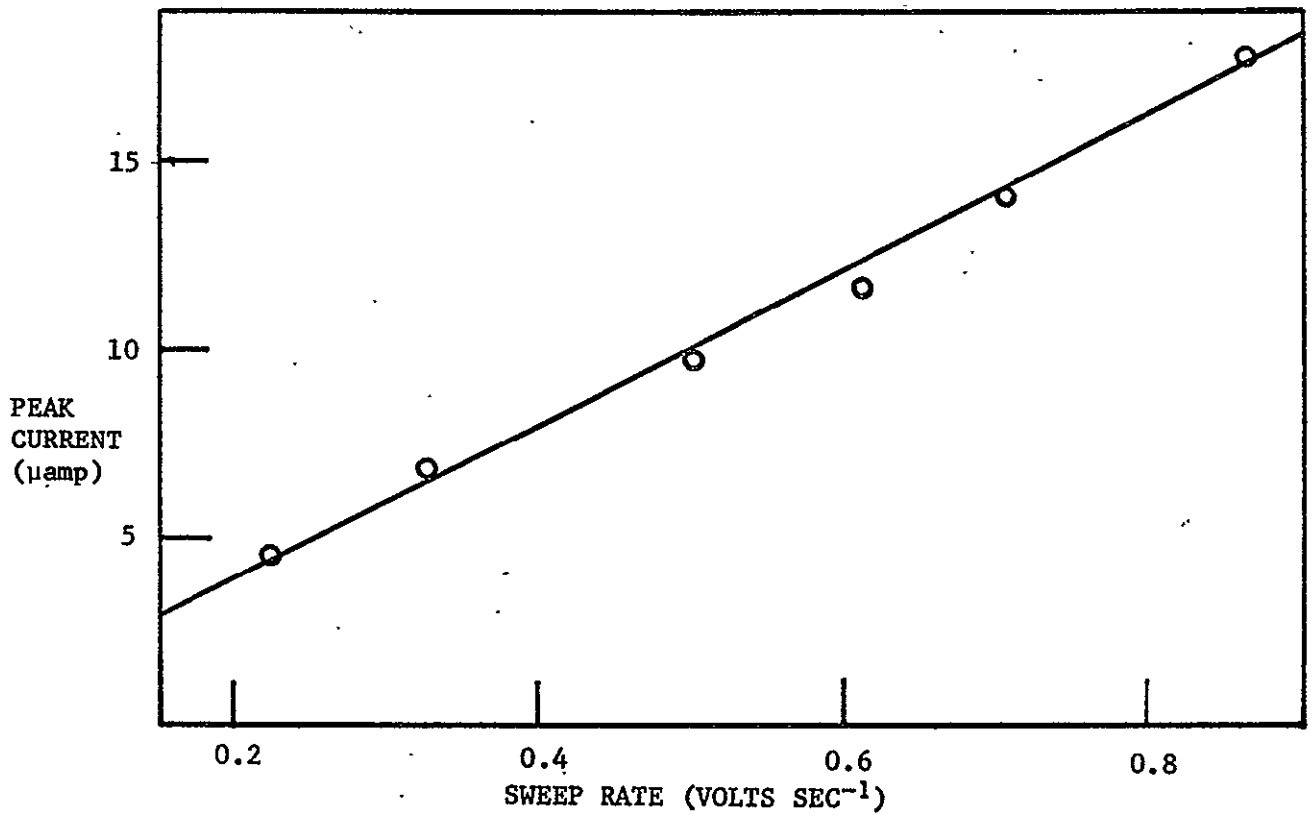Figure 8
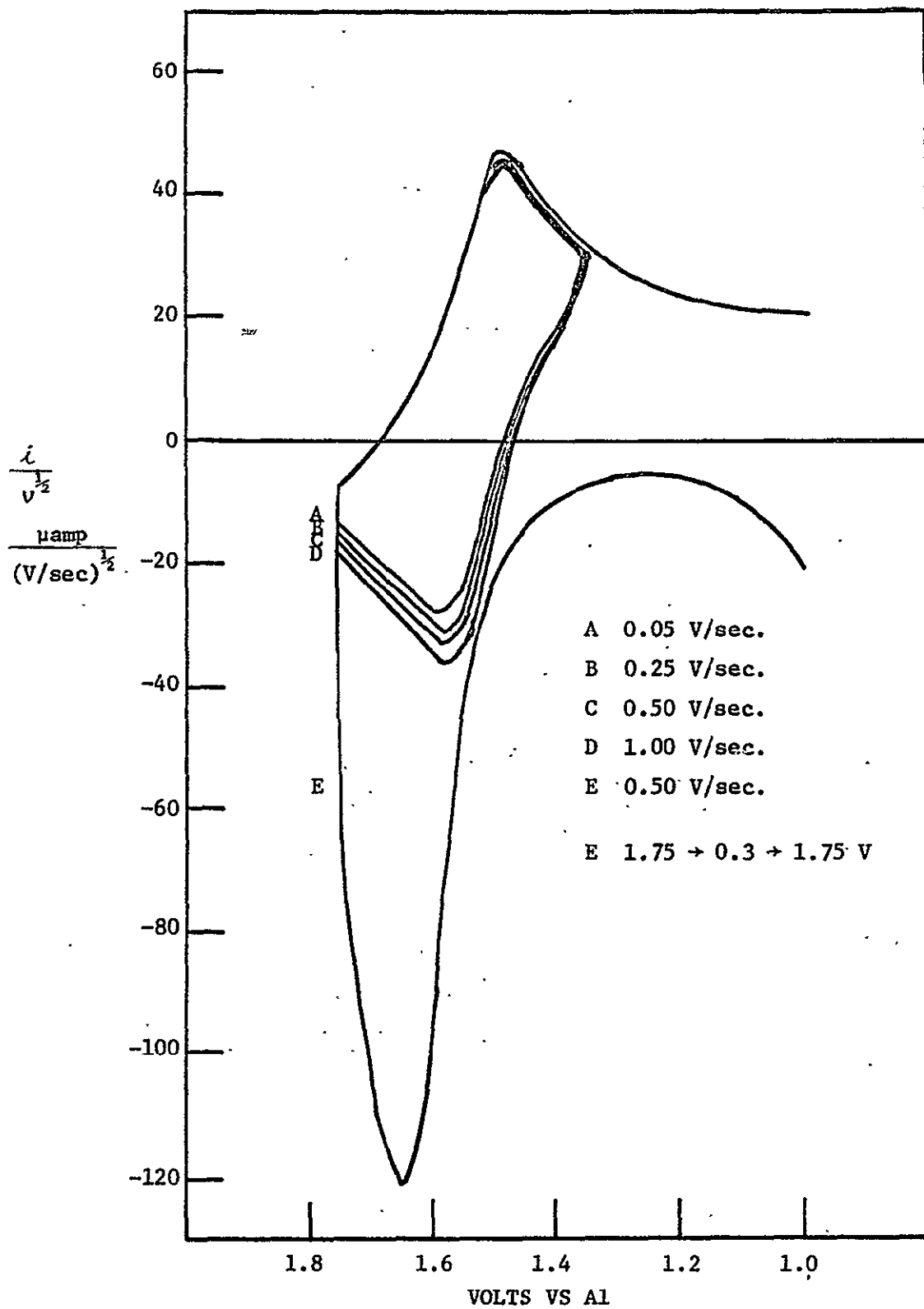
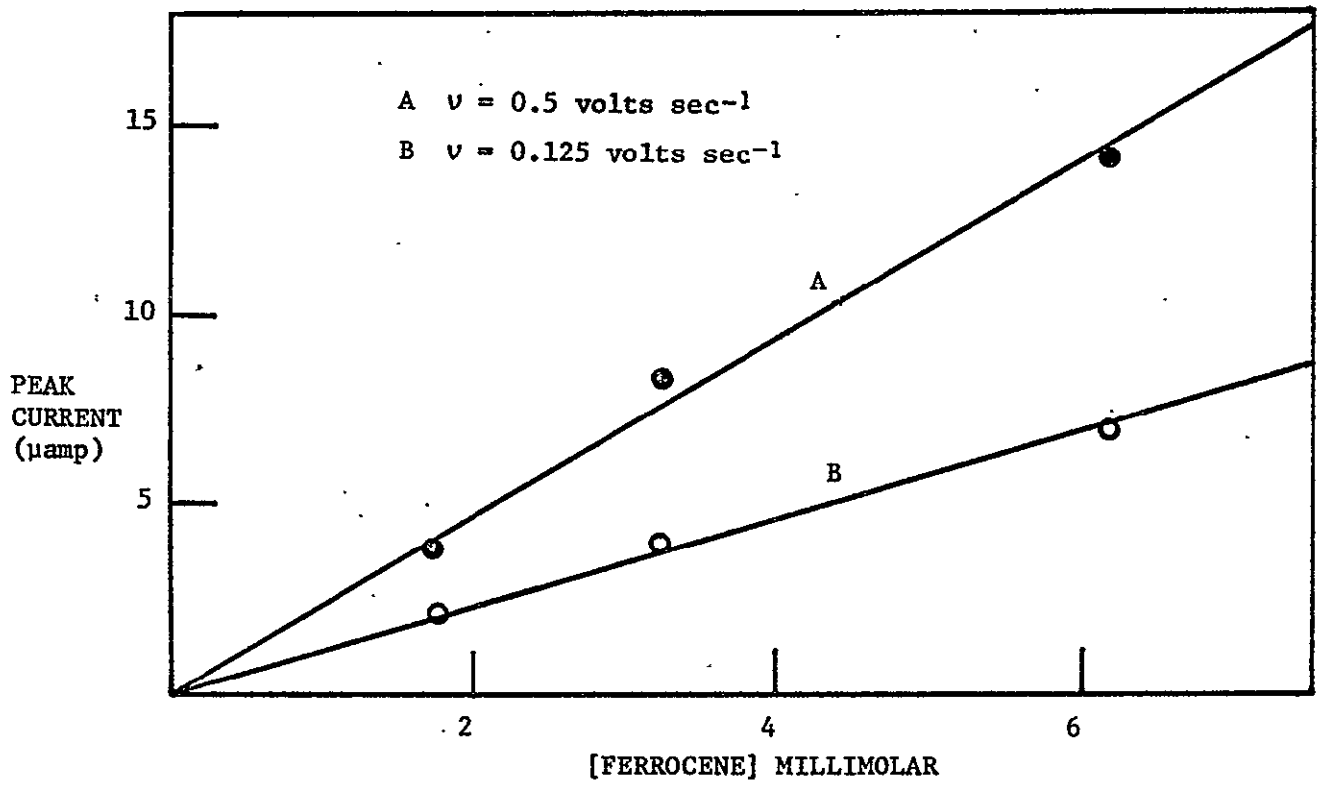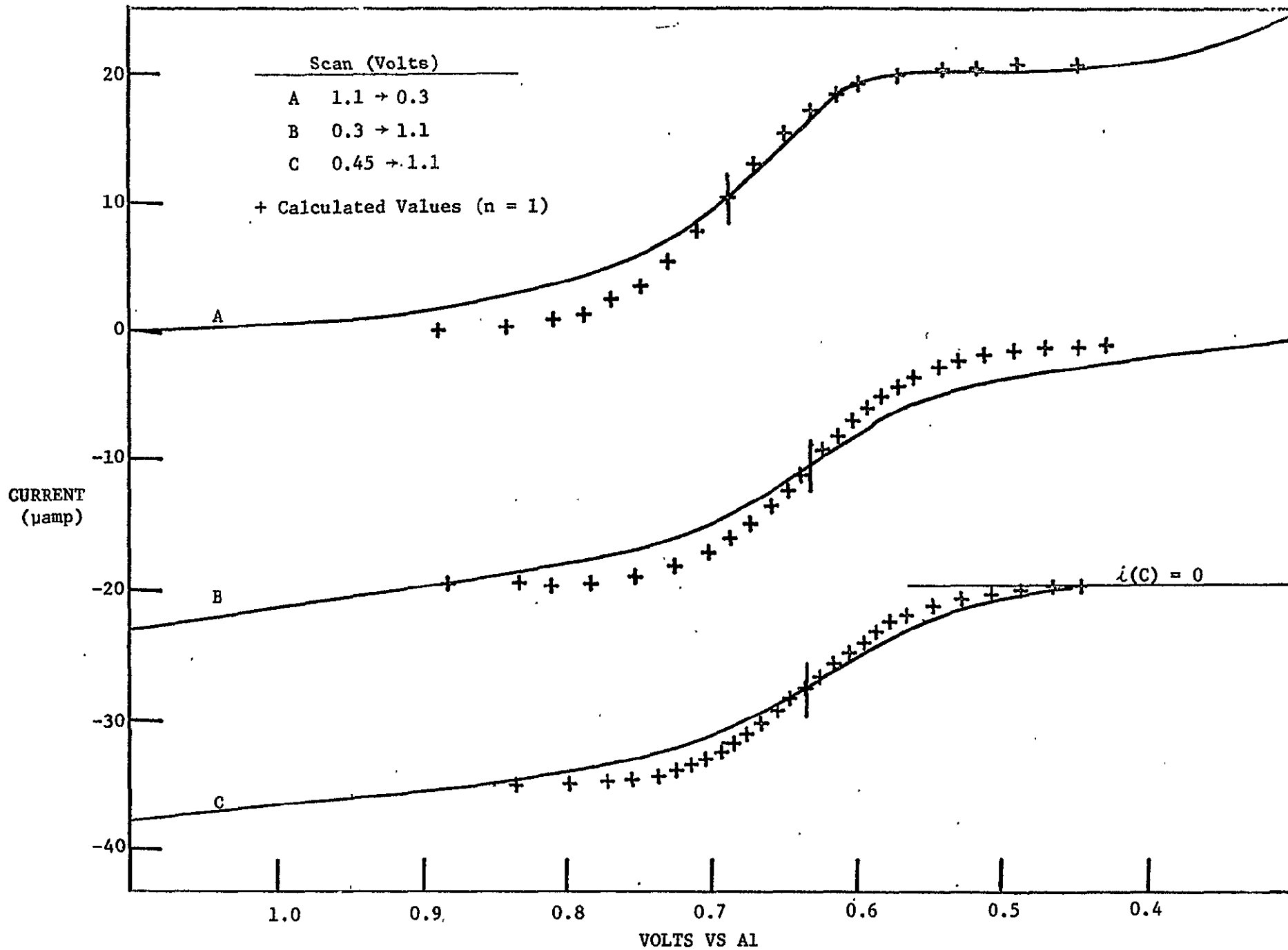Figure 9
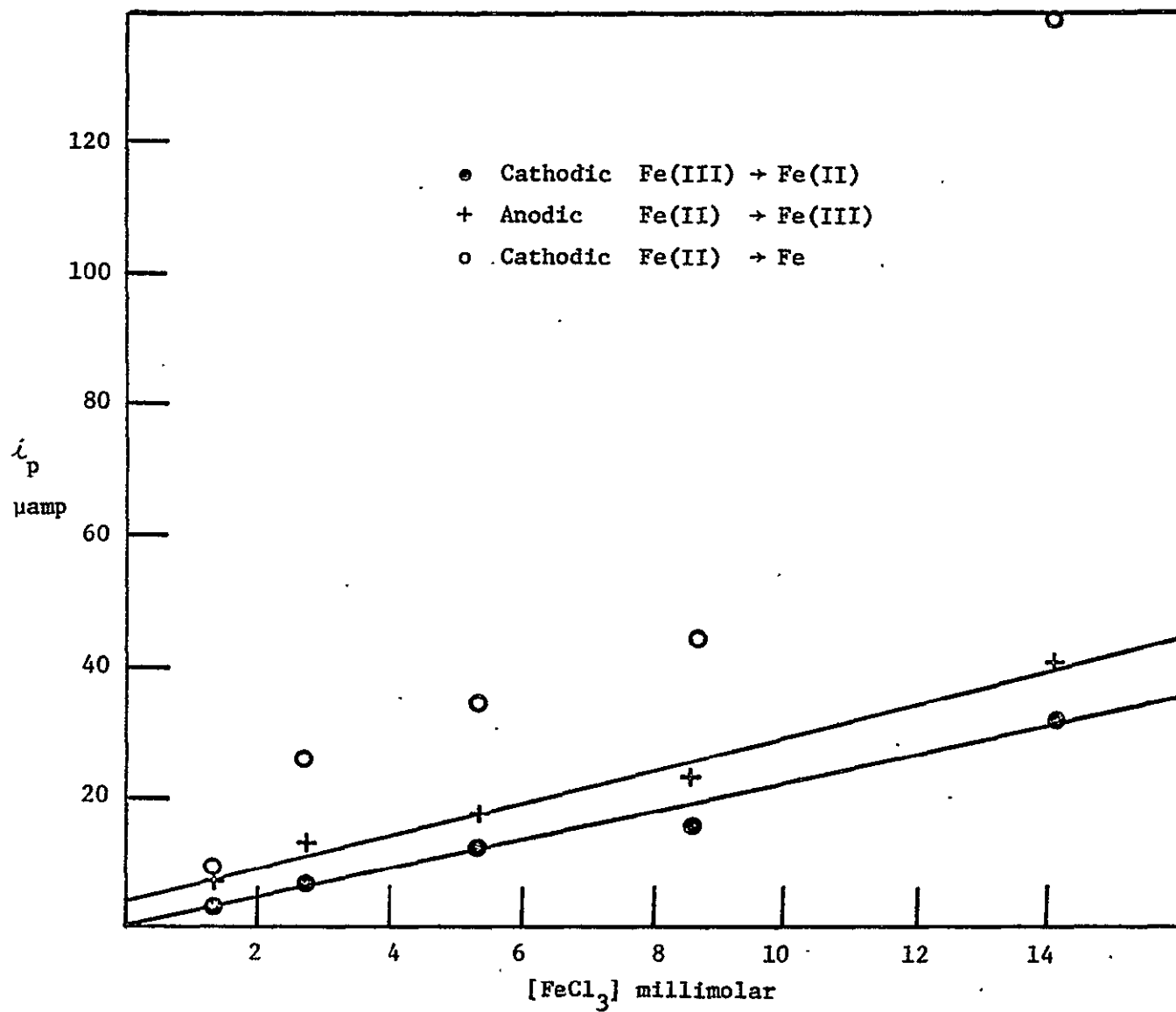
Figure 10

Figure 11

Figure 12

Figure 13

Figure 14

Figure 15

Figure 16

Figure 17

A $\nu = 0.5$ volts sec^{-1}
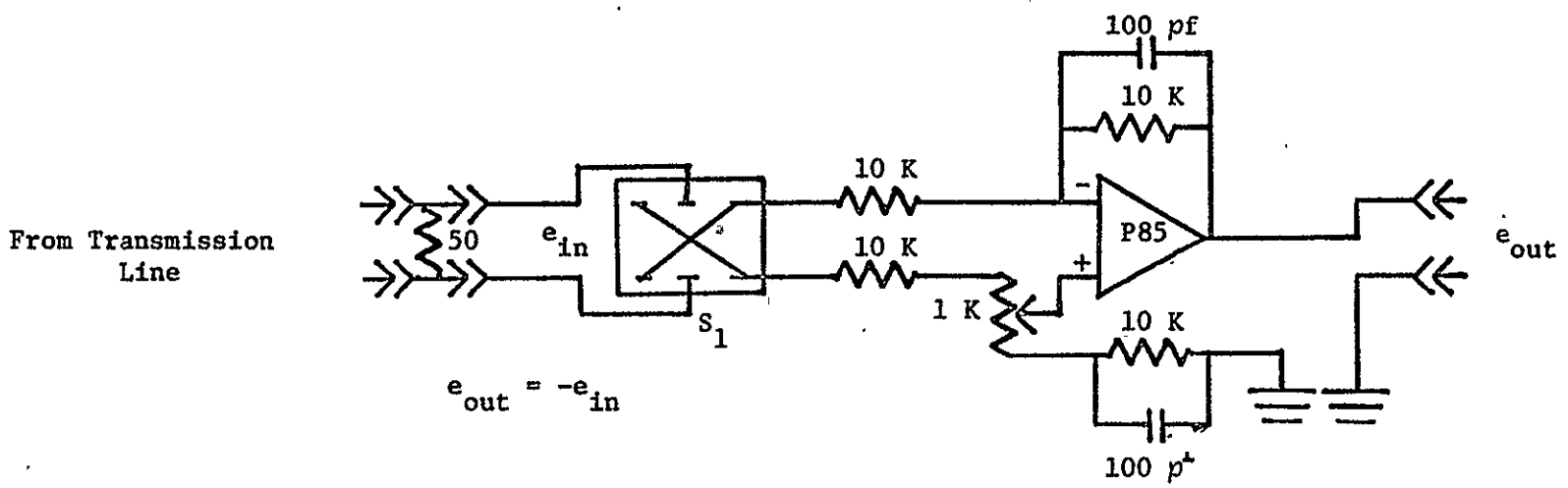B $\nu = 0.125$ volts sec^{-1}
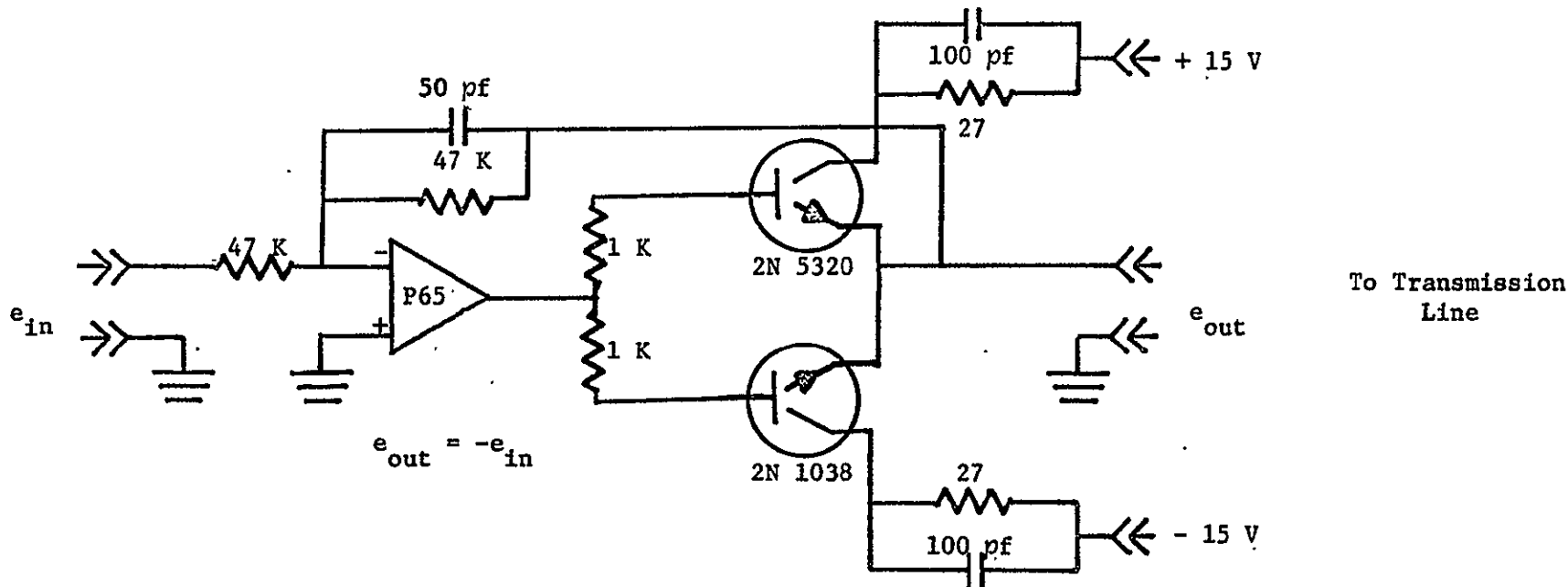
Figure 18

Figure 19

LINE DRIVER

Figure 20-A

LINE RECEIVER

Figure 20-B

Figure 21

Calibration of Transmission Lines

0 VOLTS OUTPUT

B(OUT) = +0.0000000E + 00

B(IN) = +0.0000000E + 00

V(IN) = +0.1192092E - 03

BIAS OK? N

NEW B OUT & IN = -0.00311, 0.0

B(OUT) = -0.3110000E - 02

.B(IN) = +0.0000000E + 00

V(IN) = -0.2341673E - 03

BIAS OK? N

NEW B OUT & IN = -0.00311, + 0.000234

B(OUT) = -3110000E - 02

B(IN) = +0.2340000E - 03

V(IN) = -0.1326701E - 06

BIAS OK? Y

1 VOLT OUTPUT

F(OUT) = +0.1000000E +01

F(IN) = +0.1000000E + 01

V(IN) = +0.3013372E + 00

F VALUES OK? N

NEW F OUT & IN = 0.3476157, 1.0

Figure 21 (continued)

F(OUT) = +0.3476157E + 00

F(IN) = +0.1000000E + 00

V(IN) = +0.9815831E + 00

F VALUES OK? N

NEW F OUT & IN = 0.3476157, 0.9815831

F(OUT) = +0.3476157E + 00

F(IN) = +0.9815831E + 00

V(IN) = +0.1000015E + 01

F VALUES OK? Y

THE CALIBRATION FIGURES ARE

B(OUT) = -0.3110000E - 02

F(OUT) = +0.3476157E + 00

B(IN) = +0.2340000E - 03

F(IN) = +0.9815831E + 00
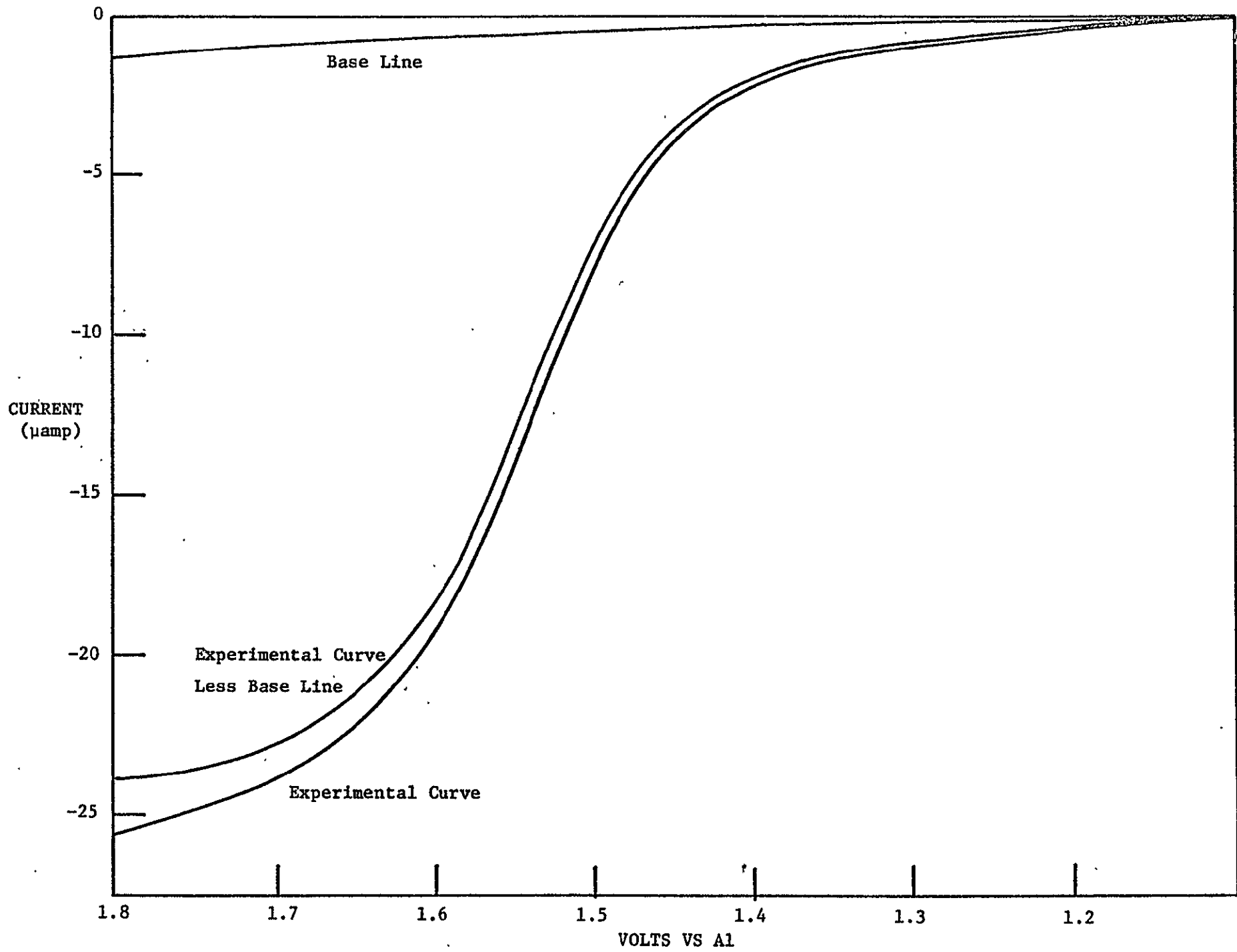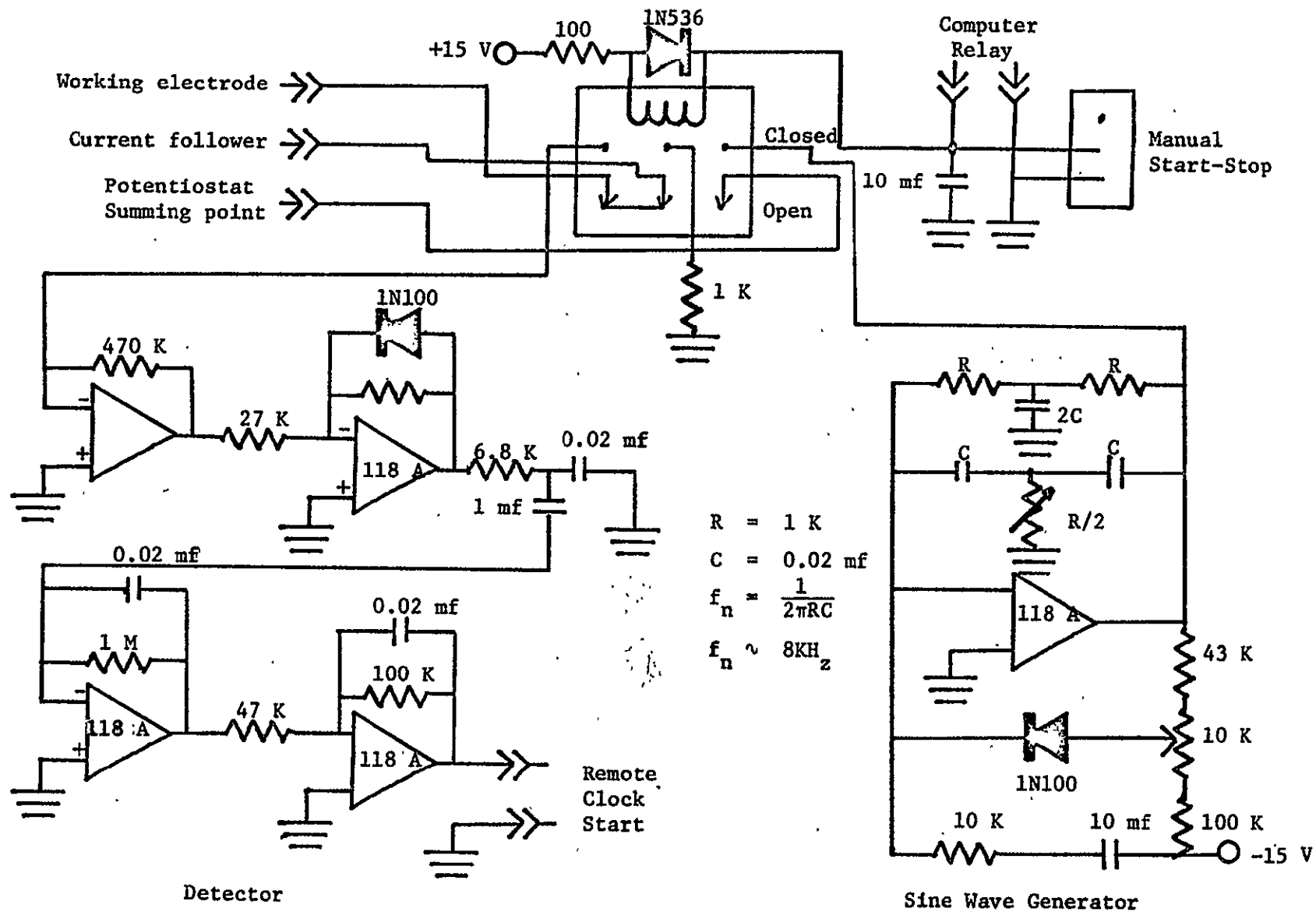
REPEAT CALIBRATION?

Figure 22

Figure 23

Figure 24

CLOCK INTERVAL = 0.1

B(IN) = 0.000234

B(OUT) = -0.00311

F(IN) = 0.98158

F(OUT) = 0.34762

PULSE HEIGHT = 0.7

INPUT TIME FOR 1ST PT, INTERVAL NUMBER OF PTS 5,5,100

TIME OF 1ST PT = +0.5000000 E + 01

TIME OF INTERVAL = +0.5000000 E + 01

R(M) = 1000

MAX I (MICROAMPS) = +0.5094067 E + 04

FOR X

MIN & MAX = 0,500

FOR X

MIN TCK & SPACE = 0,50

FOR Y

MIN & MAX = 0,5000

FOR Y

MIN TCK & SPACE = 0,500

FULL SCALE PR KY

ZERO PR KY

VALENCE CHANGE = 1

CALC A, C OR D? A

MILLI MOLAR CONC = 2.77

Figure 24 (continued)

D = 0.00000629

SCALE FAC & AVERAGE = 5,1

B OR S & BASE NO = B1

IT($\frac{1}{2}$) VS T

SLOPE = -0.2044196 E + 02

INTERCEPT = +0.1077684 E + 02

AREA IN CM SQ = +0.1077684 E + 02

REPEAT THE EXPT?   Y

SCALE FAC & AVERAGE = 5,1

B OR S & BASE NO = S1

IT($\frac{1}{2}$) VS T

SLOPE = -0.3311705 E + 01

INTERCEPT = +0.6253594 E + 02
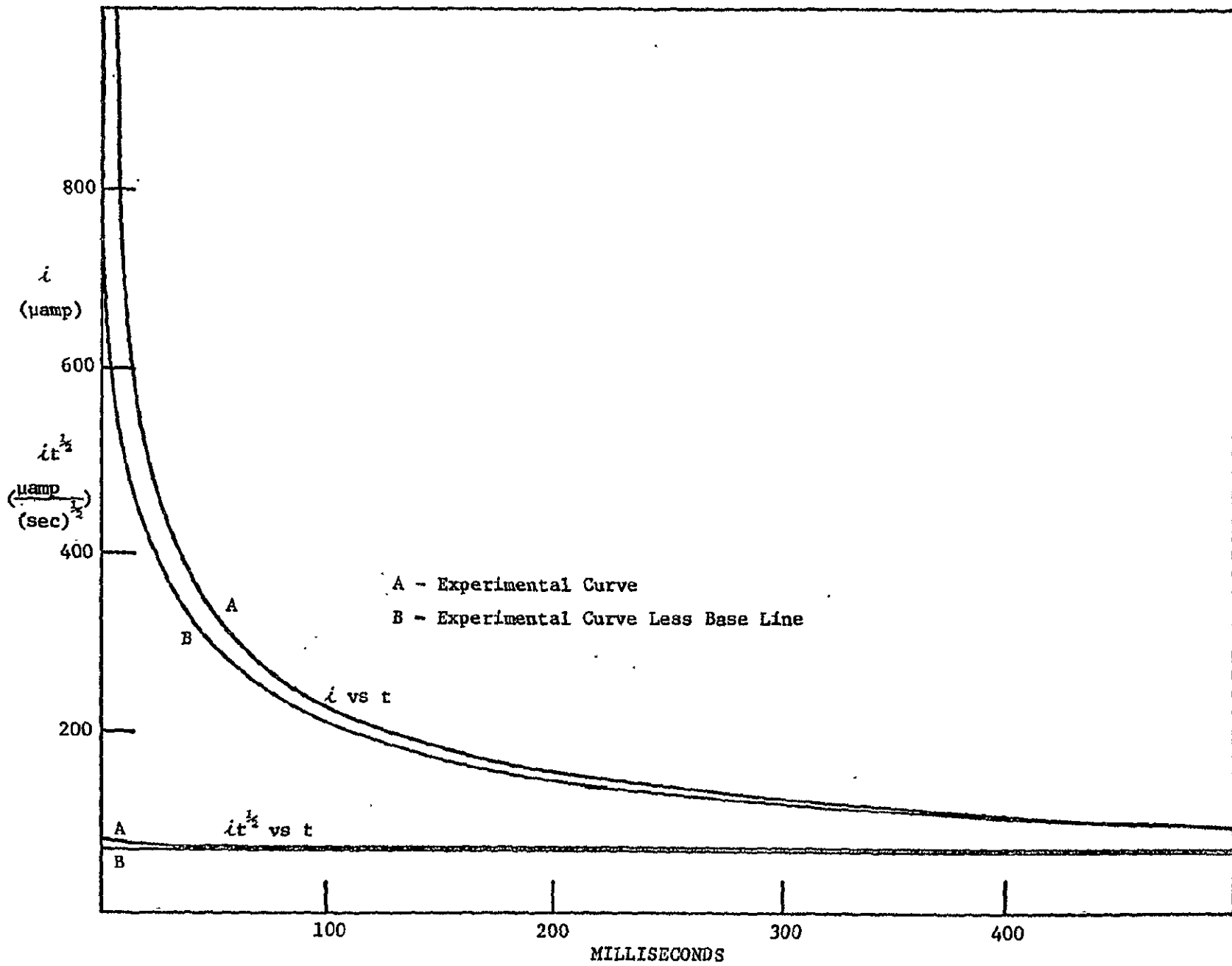
AREA IN CM SQ = +0.2016518E + 01

REPEAT THE EXPT?

Figure 25